





National Library  
of Canada

Bibliothèque nationale  
du Canada

Canadian Theses Service

Service des thèses canadiennes

Ottawa, Canada  
K1A 0N4

## NOTICE

The quality of this microform is heavily dependent upon the quality of the original thesis submitted for microfilming. Every effort has been made to ensure the highest quality of reproduction possible.

If pages are missing, contact the university which granted the degree.

Some pages may have indistinct print especially if the original pages were typed with a poor typewriter ribbon or if the university sent us an inferior photocopy.

Reproduction in full or in part of this microform is governed by the Canadian Copyright Act, R.S.C. 1970, c. C-30, and subsequent amendments.

## /IS

La qualité de cette microforme dépend grandement de la qualité de la thèse soumise au microfilmage. Nous avons tout fait pour assurer une qualité supérieure de reproduction.

S'il manque des pages, veuillez communiquer avec l'université qui a conféré le grade.

La qualité d'impression de certaines pages peut laisser à désirer, surtout si les pages originales ont été dactylographiées à l'aide d'un ruban usé ou si l'université nous a fait parvenir une photocopie de qualité inférieure.

La reproduction, même partielle, de cette microforme est soumise à la Loi canadienne sur le droit d'auteur, SRC 1970, c. C-30, et ses amendements subséquents.

UNIVERSITY OF ALBERTA  
PEDOGENIC CHARACTERISTICS OF WHITE CLAY SOILS OF THE THREE RIVER  
PLAIN, HEILONGJIANG, P.R. CHINA.

BY  
BAOSHAN XING

A THESIS  
SUBMITTED TO THE FACULTY OF GRADUATE STUDIES AND  
RESEARCH  
IN PARTIAL FULFILMENT OF THE REQUIREMENTS FOR THE DEGREE  
OF MASTER OF SCIENCE  
IN  
SOIL MINERALOGY

DEPARTMENT OF SOIL SCIENCE

EDMONTON, ALBERTA

SPRING 1990



National Library  
of Canada

Bibliothèque nationale  
du Canada

Canadian Theses Service

Service des thèses canadiennes

Ottawa, Canada  
K1A 0N4

## NOTICE

The quality of this microform is heavily dependent upon the quality of the original thesis submitted for microfilming. Every effort has been made to ensure the highest quality of reproduction possible.

If pages are missing, contact the university which granted the degree.

Some pages may have indistinct print especially if the original pages were typed with a poor typewriter ribbon or if the university sent us an inferior photocopy.

Reproduction in full or in part of this microform is governed by the Canadian Copyright Act, R.S.C. 1970, c. C-30, and subsequent amendments.

## AVIS

La qualité de cette microforme dépend grandement de la qualité de la thèse soumise au microfilmage. Nous avons tout fait pour assurer une qualité supérieure de reproduction.

S'il manque des pages, veuillez communiquer avec l'université qui a conféré le grade.

La qualité d'impression de certaines pages peut laisser à désirer, surtout si les pages originales ont été dactylographiées à l'aide d'un ruban usé ou si l'université nous a fait parvenir une photocopie de qualité inférieure.

La reproduction, même partielle, de cette microforme est soumise à la Loi canadienne sur le droit d'auteur, SRC 1970, c. C-30, et ses amendements subséquents.

ISBN 0-315-60238-4

UNIVERSITY OF ALBERTA

RELEASE FORM

NAME OF AUTHOR: BAOSHAN XING

TITLE OF THESIS: PEDOGENIC CHARACTERISTICS OF  
WHITE CLAY SOILS OF THE  
THREE RIVER PLAIN, HEILONGJIANG,  
P.R. CHINA.

DEGREE: MASTER OF SCIENCE

YEAR THIS DEGREE GRANTED: 1990

Permission is hereby granted to THE UNIVERSITY OF ALBERTA LIBRARY to reproduce single copies of this thesis and to lend or sell such copies for private, scholarly or scientific research purposes only.

The author reserves other publication rights, and neither the thesis nor extensive extracts from it may be printed or otherwise reproduced without the author's written permission.

*Baoshan Xing*  
.....

PERMANENT ADDRESS:

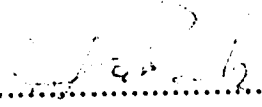
*C2B-8909 112 street*  
.....  
*Edmonton Alberta*  
.....  
*Canada T6C 2K5*  
.....

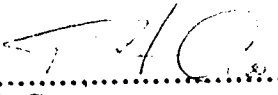
Date: *April 9*.....1990

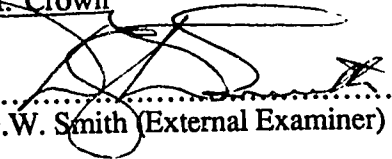
THE UNIVERSITY OF ALBERTA  
FACULTY OF GRADUATE STUDIES AND RESEARCH

The undersigned certify that they have read, and recommend to the Faculty of Graduate Studies and Research for acceptance, a thesis entitled PEDOGENIC CHARACTERISTICS OF WHITE CLAY SOILS OF THE THREE RIVER PLAIN, HEILONGJIANG, P.R. CHINA submitted by BAOSHAN XING in partial fulfillment of the requirements for the degree of MASTER OF SCIENCE in SOIL MINERALOGY.

  
.....  
M. J. Dudas (Supervisor)

  
.....  
S. Pawluk

  
.....  
P. H. Crown

  
.....  
D.G.W. Smith (External Examiner)

Date: March 30, 1998

## DEDICATION

I dedicate this thesis to my wife Tingjuan Song and mother Yuanxiang Zhou who gave me constant encouragement during this project. Without such valuable and loving support this thesis would not have been completed.

## **Abstract**

White clay soils are widely distributed in Heilongjiang Province, China and are one of the major agricultural soils in the province. However, only limited information on the soils is available.

The objective of this study was to determine the physical, chemical, micromorphological, and mineralogical characteristics of white clay soils as they relate to pedogenesis. Three representative pedons in the Three River Plain, Heilongjiang Province were selected for this study. The ratios of Ti/Zr and Zr/Sr in silt fractions were used to evaluate parent material uniformity. Trace elements including rare earth elements (REE) were analyzed by instrumental neutron activation analysis. Sr, Ti, and Zr were determined by x-ray fluorescence. Clay minerals were identified by x-ray diffraction analysis. Micromorphology of the soils was based on petrographic examination of thin sections.

Lithologic discontinuities were not detected based on the coefficients of variability associated with ratios of Zr/Sr and Ti/Zr within pedons. Argillation indices and well-oriented argillans in the Bt2 horizon indicated lessivage was a dominant process. Fe-Mn nodules were common in E horizons containing the highest levels of oxalate-extractable Fe and Mn and dithionite-extractable Fe and Mn. Bt2 horizons contained higher pyrophosphate-extractable Al and Fe than adjacent horizons. The soils of this study were acidic and had relatively uniform profile distribution of pH values.

Soil-vermiculite and vermiculite-smectite intergrades, which had not been recognized in the soils of this study before, were found to dominate the clay fractions. The clay mineral assemblage was qualitatively similar throughout profiles. Continuous addition of aerosolic dust onto surface horizons and lessivage caused quantitative variation in contents of clay minerals among horizons. Silt and sand are primarily composed of quartz and feldspar. Fe and Mn in nodules are present mainly in amorphous forms.

New information was obtained for the background levels and pedogenic behavior of 30 trace elements and 10 REE. Cl, Br, I, and Hg were enriched in Ah horizons due to inputs of aerosolic dust and their affinity for soil organic matter. Elements having an affinity for Mn and Fe oxyhydroxides (As, Co, and Mn) were concentrated in E horizons. Elements associated with clay minerals (Cr, Rb, V, and Zn) were elevated in the soil of the Bt2 due to lessivage, while elements present in resistant minerals (Sr, Ti, Hf, and Zr) were uniformly distributed within pedons.



Ce displayed positive anomalies in normalized curves of REE in E horizons. REE were enriched in clay separates. The gadolinium break, even-odd and tetrad effect were present in the soils of this study, which indicates REE can fractionate among themselves during weathering. Patterns of normalized REE curves may serve as a useful indicator of lithologic discontinuities.

Lessivage, periodic reduction-oxidation change, continuous addition of mica to the surface from aerosolic dust, and accumulation of organic matter were responsible for pedogenic characteristics of the soils of this study. The soils of this study were classified as Planosols in the FAO-UNESCO System and Boralfic Argialbolls in U.S.D.A. Soil Taxonomy.

## **ACKNOWLEDGEMENTS**

I gratefully acknowledge the contributions of the following people and organization:

- My supervisor, Dr. M.J. Dudas, for his endless patience, guidance, enthusiastic support and encouragement.
- Drs. S. Pawluk, P.H. Crown, and D.G.W. Smith (committee members) for their advice, interest, and criticism.
- Professor Z. Zhang for his suggestions and for his help with field sampling.
- M. Abley for his help with x-ray computer programs and thin sections, P. Yee for his technical assistance, and P. Geib for his help with dry-mounting.
- J. Warren and J. Arocena for discussions about this project.
- My fellow graduate students in the Department of Soil Science for their friendship and support.
- M. Calvert, M. Goh and S. Nakashima for assistance in day-to-day tasks and for providing good cheer.
- Canadian International Development Agency (CIDA) through the Black Dragon River Consortium and to NSERC for financial support.

## TABLE OF CONTENTS

CHAPTER I	INTRODUCTION.....	1
CHAPTER II	LITERATURE REVIEW .....	3
A.	GENERAL .....	3
B.	CLIMATE, RELIEF and HYDROLOGY, VEGETATION, AND PARENT MATERIAL .....	3
1.	INTRODUCTION.....	3
2.	CLIMATE .....	4
3.	RELIEF and HYDROLOGY .....	4
4.	VEGETATION.....	7
5.	PARENT MATERIAL.....	9
C.	GELOLOGY HISTORY .....	9
1.	GENERAL .....	9
2.	QUATERNARY GLACIATION .....	10
3.	LOESS .....	11
4.	ORIGIN OF HEAVY TEXTURED MATERIAL OF THE THREE RIVER PLAIN .....	12
D.	EVALUATION OF PARENT MATERIAL .....	13
E.	TRACE ELEMENTS.....	15
CHAPTER III	MATERIALS AND METHODS.....	18
A.	FEILD SAMPLE.....	18
B.	SOIL PHYSICAL and CHEMICAL ANALYSES .....	18
C.	MINERALOGICAL ANALYSIS.....	21
1.	FRACTIONATION .....	21
2.	CLAY MINERALOGY .....	22

3. SILT AND SAND MINERALOGY.....	23
D. MICROMORPHOLOGY.....	24
E. SCANNING ELECTRON MICROSCOPY.....	24
F. ELEMENTAL ANALYSIS.....	24
CHAPTER IV RESULTS AND DISCUSSION.....	32
A. PARENT MATERIAL UNIFORMITY.....	32
1. PARENT MATERIAL SIZE DISTRIBUTION OF CLAY FRACTIONS.....	33
2. ELEMENTS IN RESISTANT MINERALS.....	36
B. PHYSICAL, CHEMICAL, MICROMORPHOLOGICAL, AND MINERALOGICAL PROPERTIES AND THEIR PEDOGENIC IMPLICATIONS.....	42
1. PARTICLE SIZE DISTRIBUTION AND BULK DENSITY.....	42
2. CHEMICAL PROPERTIES.....	46
3. MICROMORPHOLOGY.....	58
4. MINERALOGY.....	68
i. CLAY MINERALOGY.....	68
ii. SILT MINERALOGY.....	79
iii. SAND MINERALOGY.....	79
C. TRACE ELEMENTS.....	82
D. RARE EARTH ELEMENTS.....	100
E. DISCUSSION OF THE GENESIS AND CLASSIFICATION.....	109
CHAPTER V SUMMARY AND CONCLUSIONS.....	111
REFERENCES.....	115
APPENDIX I.....	131
APPENDIX II.....	159

## LIST OF TABLES

TBALE 1.	Field description of pedon 1 .....	26
TABLE 2.	Field description of pedon 2 .....	28
TABLE 3.	Field description of pedon 3 .....	30
TABLE 4.	Silt size distribution and ratio.....	35
TABLE 5.	Distribution and ratio of medium and coarse fractions.....	38
TABLE 6.	Profile distribution of Sr, Ti, Zr in medium silt plus coarse silt and ratios of Zr/Sr and Ti/Zr.....	40
TABLE 7.	Particle size distribution, argillation index, and ratio of silt to clay .....	43
TABLE 8.	Bulk density of pedon 2.....	46
TABLE 9.	Cation exchange capacity and exchangeable cations for pedon 1.....	47
TABLE 10.	Cation exchange capacity and exchangeable cations for pedon 2.....	48
TABLE 11.	Cation exchange capacity and exchangeable cations for pedon 3.....	49
TABLE 12.	pH values and C, N, and P contents of the soils.....	50
TABLE 13.	Exchange acidity for horizon samples .....	52
TABLE 14.	Organic carbon content in different size fractions .....	54
TABLE 15.	Pyrophosphate, oxalate, and dithionite extractable Fe and Al .....	55
TABLE 16.	Total Fe and Al and selected ratios of Fe and Al .....	56
TABLE 17.	Micromorphological description of pedon 2 .....	60
TABLE 18.	Surface area and chemical analysis of clay separates .....	76
TABLE 19.	Distribution of clay mineral species within the clay sized fraction ...	76
TABLE 20.	Total content of trace elements in bulk soil samples of pedon 2 and literature values for terrestrial material.....	86
TABLE 21.	Total content of trace elements in clay separates of pedon 2 and literature values for terrestrial material.....	87
TABLE 22.	Profile distribution of rare earth elements in bulk soil samples of pedon 2 .....	101

TABLE 23.	Profile distribution of rare earth elements in clay separates of pedon 2.....	102
TABLE 24.	Correlation coefficients among Fe, Mn, Ce, and $\Sigma$ REE.....	108
TABLE 25.	Chemical characteristics of pedon 2 and criteria required for Podzols .....	110

## LIST OF FIGURES

FIGURE 1.	Physiographic map of China showing major mountain ranges and rivers. ....	5
FIGURE 2.	Physiographic map of Heilongjiang Province.....	6
FFIGURE 3.	Cross-section of landscape and parent material of white clay soils at Yiaoh Farm (modified form Zeng 1980).....	8
FIGURE 4.	Location map of sampling sites.....	19
FIGURE 5.	Cross-section of a typical pedon of a white clay soils.....	20
FIGURE 6.	Profile distribution of medium and coarse silts.....	34
FIGURE 7.	Profile distribution of the ratio of medium to coarse silt .....	37
FIGURE 8.	Profile distribution of ratios of Zr/Sr and Ti/Zr in silt fraction (5-50 $\mu\text{m}$ ).....	41
FIGURE 9.	Profile distribution of clay separates (< 2.0 $\mu\text{m}$ ).....	44
FIGURE 10.	Profile distribution of the ratio of silt to clay .....	44
FIGURE 11.	Profile distribution of pH and exchange acidity for pedon 2 .....	57
FIGURE 12.	Mull-granoidic fabric of the Ah horizon .....	59
FIGURE 13.	Photomicrograph of a Fe-Mn nodule from the E horizon. The matrix of the nodule is similar to the adjacent soil matrix .....	64
FIGURE 14.	Photomicrograph of a spherical Fe-Mn nodule from the E horizon. The matrix of the nodule is the same as the adjacent soil matrix ...	64
FIGURE 15.	Illuvial argillans, ferrans, and ferri-argillans in the Bt2 horizon. Argillan at upper middle, ferri-argillan at lower right, and ferran on the right .....	66
FIGURE 16.	Microlaminated clay infilling of channels in Bt2 horizon .....	66
FIGURE 17.	Ferran and ferri-argillan of the Bt2 horizon.....	67
FIGURE 18.	X-ray diffractogram of the clay separates from the Ah horizon of pedon 2 .....	69
FIGURE 19.	X-ray diffractogram of the clay separates from the E horizon of pedon 2.....	70
FIGURE 20.	X-ray diffractogram of the clay separates from the Bt1 horizon of pedon 2 .....	71

FIGURE 21.	X-ray diffractogram of the clay separates from the Bt2 horizon of pedon 2 .....	72
FIGURE 22.	X-ray diffractogram of the clay separates from the Bt3 horizon of pedon 2 .....	73
FIGURE 23.	X-ray diffractogram of the clay separates from the C1 horizon of pedon 2 .....	74
FIGURE 24.	X-ray diffractogram of the clay separates from the C2 horizon of pedon 2 .....	75
FIGURE 25.	X-ray diffractogram of Fe-Mn nodules from the E horizon of pedon 2.....	85
FIGURE 26.	Profile distribution of Br, I, and Hg in the bulk soil of Pedon 2.....	89
FIGURE 27.	Profile distribution of Br, Cl, and I in the clay separates of Pedon 2.....	89
FIGURE 28.	Total and extractable Fe with depth for pedon 3 .....	90
FIGURE 29.	Total and extractable Mn with depth for pedon 2 .....	90
FIGURE 30.	Profile distribution of As and Co in the bulk soil of Pedon 2 .....	91
FIGURE 31.	Profile distribution of Cr, Rb, Sc, V, and Zn in the bulk soil of Pedon 2.....	91
FIGURE 32.	Profile distribution of Hf, Sr, Ti, and Zr in the bulk soil of Pedon 2.....	92
FIGURE 33.	Chondrite-normalized curves of REE in bulk soil of Pedon 2. I, II, III, and IV portray tetrad effect.....	103
FIGURE 34.	Shale-normalized curves of REE in bulk soil of Pedon 2.....	103
FIGURE 35.	Chondrite-normalized curves of REE in the clay separates of Pedon 2. I, II, III, and IV portray tetrad effect.....	104
FIGURE 36.	Comparison of REE between the bulk soil and the clay separates in the E horizon for Pedon 2 .....	104
FIGURE 37.	Comparison of REE between the bulk soil and the clay separates in the Bt2 horizon for Pedon 2.....	105
FIGURE 38.	Comparison of REE between the bulk soil and the clay separates in the C2 horizon for Pedon 2 .....	105



## LIST OF PHOTOGRAPHIC PLATES

PLATE	1.	Scanning electron micrographs of quartz grains. A, smooth surfaces of a quartz grain from the E horizon. B, rounded edges of a quartz grain from the C horizon .....	80
PLATE	2.	Scanning electron micrographs of feldspar. A, highly weathered feldspar grain from the E horizon. B, close-up of A. C, relatively less weathered feldspar grain from the C horizon. D, close-up of C. ....	81
PLATE	3.	Scanning electron micrographs of Fe-Mn nodules of the E horizon . A, a rounded nodule, B, a hollow nodule, C, a compound nodule, D, close-up of C.....	83
PLATE	4.	Scanning electron micrographs of an Fe-Mn nodule of the E horizon. A, the surface of the nodule. B and C, close-up of A showing quartz and feldspar grains embedded in the nodule .....	84

## LIST OF APPENDIX TABLES

TABLE 1.	Profile distribution of total trace elements in the bulk soil samples of pedon 1 (mg/kg).....	149
TABLE 2.	Profile distribution of total trace elements in the bulk soil samples of pedon 3 (mg/kg).....	150
TABLE 3.	Profile distribution of total trace elements in clay separates of pedon 1 (mg/kg) .....	151
TABLE 4.	Profile distribution of total trace elements in clay separates of pedon 3 (mg/kg) .....	152
TABLE 5.	Profile distribution of rare earth elements (REE) in bulk soil samples of pedon 1 (mg/kg) .....	153
TABLE 6.	Profile distribution of rare earth elements (REE) in bulk soil samples of pedon 3 (mg/kg) .....	153
TABLE 7.	Profile distribution of rare earth elements (REE) in clay separates of pedon 1 (mg/kg) .....	154
TABLE 8.	Profile distribution of rare earth elements (REE) in clay separates of pedon 3 (mg/kg) .....	154

## LIST OF APPENDIX FIGURES

FIGURE 1.	X-ray diffractogram of the clay separates from the Ah horizon of pedon 1 .....	131
FIGURE 2.	X-ray diffractogram of the clay separates from the E horizon of pedon 1 .....	132
FIGURE 3.	X-ray diffractogram of the clay separates from the Bt1 horizon of pedon 1.....	133
FIGURE 4.	X-ray diffractogram of the clay separates from the Bt2 horizon of pedon 1.....	134
FIGURE 5.	X-ray diffractogram of the clay separates from the Bt3 horizon of pedon 1.....	135
FIGURE 6.	X-ray diffractogram of the clay separates from the C1 horizon of pedon 1 .....	136
FIGURE 7.	X-ray diffractogram of the clay separates from the C2 horizon of pedon 1 .....	137
FIGURE 8.	X-ray diffractogram of the clay separates from the Ah horizon of pedon 3 .....	138
FIGURE 9.	X-ray diffractogram of the clay separates from the E horizon of pedon 3 .....	139
FIGURE 10.	X-ray diffractogram of the clay separates from the Bt1 horizon of pedon 3.....	140
FIGURE 11.	X-ray diffractogram of the clay separates from the Bt2 horizon of pedon 3.....	141
FIGURE 12.	X-ray diffractogram of the clay separates from the Bt3 horizon of pedon 3.....	142
FIGURE 13.	X-ray diffractogram of the clay separates from the C1 horizon of pedon 3 .....	143
FIGURE 14.	X-ray diffractogram of the clay separates from the C2 horizon of pedon 3 .....	144
FIGURE 15.	X-ray diffractogram of the total silt fraction of pedon 1.....	145
FIGURE 16.	X-ray diffractogram of the total silt fraction of pedon 2.....	146
FIGURE 17.	X-ray diffractogram of the total silt fraction of pedon 3.....	147
FIGURE 18.	X-ray diffractogram of the Fe-Mn nodules from the E horizons of three pedons .....	148

## CHAPTER I

### INTRODUCTION

White clay soils are the prominent soils in Northeast China. In Heilongjiang Province, there are about 3.2 million hectares of the white clay soils most occurring on the Three River Plain, which lies in the northeast of Heilongjiang Province. White clay soils are one of the major agricultural soils in China. These soils are fertile and are associated with nearly flat lying terrain which facilitates farm mechanization. However, the white clay soils have a thick, impermeable and compact B horizon and the overlying horizon appears leached of clay. Root penetration into the B horizon is limited and affects nutrient and moisture uptake. Due to a perched water table, stagnant water accumulates on the surface in wet seasons, and the surface becomes very hard upon drying. The physical properties adversely affect crop yield. Documentation of white clay soils in China has largely been confined to physical properties and the knowledge of how to improve and cultivate the soils.

Only limited information exists on the nature of pedogenesis and the chemistry of white clay soils. Such information is needed in order to develop appropriate management schemes to increase their productive capacity and quality.

In some studies of white clay soils, different investigators examining the same soils report dissimilar pedogenic theories which resulted in many names for white clay soils such as podzol and solod in the literature. Until the 1980's, in order to avoid confusion, the accepted name was the white clay soil, since there is an albic horizon overlying heavy textured solums (Gao 1988 and Zhang 1987).

In describing the genesis of this soil, Zeng (1963) emphasized the role of the seasonal perched water table and the stagnant surface water and its effect on lateral movement of clay. Xu (1979) proposed that the temporary stagnant water on the surface could cause the reduction of iron and manganese which acted to cement soils particles. The dispersed particles were then susceptible to eluviation. However, Zhang and Zhang (1983) found the Eh of the A and B horizons of white clay soils were all about +500 mv for three consecutive years (80-82). He concluded Fe and Mn were not likely to be reduced.

There are controversies about the formation of white clay soils partly because of a lack of data on the mineralogical, morphological, and chemical properties. Further studies

are needed to characterize the inorganic fraction and to determine the genesis of these soils. Decisions on the use and management of the white clay soils are particularly dependent on such information. Three representative undisturbed pedons of the typical white clay soils were chosen in Mishan County and Hulin County on the Three River Plain, Heilongjiang Province, China. Soils collected for this study were examined with the following objectives in mind:

1. To establish parent material uniformity of three pedons of the white clay soils.
2. To conduct characterization studies to determine the major chemical, mineralogical, physical, and micromorphological properties.
3. To determine trace element chemistry including rare earth elements (REE)
4. To propose genetic processes and classification of the white clay soils.

## **CHAPTER II**

### **LITERATURE REVIEW**

#### **A. General**

In China, white clay soils are defined as soils having light colored eluvial horizons with an overlying humic horizon of 10 to 20 cm, and an underlying illuvial B horizon in which silicate clay has accumulated (Zhang 1987). The process responsible for the formation of white clay soils was named the Baijiang<sup>1</sup> process which was explained by Zhu (1984) as follows:

Downward and lateral movement of reduced iron and manganese along with water and clay leads to the bleached horizons and heavy texture horizons. He also suggested that organic matter plays an important role in the process.

White clay soils are classified as one group of semi-hydromorphic soils in the Chinese Classification System (Zhu 1984). White clay soils are further divided into subgroups called typical, meadow, and gleyed white clay soils. These soils have not been classified with the U.S.D.A. 7th Approximation or other international classification schemes.

The majority of the typical and meadow white clay soils has been cultivated. Wheat and corn are the dominant grain crops with soybean and sugarbeet the major economic crops, while other areas are used for forage production and grazing of cattle and sheep on pastures. Most of the gleyed white clay soils remain uncultivated, since it is difficult to drain water in such low lying land, especially in some area of the Three River Plain, Heilongjiang.

#### **B. Climate, Relief and Hydrology, Vegetation, and Parent Material**

##### **1. Introduction**

The genesis of soils has been considered to be a function of the factors of soil formation. Boul et al. (1973) define a factor of soil formation as "an agent, force, condition or relationship, or combination of these, which influences, has influenced, or may

---

<sup>1</sup> Baijiang means white clay.

influence a parent material of a soil, with the potential of changing it". Factors of soil formation are still of paramount importance in studies in pedogenesis, although static (Howitt and Pawluk 1985a; Ugoloni 1977) and dynamic (Howitt and Pawluk 1985b) approaches have been used recently. The factors of soil formation are considered to be climate, vegetation, parent material, relief, and time. Other forces have been considered as factors of soil formation; for example, water, gravity and man as proposed by Rode (1961) and Kabata-Pendias and Peddias (1984). The five generally accepted factors could be divided into active and passive factors. The active factors are climate and vegetation, while parent material and relief are passive factors. Time is required for a steady state to be obtained (Lavkulich 1969).

## **2. Climate**

The climate of Three River Plain lies within the sub-humid, cool temperate, continental, monsoon climatic zone characterized by long, cold winters and short, warm summers. The northwest wind is dominant. The mean annual temperature within the area varies from 2.0 to 3.8° C, and the mean temperatures of Winter (Nov.-Mar.), Spring (Apr.-May), Summer (June -July), and Fall (Sept.- Oct.) are -11.8° C, 8.9° C, 19.7° C and 9.6° C, respectively. The warmest month is July with an average maximum of over 21.3° C. The coldest month is January with an average minimum of minus 18.2° C. The frozen depth of soils ranges from 1.5 to 2.0 m. The frost free period ranges from 120 to 141 days and the accumulated temperature >10° C varies from 2000 to 2500° C. The mean annual precipitation is 550 mm with 70 % occurring in June to September. The mean precipitation during Winter, Spring, Summer, and Fall is 43 mm, 78 mm, 318 mm, and 110 mm, respectively. In Spring, wind is strong and evaporation is greater than precipitation so that droughts are likely to occur.

## **3. Relief and Hydrology**

The Three River Plain is located at the base of the Xiaoxingan Mountain Range and the Wanda Mountain, northeast of Heilongjiang Province, China (Fig. 1 and Fig. 2). The altitude of the Three River Plain varies from 60 to 120 m above sea level. White clay soils are found in the very gentle slopes (1 to 5 %) with heavy textured material. If soil parent materials are light textured in this area, drainage is relatively good and oxygenated condition dominates. Dark brown and Meadow forest soils have developed on these lighter textured parent materials. Dark brown forest soils have also formed on steeper slopes (Zeng 1963). Gleysols and bog soils have developed in depressional areas where reduced

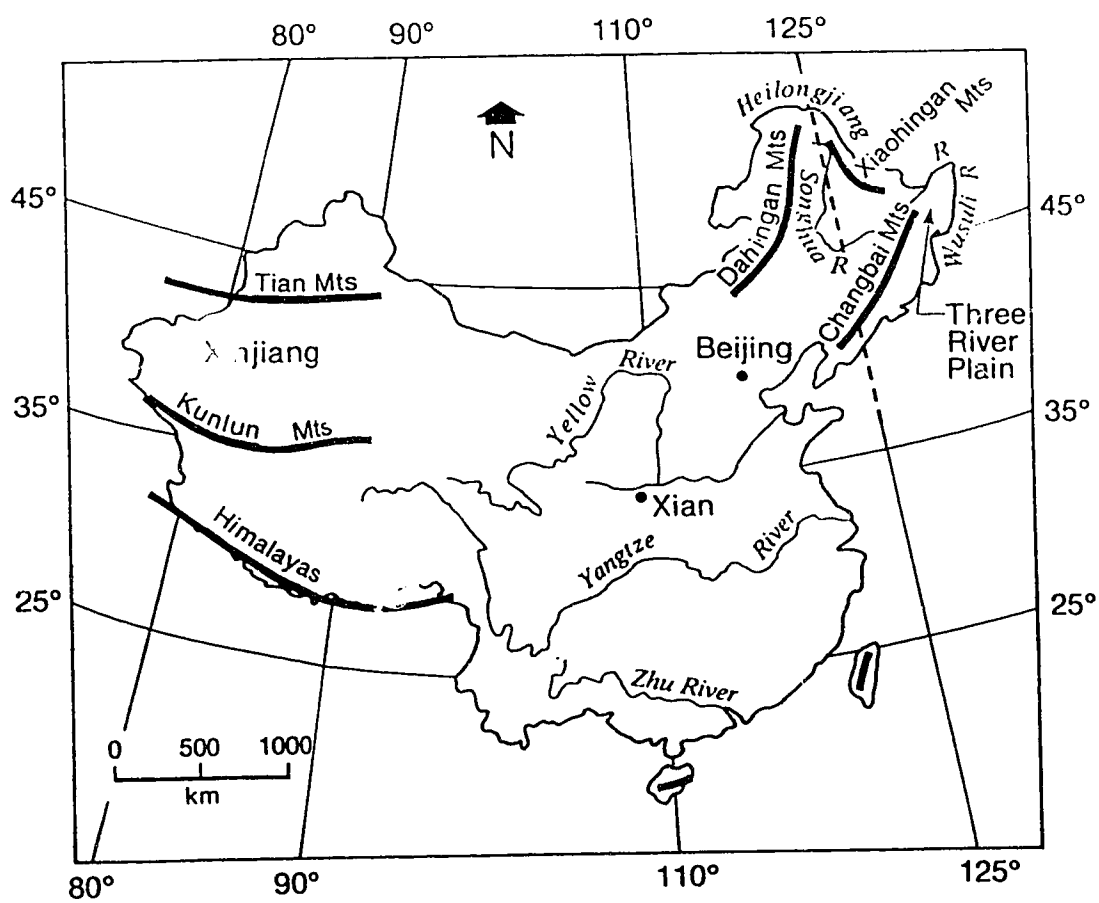


Figure 1. Physiographic map of China showing major mountain ranges and rivers.



**Figure 2. Physiographic map of Heilongjiang Province.**

conditions dominate. In landscapes with slightly rolling, gentle slopes and heavy textured parent material, conditions of alternate wetness and dryness are associated with white clay soils (Fig. 3).

Heilongjiang, Songhua, and Wusuli rivers and their tributaries constitute the major drainage system of the Three River Plain. The Plain is named after the above mentioned rivers. The Muling River plays an important role in the drainage near the sampling sites of this study. The permanent water table of white clay soils is 8 to 10 m deep (Zeng 1980). Zeng (1980) proposed that the heavy parent material has low infiltration rate. Hence, the pedogenesis of this soil is not directly affected by ground water. The internal drainage of this soil is poor and a perched water table exists during wet seasons. However, the external drainage is relatively good because of slope. Thus, the perched table disappears and the soil surface becomes dry during dry seasons.

Soil moisture fluctuates with seasons (Xia and Shang 1981) and soil moisture regimes during a year can be divided into five periods. They are: 1. thawing period (the end of March to the end of April), 2. drying period (from beginning of May to the middle of July), 3. rainy period (the middle of July to the middle of September), 4. relatively stable period (the middle of September to the beginning of November), and 5. frozen period (from the beginning of November to the end of March). The development of irrigation and drainage systems of the white clay soils for high crop yield, especially for spring wheat, is very much dependent on understanding these soil moisture regimes.

#### 4. Vegetation

Vegetation is an active factor of soil formation. Vegetation plays a very important role in the genesis of soils. The influence of vegetation is discussed by Pettapiece (1969) in a study of the forest-grassland transition. The white clay soils lie within the mixed Conifer-hardwood forest region (Liu 1988; Wu 1980). The study sites have mixed vegetation of forest and grass within the mixed Conifer-hardwood forest region. The dominant upper canopy consists of Oak (*Quercus mongolica* Fisch), Poplar (*Populus davidiana* Dode), Birch (*Betula dahurica* Pallas), and *Tilia amurensis* Kom. Understory vegetative cover consists of grasses and shrub. Common grasses are *Clematis mandshurica*, *Convallaria keiskei*, *Adenophora nikoensis* Lamb, *Carex* sp, and *Palonia obovata* Maxim. Main shrubs are comprised of *Corylus heterophylla* Fisch and *Lespedeza bicolor* Turcz.

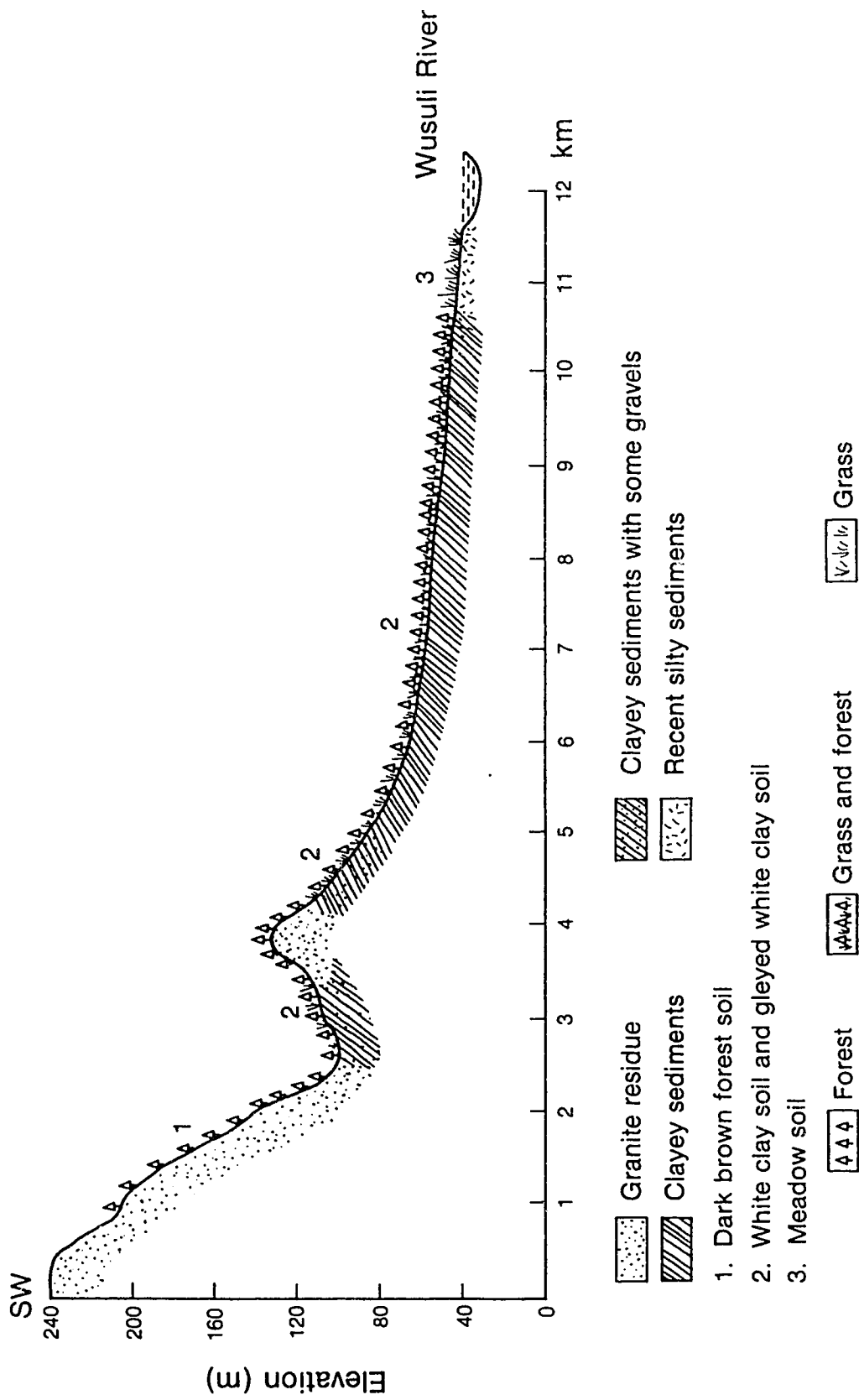


Figure 3. Cross-section of landscape and parent material for white clay soils at Yiaoh State Farm (modified from Zeng 1980).

In Summer, areas with white clay soils are warm and moist and, therefore, trees and grasses grow vigorously. The annual addition of organic matter is high. Nan and Huang (1965) reported accumulations of 304.2 g dry matter per square meter of soil for the above ground portions of natural vegetation at Yiaohé, Hulin County, Heilongjiang. Roots are largely distributed in the Ah horizon and are horizontally oriented since the lower solums are very hard for roots to penetrate. Zeng (1980) showed that there was 1346 g of roots per square meter in Ah horizons under Oak-mixed grass cover, which was 80 % of total weight of roots.

## 5. Parent Material

The parent material of white clay soils is transported material. The material is mainly Quaternary alluvial sediments and sometimes, lacustrine deposits (Zeng 1980; Xia and Shang 1981). The depth of the sediment varies from 3 to 15 meters. The underlying material is sands and gravels of variable depth (Xie 1982). White clay soils are primarily developed on the parent material with no or little carbonates and excess salts (Zhang<sup>2</sup> 1988, pers. commun.). Occasionally, white clay soils are developed on the basalt terrace in Jilin Province but these soils are not directly affected by basalts since soils are formed on the layer of lacustrine deposits covering the basalts (Soil Survey of Jilin Province 1960).

## C. Geological History

### 1. General

China is a country with a great expanse of hills, mountains, and plateaus. It is marked by great changes in relief: highest in the west, becoming lower and lower to the east, like a giant inclined staircase. Over this staircase great rivers, such as the Yangze River, the Yellow River, and Heilongjiang River flowed eastward and emptied into the Pacific (Fig. 1). In Heilongjiang Province, Dahingan and Xiaohingan Mountains occur in the northwest, Wanda mountains in the southeast, and the Three River Plain in the northeast sharing the border with USSR (Fig. 2).

Tectonic activity in Northeast China was very active during the Lower Paleozoic. In fold zones in this region belong to the Paleozoic geosynclinal area, i.e., the Korean Fold Zones. The Wusuli Fold Zone in the northeast of Heilongjiang Province

---

<sup>2</sup> Professor Zhang, Dept. of Agronomy, Heilongjiang Agricultural Land Reclamation University (HALRU), Mishan County, Heilongjiang Province, China.

was formed in the Mesozoic geosynclinal area on the base of Hercynian Fold Zones. The Nadanhada Mesozoic Geosynclinal Synclinorium and Tongjiang Inland downcast fault occur in Wusuli Fold Zone. The latter began to form in the Jurassic Period and continued into the Tertiary Period. This downcast fault is filled with loose Cenozoic sediments, which built the foundation of the present Three River Plain.

After the Mesozoic Yenshan Movement which formed the basic geomorphic sketch of Northeast China, Tertiary Neotectonic movement also had an effect on the geomorphic development. Existing mountains and hills became peneplains through erosion during the Oligocene Epoch. The peneplains through the Cenozoic uplift become rejuvenated mountains and hills. The Dahingan Mountains, Xiaohingan Mountains, and Wanda Mountains were formed at this time. These mountains consist of mainly igneous rocks (Cheng 1986).

## 2. Quaternary Glaciation

The Quaternary, which is the most recent chronostratigraphic unit, was studied to a limited extent in China (Liu 1988; Derbyshire 1987; Shi et al. 1986; Su 1984; Lee 1947). The world-wide Quaternary glacial and interglacial climates also exerted their influence in China. Glacial geology in China was first studied by Lee (1922). He reported the Pleistocene glaciation occurred at several mountains such as Hengshan (2017 m elevation; latitude 29°30' N) as evidenced by the existence of edge-rounded and scratched granitic boulders in a matrix of sandstone and conglomerate debris in the Datong basin, northern Shanxi Province. Later, he described similar deposits in the Lushan (1470 m elevation; latitude 19°30' N) (Lee 1933) extending down to 20 m above sea level on the floodplain of the Yangtze River. The work of Barbour (1934) was strongly critical of the glacial explanation. Lee (1947) still went on to propose a Pleistocene glacial stratigraphy consisting of three stages based on differential weathering of the drifts. He named them, using the model of Penck and Brückner (1909), the Poyang (Günz), Da Gou (Mindel) and Lushan (Riss) glacial stages. This became the standard stratigraphic framework for China. Lee extended his observations throughout the mountain massifs of the south and east. He used criteria of stony clay in which subangular cobbles and boulders with one or more polished faces to delineate glacial units. Lee's stratigraphic model has continued to dominate Pleistocene geology in China. Acceptance of the idea that multiple glaciation had affected most of the mountain massifs of eastern China during the Pleistocene was widespread by the time of the publication of the map by Sun and Yang (1961). The mountain glaciers were observed at Dahingan Mountains and Wanda Mountains (Sun and

Yang 1961). These mountain glaciers are different from the continental glaciations in North America in that the continental Pleistocene glaciers travelled a long distance and covered a large area.

Recent studies (Zhang and Mou 1982; Shi and Deng 1983; Shi *et al.* 1986; Derbyshire 1987; Liu 1988) have thrown doubt on Lee's stratigraphic model by showing that the abundant stony clay deposits in Lushan were produced by the combination of humid subtropical monsoonal weathering and a well-documented history of uplift. Then, these stony clays were reworked by debris flow and by piedmont fan sedimentation rather than by glaciation. Derbyshire (1982, 1983) observed that there are no glacial deposits or landforms of glacial erosion in Lushan. Similar forms and sediments formerly attributed to glaciation in all mountain regions in east China must now be regarded as doubtful (Shi *et al.* 1986). Shi *et al.* (1986) reported that sediments of Baitushan (Heilongjiang Province in the NE) are fluvial and proluvial in origin rather than glacial. The hypothesis of widespread glaciation in East China is opposed by Yang (1986). Research is clearly needed to resolve the questions of glaciation. In the Three River Plain, Heilongjiang Province, the lack of evidence of glaciation, such as the presence of cobbles and boulders, probably suggests that there was no Pleistocene glaciation.

### 3. Loess

Loess is typically a well sorted, non stratified, buff colored, non indurated material (Lewis *et al.* 1975). The word loess comes from the German words loss or losch meaning loose (Gary *et al.* 1972). Classically, loess consists of 50 - 80% silt sized particles and contains less than 10% clay sized particles (Brierley 1988). Loess is defined as "windblown dust of Pleistocene age, carried from desert surfaces, alluvial valleys and outwash plains lying south of the limits of the ice sheets, or from unconsolidated or glaciofluvial deposits uncovered by successive glacial recessions but prior to invasion by a vegetation mat" in the Glossary of Geology (Gary *et al.* 1972). Kukla (1987) described loess as a silt, transported and deposited by wind, loosely cemented by a fine syngenetic carbonate incrustation, formed in semi-arid continental climates. In simple terms, loess may be defined as "wind blown silt deposits" (Brierley 1988). However, no single definition has been universally accepted (Pye 1983).

Loess deposits of Pleistocene age cover large areas in the middle latitudes of the Northern Hemisphere, stretching in a discontinuous belt from southern Britain across central Europe to eastern Asia, and from Alaska and eastern Washington State into the

Mississippi and Ohio valleys (Kukla 1987). Loess also occurs in New Zealand and South America (Kukla 1987).

Loess is widespread in China with the most extensive deposits comprising the Loess Plateau of central China. The thickness of loess varies throughout areas. Loess of appreciable thickness covers an area of at least 440,000 km<sup>2</sup> in China between 33° and 47° N latitude and 75° and 125° E longitude (Liu 1986). There is no distinct loess deposits in Three River Plain and adjacent areas in Heilongjiang Province, Northeast China. The origin of the loess in China is still contentious. The mineralogy of loess is dominated by quartz, feldspar and muscovite with the main clay minerals being mica, kaolinite and montmorillonite. The most common soluble salt is CaCO<sub>3</sub>, making up 10 - 20 % by volume (Liu 1986).

#### **4. Origin of heavy textured materials of the Three River Plain**

In the 1950's, people began to settle in the Three River Plain, reclaiming and cultivating the land. Since then, soils in the Plain have been studied with focus on how to reclaim the soils effectively for agricultural production. Recent studies on the genesis of the soils in the Three River Plain, especially of white clay soils have been conducted (Xu 1979; Zhang 1987; Gao *et al.* 1988) which resulted in disagreement on the origin of the heavy textured parent material. Clayey loess was claimed to be the parent material of white clay soils by Zhang (Pers. commun. 1987). The origin of lacustrine deposits was favoured by Zeng (1963) and Gao *et al.* (1988). Others believe that the heavy textured material is derived from glaciation based on the theory of Sun and Yang (1961).

Liu (1988) reported that the temperate forest regions of China had undergone drastic environmental changes during the Pleistocene, corresponding to glacial/interglacial climatic cycles. However, the temperate regions of China had not been affected by continental Pleistocene glaciations like their North American or European counterparts. Sporo-pollen analysis of samples from the Three River Plain (Liu 1988; Ye *et al.* 1983; Xie 1982) show formation of the clayey sediments is closely related to the climatic and environmental changes during the Quaternary period. At the Late Pleistocene, this region experienced the cold period. The vegetation was very sparse, and rocks had undergone strong mechanical and physical weathering (Xie 1982). Large amounts of weathered sands and gravels of granitic rocks on the Xinghingan and Wanda Mountains had been carried away and deposited at the Three River Plain by running water. Then, thick layers of the sands and gravels formed. Between the end of the Late Pleistocene and beginning of the

Early Holocene, precipitation and temperature increased, which promoted a dense vegetation cover in this region. Strong chemical weathering produced large quantities of clay and silt. Clay and silt particles were carried away by water from the Mountains and deposited on the surface of the Three River Plain. Therefore, the origin of the heavy textured parent material in the Three River Plain was concluded to be alluvial with some lacustrine deposits (Xie 1982). The sudden change in pollen composition indicated the climate changed from cold to warm in Northeast China at the beginning of the Holocene (Liu 1988).

#### D. Evaluation of Uniformity of Parent Material of Soils

Soils are derived from their parent materials, and the establishment of parent material uniformity in pedological studies is an indispensable step in the evaluation of pedogenic changes within the soil solum. Evans (1978) stated that "the identification of lithologic discontinuities in parent materials is an essential prerequisite in differentiating soil properties that are pedological in origin from those that are geological". When the parent material of a soil is assessed to be relatively uniform, then the changes in the upper solum can be attributed to pedogenic processes.

To establish parent material uniformity, certain immobile and resistant soil constituents must be quantitatively determined throughout the pedon. Several resistant components or standards have been used: Quartz and Ti (Sudom and St. Arnaud 1971; Smeck and Wilding 1980), Zr (Khan 1959; Smeck and Runge 1971), and acid-resistant residue (Akhtyrtsev 1968). Despite the fact that no internal standard is completely inert, seldom have a number of internal standards been assessed (Abder-Ruhman 1980). There are a number of criteria commonly used for establishing uniformity (Barshad 1964). The most useful ones in Barshad's list were given as follows (Evans 1978):

1. particle-size distribution of resistant minerals. e.g., percentage of total rutile in each size fraction.
2. particle-size distribution ratio of non-clay fraction.  
e.g.,  $\frac{\text{medium silt}}{\text{coarse silt}}$ ,  $\frac{\text{fine sand}}{\text{silt}}$  and  $\frac{\text{coarse sand}}{\text{fine sand}}$ .
3. ratio of the contents of two resistant minerals in any one silt fraction.  
e.g., quartz/zircon in silt fraction.



Other somewhat more subjective criteria such as the presence of unexpected minerals or a non-pedological distribution of soil constituents may also be used (Evans 1978). Runge *et al.* (1974) suggested phosphorus could be used for identifying paleosols.

Selection of certain criteria for the evaluation of parent materials is to a large extent determined by the nature of the parent materials themselves. Particle-size distribution of the non-clay fraction has proved to be a very useful parameter for identifying lithologic discontinuities in some soils (Raad and Protz 1971; Wang and Arnold 1973; Abder-Ruhman 1980). However, the usefulness of particle-size distribution of the non-clay fraction is questionable, if physical breakdown of sand and silt sized particles occurs during pedogenesis (St. Arnaud and Whiteside 1963; Evans and Adams 1975). The particle size distribution of quartz and contents of  $ZrO_2$  and  $TiO_2$  did not distinguish between two visibly different tills in Canada (Sudom and St. Arnaud 1971). This limitation may be caused by the presence of inclusions which render quartz and zircon susceptible to physical breakdown (Raeside 1959).

The most common method of assessing the uniformity of soil parent materials is to compare the ratio of the amounts of two resistant minerals in one or more size fractions (Roonwall and Bhumbra 1969; Evans and Adams 1975; Evans 1978; Abder-Ruhman 1980). If a chemical element is exclusively in the resistant mineral, such as may be the case of Zr in zircon, Ti in rutile or anatase, or B in tourmaline, the resistant mineral may be assessed by chemical rather than mineral analysis (Khangarot *et al.* 1971; Ritchie *et al.* 1974; Evans and Adams 1975).

After choosing a suitable ratio, the degree of variation in ratios among soil solum or horizons indicative of the lithologic discontinuities must be established. Drees and Wilding (1973) in a study of elemental variation within a sampling unit in tills, loess and outwash suggested that if a lithological discontinuity is present, there should be a significant difference between stratigraphic units which exceeds the random variations (e.g. lateral variations within each horizon) by the value of  $t$  for a given probability level. Their study suggests that a relative standard deviation in the Ti:Zr ratio between two horizons must exceed 28% to show a significant lithological break in profiles developed on glacial till. A coefficient of variation in excess of 100% in the Ti:Zr ratio for two horizons was required to confidently detect lithologic discontinuities in soils developed on sandstones, siltstones and cherty limestone (Chapman and Horn 1968). Deviations of 4.8 to 21% from the mean for the Ti:Zr ratios in silt and 8.1 to 17.6% for quartz:illite ratios in silt fractions were not

considered indicative of discontinuities in soils developed from scree deposits of Lower Paleozoic mudstones (Evans and Adams 1975). Abder-Ruhman (1980) used cumulative-frequency curves for particle size distribution of the non-clay fraction to determine the uniformity of parent materials of soils developed on glacial deposits. From the wide differences in the level of variation accepted for a uniform material it would seem that the nature of the deposit, the nature of the parameters used (e.g., Ti:Zr ratio or quartz:feldspar ratio, etc.) and the accuracy of the determination for that parameter are important factors in determining the acceptable level of variation for a uniform material. Unfortunately, there is still no general agreement as to what degree of variation defines a discontinuity.

### E. Trace Elements

The trace element status of soils plays an ever increasing role with the increasing demand of agricultural production and the increasing concern about environmental quality. Trace elements play a major role in soil fertility. Excessive levels of these elements can cause nutrient deficiencies or toxicities in crop plants and, ultimately, in the animals which feed upon them. Agronomists, geochemists, pedologists, and biochemists have conducted a variety of studies on the behavior of trace elements in the ecosphere for the last three or so decades (Yoe and Koch 1957; Goldschmidt 1954; Mitchell 1964; Aubert 1977; Adriano 1986; Rai *et al.* 1986, 1988; Hall 1988). The significance of trace elements in the environment was underlined during the Conference on Human Environment organized by the Royal Swedish Academy of Science (1982). Adriano (1986) suggested a list of current universal interests in trace element studies. These are: 1. to increase food, fiber, and energy production; 2. to determine trace element requirements and tolerance by organisms, including relationships to animal and human health and disease; 3. to evaluate the potential biomagnification and biotoxicity of trace elements; 4. to understand trace element cycling in nature, including their biogeochemistry; 5. to assess trace element enrichment in the environment by recycling wastes; 6. to discover additional ore deposits; and 7. to comply with stringent regulations on releases of effluents (both aqueous and gaseous) to the environment.

The term "trace element" is rather loosely used in the literature and has differing meanings in various scientific disciplines. Often it designates a group of elements that occur in natural systems in minute concentration. Trace elements have been defined as those elements whose individual contributions do not exceeded 1000 ppm in soils (Mitchell 1964). Some geochemists view "trace elements" as those other than the eight abundant rock-forming elements found in the lithosphere (O, Si, Al, Fe, Ca, Na, K, and Mg).

Sometimes, trace elements are considered to be those elements used by organisms in small quantities but believed to be essential to their nutrition. However, the definition broadly encompasses elements including those with no known physiological functions. Biochemists treat trace elements as those that are ordinarily present in plant or animal tissue in concentrations comprising less than 0.01% of the organisms. In food science, "trace element" may be defined as an element which is of common occurrence but whose concentration rarely exceeds 20 parts per million (ppm) in the foodstuffs as consumed, but, as Adriano (1986) pointed out, some of the "nutritive" trace elements (e.g., Mn and Zn) may often exceed this concentration (20 ppm). Adriano (1986) referred to trace elements as those that occur in natural or perturbed systems in small amounts and, when present in sufficient concentrations, are toxic to living organisms. Therefore, "trace element" has different connotations in different disciplines.

The term trace element is used interchangeably with trace metal, micronutrients, heavy metal, minor element, and trace inorganic. Heavy metals usually refer to elements having densities greater than 5.0 g/cm<sup>3</sup>. Micronutrients such as Zn, Mn, and B are often restricted to those elements required by higher plants. The selection of terms for trace elements is determined by practical purposes.

The content of trace elements in the soil is largely dependent on the content in rocks from which the soil parent material was derived and on the processes of weathering to which the soil-forming materials have been subjected. Pedogenesis affects the distribution of trace elements in soil profiles. During early stages of weathering and pedogenesis, the trace element composition of the soil will closely reflect composition and distribution in the parent material. With time, however, the trace element characteristics of soil reflects pedogenic processes. Podzolization, for instance, leads to the accumulation of some trace elements (Co, Cu, Mn, Ni, etc.) in the illuvial horizons (Kabata-Pendias and Pendias 1984). McKeague and Wolynetz (1980) reported that levels of most minor elements determined in their study were depleted in Ae horizons compared to the associated B and C horizons of Canadian soils. Some trace elements such as Cr and Zn were reported to be enriched in clay separates (Dudas and Pawluk 1980). Jenne (1977) stressed that oxides and oxyhydroxides of Fe and Mn, organic matter, sulfides, and carbonates are important sinks for trace elements. Of less importance are the clay size aluminosilicate minerals. The accumulation and redistribution of arsenic in acid sulphate soils are closely related to the translocation and reaction of iron released by the oxidation of pyrite (Dudas and Pawluk 1980; Dudas 1987). The accumulation of organic matter can affect the behavior of some

trace elements. The degree of the redistribution of trace elements in parent material depends on the nature and intensity of imposed physical, chemical, and biological reactions involved in soil formation, and on the length of time they have been in operation.

There is limited information about the trace element chemistry of the white clay soils in the Three River Plain. Some micronutrients (e.g., Zn, Cu) have been determined only for assessing deficiency and toxicity to crop growth. The determinations were mainly restricted to plow layers (Ap). As a result, pedogenic impacts on the distribution of trace elements remain unknown.

## CHAPTER III

### MATERIALS AND METHODS

This chapter describes the methods and procedures used for the field sampling of pedons. Analytical methods and procedures used for the laboratory study of soils are also described in this chapter.

#### A. Field Sampling

Representative pedons were chosen after examining several sites in the Three River Plain, Heilongjiang Province under the guidance of Professor Zhang<sup>3</sup>. The objectives in sampling were to select undisturbed, typical white clay soil profiles on landscape positions with minimal relief and with native vegetation. Three large pits (1.2 m x 2.0 m x 2.0 m) were excavated to facilitate study and sampling of the profiles. One site was located in State Farm 857 and the other two sites in State Farm 854 (Fig. 4). Bulk soil samples were taken from each horizon recognized in the field to a depth of 1.8 meters. The bulk soil samples were air-dried at room temperature, packed in paper cartons and shipped to Canada. The air-dried samples were crushed, passed through a 2 mm sieve, mixed, and stored for analysis. Detailed site information and morphological description of the three pedons sampled are displayed in Tables 1, 2, and 3. These tables can be found at the end of this chapter. A typical pedon is shown in Figure 5.

Seven soil samples for micromorphological analysis were taken from various horizons observed in pedon 2 using boxes 10 cm x 8 cm x 12 cm in size. The samples were air-dried at room temperature, carefully packed with wrapping paper, and personally carried back to Canada to avoid disturbance.

#### B. Soil Physical and Chemical Analyses

Procedures followed for soil analysis were generally those outlined by the Canada Soil Survey Committee (1981).

---

<sup>3</sup> Professor Zhang, Dept. of Agronomy, HALRU, Mishan County, Heilongjiang Province, China.

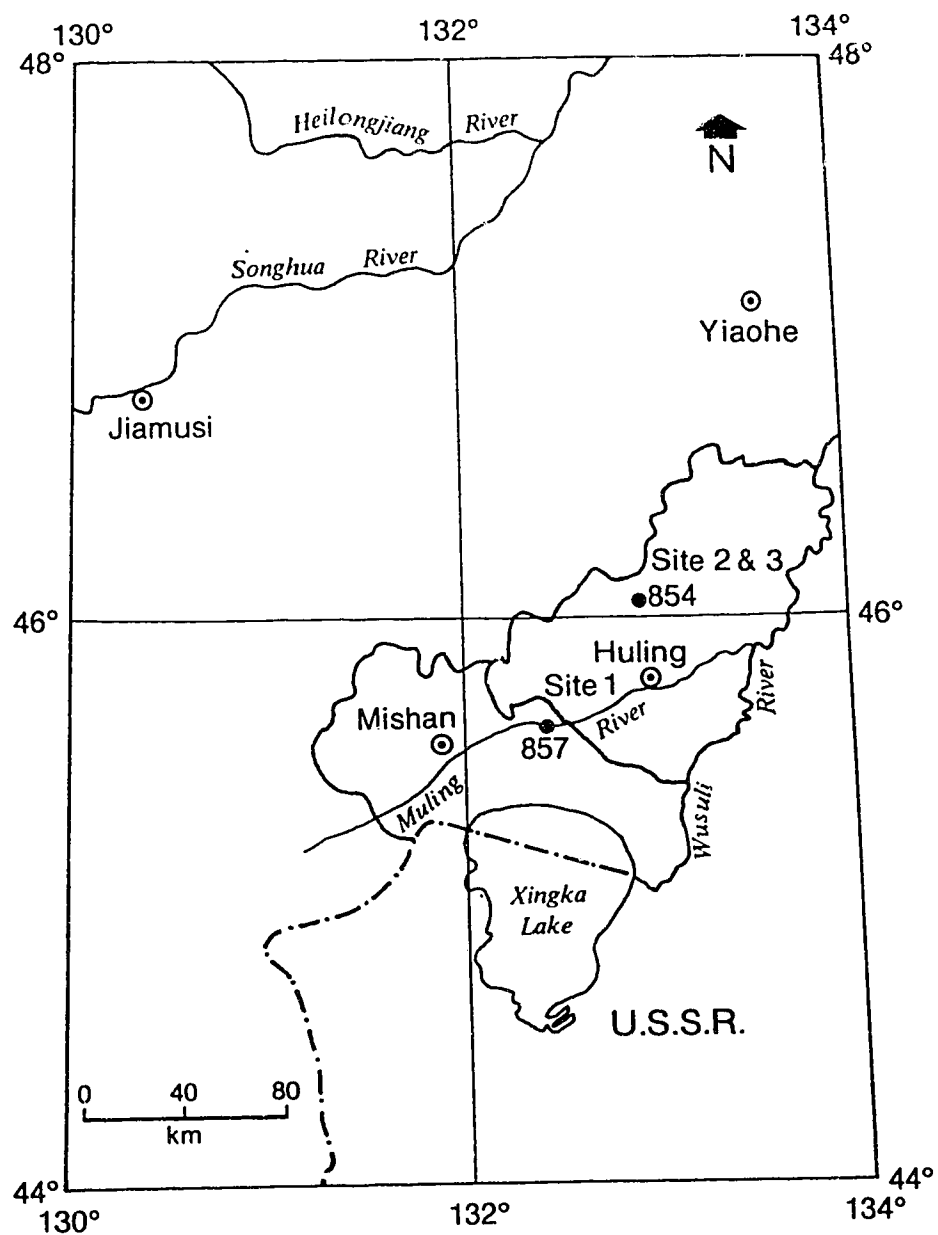


Figure 4. Location map of sampling sites.

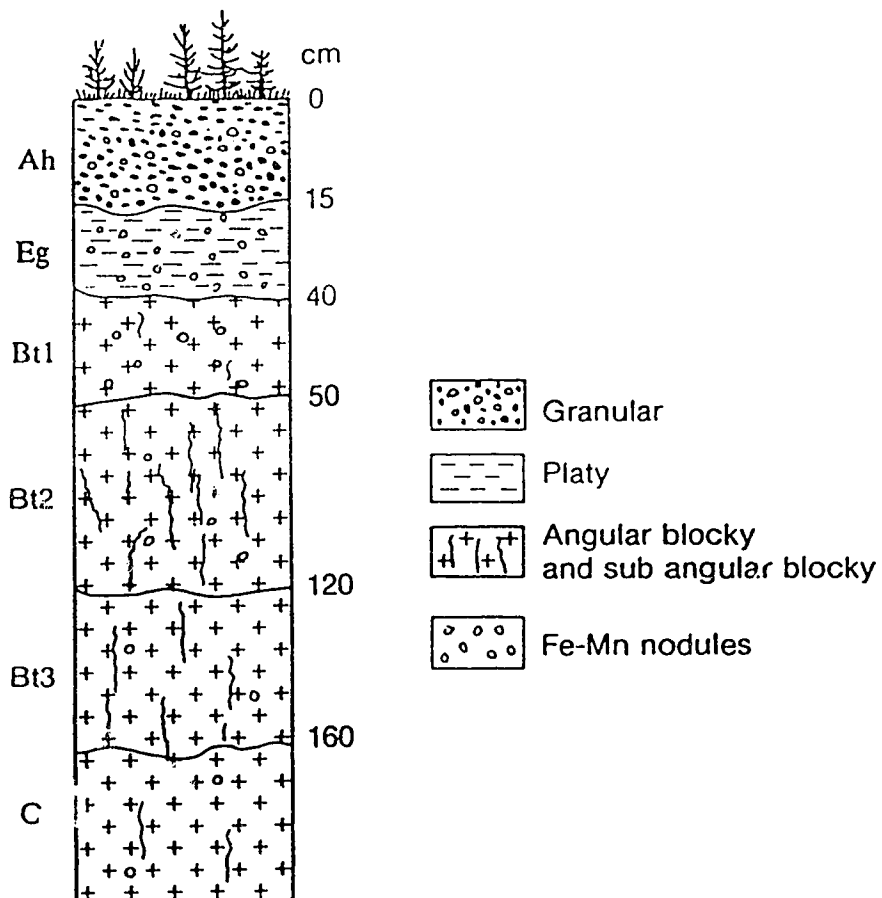


Figure 5. Cross-section of a typical pedon of a white clay soil.

Total cation exchange capacity for bulk soil was determined by the  $\text{NH}_4\text{OAc}$  method as described by McKeague (1978). Exchangeable cations displaced by  $\text{NH}_4\text{OAc}$  were determined by atomic absorption spectroscopy (Pawluk 1967). Exchangeable hydrogen (or exchangeable acidity) was measured using  $\text{BaCl}_2$ -triethanolamine as outlined by Peech *et al.* (1962).

Particle size distribution was determined using the pipette method as described by McKeague (1978). Samples from Ah horizons were treated with 30 % peroxide ( $\text{H}_2\text{O}_2$ ) to remove organic matter before conducting particle size analysis. The methods outlined by McKeague (1978) were also used for the pH measurement in distilled water and in 0.01 M  $\text{CaCl}_2$ . The bulk densities of selected horizons from pedon 2 were determined using the core method of McKeague (1978).

Organic carbon for bulk soil, clay, and silt was determined by dry combustion using a Leco Model 577-100 induction furnace with IR detection of evolved  $\text{CO}_2$  (McKeague 1978). Organic carbon of sand was calculated by difference. Total nitrogen (N) and phosphorous (P) were also determined using the method as outlined by McKeague (1978). The acid ammonium oxalate method (McKeague 1978) was utilized for the measurement of amorphous Al, Fe, and Mn for each horizon. The sodium pyrophosphate extraction as described by McKeague (1978) was used to determine amounts of organic complexed Al, Fe, and Mn for each horizon. The dithionite-citrate-bicarbonate method (McKeague 1978; Mehra and Jackson 1960) was used to assay the amounts of "free" (non-silicate) Al, Fe, and Mn for each horizon. Atomic absorption spectroscopy was used in conjunction with these methods for determination of Al, Fe, and Mn in extracted solutions.

## C. Mineralogical Analysis

### 1. Fractionation

Bulk soil samples of about 50 grams were dispersed in 250 ml of distilled water using a Braunsonic 1510 vibrator probe for three minutes at 380 watts (Edwards and Bremner 1967). Following sonification, samples were quantitatively transferred into 2 litre beakers for fractionation. Clay was separated from silt and sand by gravity sedimentation as described by Jackson (1979). During separation of clay, the samples were dispersed a second time by sonification in order to obtain complete dispersion of the clay fraction. Separated clay samples were flocculated using 1 M  $\text{CaCl}_2$  solution. Flocculated



clays were then washed free of excess  $\text{CaCl}_2$  by centrifuge washing with distilled water after which they were freeze-dried for storage and subsequent analyses. Following clay separation, the samples were quantitatively washed through a 300 mesh sieve (0.05 mm) to separate sand and silt fractions which were then oven-dried, weighed, and stored for subsequent analyses.

Silt samples were again sonified and all released clay was removed by gravity sedimentation to ensure the silt separates were free of clay. Silt samples were then further separated into fine (2 to 5  $\mu\text{m}$ ), medium (5 to 20  $\mu\text{m}$ ), and coarse (20 to 50  $\mu\text{m}$ ) fractions by the sedimentation method as outlined by Jackson (1975). Each subfraction of the silt separates was weighed and stored for analyses. Similarly, sand samples were fractionated into the very fine (0.05 to 0.01 mm), fine (0.01 to 0.25 mm), medium (0.25 to 0.50), coarse (0.50 to 1.0 mm), and very coarse (1.0 to 2.0 mm) fractions by dry sieving. The weights of individual fractions were recorded before storage.

## 2. Clay Mineral Analyses

Cation exchange capacity of freeze-dried clays (< 2  $\mu\text{m}$  fraction) was determined by the method described by Dudas (1987). The clays were subjected to a sonification treatment for about thirty seconds during the final saturation and washing steps in order to attain complete saturation and thorough washing.

The surface area of clays was determined by equilibrating Ca-saturated, oven-dried clays with ethylene glycol monoethyl ether (EGME) under vacuum for 48 hours. The weight gain due to the adsorption of EGME is proportional to the surface area of the clay (Carter *et al.* 1965). The measurement for each clay sample was conducted in triplicate.

The determination of amounts of vermiculite in clays was conducted using the method described by Coffman and Fanning (1974) and Abder-Ruhnan (1980). A short sonification (30 seconds) treatment was utilized at the last saturation and ion displacement step in the procedure.

The total dissolution of Ca-saturated clays was conducted by the microwave method outlined by Warren *et al.* (1990). Following sample ignition at 850° C, the dissolution was conducted using  $\text{HNO}_3$ -HF in teflon bombs which were placed in a microwave oven (Kenmore Model No. 88145) for digestion. Potassium was determined by atomic absorption spectroscopy and the  $\text{K}_2\text{O}$  content was used to determine content of mica in the clay fraction.

Fractionated clay samples (part 1 of the mineralogical analyses) were used for x-ray diffraction (XRD) analysis. Slides were made of the Ca- and K- saturated clays using the paste method described by Theisen and Harward (1962). The slides were subjected to the following treatments before x-ray diffraction analyses:

1. Ca-saturated clay, equilibrated at 54% relative humidity overnight and analysed at 54% relative humidity.
2. Ca-saturated clay equilibrated with ethylene glycol at 105° C for 2 hours and analyzed at ambient conditions after cooling.
3. Ca-saturated clay, equilibrated with glycerol at 65° C for at least 12 hours and run at ambient conditions after cooling.
4. K-saturated clay, heated at 105° C overnight and analysed at 0% relative humidity.
5. K-saturated clay, heated at 105° C overnight, then equilibrated to 54% relative humidity, and analysed at 54% relative humidity.
6. K-saturated clay, heated at 300° C for 2 hours and analysed at 0% relative humidity after cooling.
7. K-saturated clay, heated at 550° C for 2 hours and analysed at 0% relative humidity after cooling.

X-ray diffraction analyses were performed using a phillips PW1730 X-ray generator, a PW1710 diffractometer, and using Co K $\alpha$  radiation at 50 kV and 25 mA. The step scanning speed was 2 seconds for each step of 0.05° 2 $\theta$ .

### 3. Sand and silt mineralogy

The selected sand fraction samples was separated into a heavy (S.G. > 2.75) and a light (S.G. < 2.75) fraction using tetrabromoethane in separatory funnels (Dudas 1987). Some nodules in the sand fraction were separated by hand picking under the microscope. Separated nodules were then ground and placed in aluminium specimen holders for powder X-ray diffraction analysis of both normal scanning (2 seconds for each step of 0.05° 2 $\theta$ ) and step scanning (10 seconds for each step of 0.02° 2 $\theta$ ) modes. Some selected nodules were prepared as thin sections and used for petrographic analysis. Samples of total silt from each horizon were characterized by powder X-ray diffraction analysis. In addition, grain mounts for the total silt fraction were prepared for optical examination using the method described by Innes and Pluth (1970).

#### **D. Micromorphology**

The oriented core samples of soil for micromorphological examination were prepared by impregnating the soil cores with 3M Scotchcast™ epoxy resin #3 under vacuum after drying at 65° C. The impregnated sample blocks were then cut and mounted with a vertical orientation on ground glass slides (5 cm x 7 cm). Grinding and polishing of the thin sections to 30 µm thickness was accomplished utilizing a semi-automated procedure involving the Logitech thin section precision polishing system. Cover slips were attached to protect the thin sections. Fe-Mn nodules were mounted on 2x7 cm slides by a similar procedure.

The thin sections were examined using a petrographic microscope. The micromorphology was described using the terminology of Brewer (1976), Pawluk (1987), Pawluk and Bal (1985), Brewer *et al.* (1983), Brewer and Pawluk (1975), and Fox and Protz (1981). The photography of the thin section was carried out with a Carl Zeiss model 65151 photomicroscope. Kodak Ektachrome film (ASA 100, daylight) was used for photography.

#### **E. Scanning Electron Microscopy**

Selected nodules, quartz, and feldspar grains of sand separates from the major genetic horizons were examined by scanning electron microscopy (SEM). Samples were placed on stubs which were then sputter coated with gold to prevent charging of the samples. Electron micrographs were obtained using a Cambrige Stereoscan scanning electron microscope, and the semi-quantitative elemental compositions of feldspar and nodules were determined using the Kevex 7000, Energy Dispersive X-ray analyzer. The purpose of this examination was to document the surface morphology of feldspar and quartz in order to gain some additional information on morphological features related to weathering and transportation modes and to estimate the exterior and interior composition of nodules.

#### **F. Elemental Analysis**

Bulk soil and clay samples from each sampled horizon were analyzed for elemental composition including major, trace, and rare earth elements by Instrumental Neutron

Activation Analysis (INAA<sup>4</sup>). Following grinding which facilitates homogeneous packing, about 2 grams of the clay and bulk soils were packed into small plastic vials. The weight of soil samples were accurately recorded prior to shipment. Medium and coarse silt samples of around 5 grams from each sampled horizon were analyzed for Ti, Zr, and Sr by means of X-ray fluorescence using the commercial facilities of the Nuclear Activation Services Ltd.

---

<sup>4</sup> INAA, Nuclear Activation Services Limited, C/O X-ray Assay laboratories, 1885 Leslie Street, Don Mills, Ontario, M3B 3J4, Canada, Tel:(416) 445-5755.

Table 1. Field Description of Profile 1 (in FAO system, 1988).

---

The setting:

Condition : Native land

Location : 857 farm, Mishan County, Heilongjiang Province, China. Latitude 45°37' North, longitude 132°26' East.

Slope and aspect: 3 - 5%, northwest

Sample position : Upper middle position

Drainage : Well-drained externally (lateral surface), poorly drained internally  
perched water table present at 35 cm.

Parent material : alluvial sediments

Vegetation :

1. Forest: *Quercus monolica* Fisch, *Populus davidiana* Dode, *Tilia amurensis* Kom, *Lorylus heterophylla* Fisch, *Lespedeza bicolor* Turcz.
2. Grass: *Clematis manshurica*, *Convallaria keiskei*,  
*Adenophora nikoensis* Lamb, *Carex sp.* *Palonia obovata* Maxim, *Potentilla discolor* Bunge.

Elevation : 101 meters above sea level

---

Sample No.	Horizon	Depth	Description
11	Ah	0 - 15 cm	Very dark gray (10YR 3/1,D); clay loam; moderate, fine granular; very friable; abundant, very fine to medium, random roots, inped and exped, and very few coarse, horizontal roots; no carbonates; no coarse fragments; gradual, wavy boundary; 10 - 20 cm thick; medium acid reaction.
12	Eg	15 - 37 cm	Light gray (10YR 7/1, D); silty clay loam; weak, medium platy; slightly hard; few, fine to medium, random roots, inped and exped; no carbonates; common, fine, prominent reddish brown nodules, (5YR 4/4, D); mottles; no coarse fragments; clear smooth boundary; 18 - 24 cm thick; medium to strong acid reaction.

13	Bt1	37- 55 cm	Light brownish gray (10YR 6/2, D); silty clay; moderate, medium angular blocky; hard; few, fine to medium, random roots, inped and exped; no carbonates; few, fine, prominent yellowish red nodules (5YR 5/6, D); no coarse fragments; gradual smooth boundary; 10 - 20 cm thick; strong acid reaction.
14	Bt2	55-125 cm	Brown (10YR 5/3, D); clay; strong, medium to coarse angular blocky; very hard; very few, very fine to fine, random roots; exped; no carbonates; no coarse fragments; gradual smooth boundary; 68 - 72 cm thick; strong acid reaction.
15	Bt3	125-167 cm	Yellowish brown (10YR 5/4, D); clay; moderate to strong, medium to coarse angular blocky; very hard; no root; no carbonates; no coarse fragments; gradual smooth boundary; 40 - 44 cm thick; strong acid reaction.
16	C1	> 167 cm	Dark yellowish brown (10YR 4/4, D); clay; subangular block; very hard; no root; no carbonates; no coarse fragments; medium to strong acid reaction.

---

Table 2. Field Description of Profile 2 (in FAO system, 1988).

The setting:

Condition : Native land

Location : 854 State Farm, Huling County, Heilongjiang Province, China. latitude 46°05' North, longitude 132°58' East.

Slope and Aspect : 3 - 5 %, north.

Position : Upper middle slope

Drainage : Well-drained externally (lateral surface), poorly drained internally  
perched water table: 40 cm.

Parent material : Alluvial sediments

Vegetation:

1. Forest: *Quercus monolica* Fisch, *Populus davidiana* Dode, *Betula dahurica* Pallas, *Corylus heterophylla* Fisch, *Lespedeza bicolor* Turcz.

2. Grass: *Clematis manshurica*, *Convallaria keiskei*, *Adenophora nikoensis* Lamb, *Carex sp*, *Palonia obovata* Maxim, *Vicia amoena*

Elevation : 90 meters above sea level

Sampe No.	Horizon	Depth	Description
21	Ah	0 - 15 cm	Dark gray (10YR 4/1,D); clay loam; moderate, fine to medium granular; friable; abundant, very fine to medium, random roots, inped and exped, and few coarse, horizontal roots; no carbonates; no coarse fragments; gradual, wavy boundary; 10 - 20 cm thick; medium acid reaction.
22	Eg	15 - 41 cm	Light gray (10YR 7/1, D); silty clay loam; weak, medium platy; slightly hard; few, fine to medium, random roots, inped and exped; few, fine, tubular pores; no carbonates; common, fine, prominent reddish brown nodules (5YR 4/4, D); hard; mottles; no coarse fragments; clear smooth boundary; 24 - 28 cm thick; medium to strong acid reaction.
23	Bt1	41 - 53 cm	Light gray (10YR 7/2, D); clay loam; weak, fine to medium subangular blocky; hard; few, very to fine, random roots, inped and exped, very few, coarse

roots; no carbonates; few, fine, prominent yellowish red nodules (5YR 5/6, D); no coarse fragments; gradual smooth boundary; 10 - 14 cm thick; strong acid reaction.

24	Bt2	53- 123cm	Dark brown (10YR 4/3, D); clay; strong, medium to coarse angular blocky; very hard; very few, very fine to fine, random roots; expd; no coarse root; no carbonates; no coarse fragments; gradual smooth boundary; 68 - 72 cm thick; strong acid reaction.
25	Bt3	123-165cm	Dark yellowish brown (10YR 4/4, D); clay; moderate, medium angular blocky; very hard; no roots; no carbonates; no coarse fragments; gradual smooth boundary; 40 - 44 cm thick; medium to strong acid reaction.
26	C1	> 165 cm	Dark yellowish brown (10YR 4/4, D); clay; subangular block; very hard; no root; no carbonates; no coarse fragments; medium to strong acid reaction.

---



Table 3. Field Description of Profile 3 (in FAO system, 1988).

The setting:

Condition : Native land

Location : 1000 m away from profile 2, 854 state farm, Huling County.

Slope and Aspect : 1 - 2%, northwest

Position : Middle slope

Drainage : Well-drained laterally(surface), poorly drained internally  
perched water table present at 40 cm.

Parent material : Alluvial deposits

Vegetation:

1. Forest: *Quercus monolica* Fisch, *Betula dahurica* Pallas, *Corylus heterophylla* Fisch, *Lespedeza bicolor* Turcz.

2. Grass: *Clematis manshurica*, *Adenophora tetraphylla*, *Trifolium lupinaster*, *Carex* sp., *Palonia obovata* Maxim, *Veratum nigrum*.

Elevation : 90 meters above level

Sample No.	Horizon	Depth	Description
31	Ah	0 - 21 cm	Dark gray (10YR 4/1,D); clay loam; moderate, fine granular; very friable; abundant, very fine to medium, random roots, inped and exped, and very few coarse roots; no carbonates; no coarse fragments; gradual, wavy boundary;15 - 26 cm thick; medium acid reaction.
32	Eg	21 - 48 cm	Light gray(10YR 7/1, D); silty clay loam; weak, fine to medium platy; slightly hard; few, fine to medium, random roots, inped and exped; few, fine, tubular pores; no carbonates; common, fine, prominent reddish brown nodules (5YR 4/4, D); hard; mottles; no coarse fragments; clear smooth boundary; 25 - 29 cm thick; strong acid reaction.
33	Bt1	48 - 64 cm	Light gray (10YR 7/2, D); silty clay; weak, fine to medium subangular blocky; hard; few, very to fine, random roots, inped and exped, very few, coarse

roots; no carbonates; few, fine, prominent yellowish red nodules (5YR 5/6, D); hard; no coarse fragments; gradual smooth boundary; 14 - 18 cm thick; strong acid reaction.

- |    |     |            |  |
|----|-----|------------|--|
| 34 | Bt2 | 64 -130 cm | Dark brown(10YR 4/3, D); clay; strong, medium to coarse angular blocky; very hard; very few, very fine to fine, random roots; expd; no coarse root; no carbonates; no coarse fragments; gradual smooth boundary; 64 - 68 cm thick; strong acid reaction. |
| 35 | Bt3 | 130-160 cm | Dark yellowish brown(10YR 4/4, D); clay; moderate, medium angular blocky; very hard; no roots; no carbonates; no coarse fragments; gradual smooth boundary; 40 - 44 cm thick; medium to strong acid reaction.  |
| 36 | C1  | > 160 cm   | Dark yellowish brown(10YR 4/4, D); clay; subangular block; very hard; no root; no carbonates; no coarse fragments; medium to strong acid reaction.   |
-

## **CHAPTER IV**

### **RESULTS AND DISCUSSIONS**

In this chapter, the results of the laboratory analyses will be presented along with discussion of the pedogenesis of the white clay soils. In accordance with the main objectives of this study, the results and discussion section will be divided into five parts: A. parent material uniformity; B. physical, chemical, micromorphological and mineralogical soil properties and their pedogenic implications; C. trace element chemistry; D. rare earth elements; and E. discussion of the genesis and classification of the white clay soils.

#### **A. Parent Material Uniformity**

In order to enable assessment of changes during profile development, the soil should be formed throughout from a single parent material with variations less than those incurred in sampling, pre-treatment, and the estimation of constituents (Brewer 1964). When uniformity of parent material of a profile is established, the changes in chemical, physical, mineralogical, and morphological properties of soils along profiles can be attributed to pedogenic processes and quantitative pedological studies on soils may be conducted.

The parent materials of white clay soils are mainly Quaternary alluvial and lacustrine clayey deposits (Zeng 1980; Xia and Shang 1981; Xie 1982). Zeng (1963, 1980) reported that the parent materials for white clay soils were uniform based on the field observation. However, evaluation of uniformity should be based on as many lines of evidences as possible due to the complexity of pedogenesis and the nature of the variations in parent materials (Evans 1978).

In this study, horizons within profiles are treated as individual homogeneous unit. Each horizon is assumed to be laterally and vertically uniform. The possibility of discontinuities between these horizon units within a profile was determined on the basis of deviation from the mean (coefficient of variation or relative standard deviation in percentage) for a number of parameters suggested in the literature. Also, the generally accepted deviations for certain parameters in the literature will be compared to the deviations in this study for identification of lithological discontinuities.

There was no evidence of depositional stratification in the field. The observed changes in color, texture, and structure within each profile (Tables 1, 2 and 3 and Fig. 5) were attributed to pedological processes rather than geological origin.

### 1. Particle Size Distribution of Non-clay Fractions

Particle size distribution has been widely studied by pedologists for a number of decades. Information on the particle size distribution has been utilized by many investigators as criteria for evaluating the parent material uniformity of soils (St. Arnaud and Whiteside 1963; Barshad 1964; McKeague and Brydon 1970; Miller *et al.* 1971a,b; Sudom and St. Arnaud 1971; Sneddon *et al.* 1972; Evans and Adams 1975; Price *et al.* 1975; Rutledge *et al.* 1975; Evans 1978; Abder-Ruhman 1980; Puan 1988).

Clay particles may translocate within the soil solum during pedogenesis, therefore, the non-clay fractions should be selected. Sand fractions were generally below 6 % in the samples of white clay soils of this study. The sand fractions were partly composed of pedogenic Fe-Mn nodules, especially in the eluviated horizon (E horizons). As a result, it would not be appropriate to chose the sand fraction to detect lithologic breaks for white clay soils even though sands are relatively immobile during soil formation (Raad and Protz 1978). Silt constitutes the major fraction in all soil horizons of the selected pedons. Thus, silt fractions were chosen to evaluate the parent material uniformity in this study.

Profile distribution of individual silt fractions on a non-clay basis are shown in Figure 6 and Table 4. Content of fine silt in Ah and E horizons are less than the underlying horizons. For instance, the fine silt content in the E horizon of pedon 1 is 22% less than the average fine silt content of the remaining horizons, and the fine silt content in the E horizon of pedon 3 is 20% less than the average content of the remaining horizons. The coefficient of variation of fine silt within profiles are relatively large. The values were 13, 20 and 12 % for pedon 1, 2, and 3, respectively.

The large variation in fine silt distribution within profiles may be associated with pedogenic processes. Decrease of fine silt in Ah and E horizons with accumulation of fine silt in Bt horizons may have been caused by the translocation of fine silt during pedogenesis (Wright and Foss 1968; Abder-Ruhman 1980). Also, due to the relatively large surface area compared with medium and coarse silt, fine silt at the surface horizons may be broken down physically, biologically, and chemically to clay-size material. The

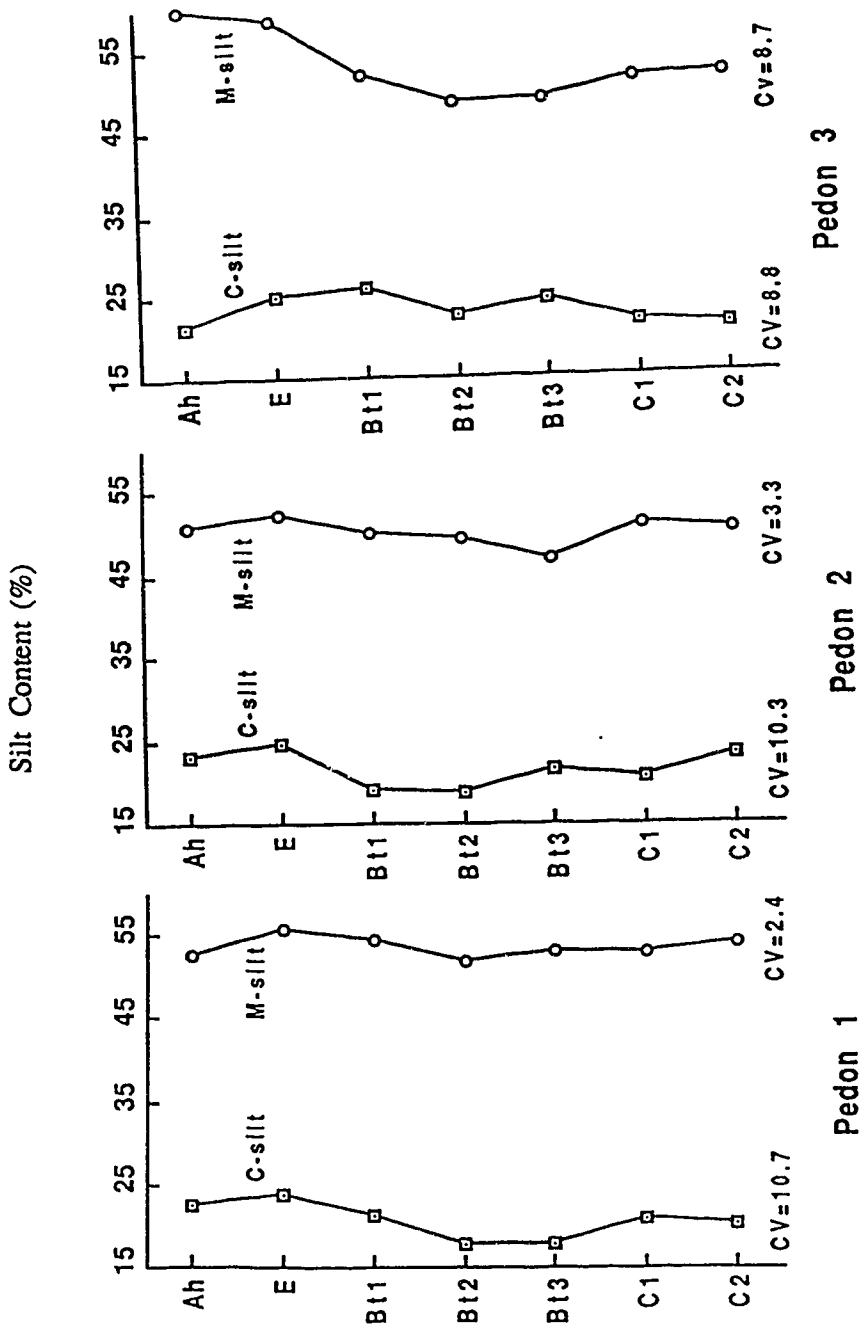


Figure 6. Profile distribution of medium and coarse silts.

Table 4. Silt size distribution and ratio.

Sample No.	Horizon	Fine silt	Medium silt	Coarse silt	Medium/Coarse
Pedon 1					
11	Ah	25	52	23	2.3
12	E	21	56	24	2.4
13	Bt1	24	54	21	2.6
14	Bt2	30	52	18	2.9
15	Bt3	29	53	18	3.0
16	C1	25	53	21	2.6
17	C2	26	54	20	2.7
Mean $\pm$ S. D.†		26 $\pm$ 3	54 $\pm$ 2	21 $\pm$ 2	2.6 $\pm$ 0.3
C V %‡		13	2.4	11	11
Pedon 2					
21	Ah	19	60	21	2.8
22	E	16	59	25	2.4
23	Bt1	23	52	26	2.0
24	Bt2	29	49	22	2.2
25	Bt3	27	49	24	2.0
26	C1	27	51	21	2.4
27	C2	28	52	21	2.5
Mean $\pm$ S. D.		24 $\pm$ 5	53 $\pm$ 5	23 $\pm$ 2	2.3 $\pm$ 0.3
C V %		20	8.7	8.8	13
Pedon 3					
31	Ah	26	51	23	2.2
32	E	23	52	25	2.1
33	Bt1	31	50	19	2.6
34	Bt2	32	50	19	2.6
35	Bt3	32	47	22	2.2
36	C1	28	51	21	2.5
37	C2	26	51	23	2.2
Mean $\pm$ S. D.		28 $\pm$ 3	50 $\pm$ 2	22 $\pm$ 2	2.4 $\pm$ 0.2
C V %		12	3.3	10	9.7

† denotes standard deviation.

‡ denotes coefficient of variation expressed as %.

clay-sized material may then leach down to lower horizons. St. Arnard and Whiteside (1963) and Abder-Ruhman (1980) reported that fine particles could be produced by frost action, especially at the surface of the solum, where the freeze-thaw cycle was most pronounced. Organic acids, produced from the mineralization of soil organic matter and from plant root exudates, can enhance the breakdown of coarse particles to fine particles. Therefore, a pedogenic rather than a lithologic cause may account for the observed differences in fine silt content between horizons. The largest variation (CV) from the mean of fine silt is 20% which is not large enough to indicate a lithologic break by the traditional standards.

There is no apparent change in distribution of medium and coarse silt. Thus, small coefficients of variation were associated with medium and coarse silts. Profile distribution of medium and coarse silts and their respective coefficients were displayed in Figure 6. These results indicated that lithologic discontinuities did not occur within profiles.

Ratios of clay-free fractions were mostly used as criteria for establishing parent material uniformity by a number of investigators (Barshad 1964; Evans 1978; Abder-Ruhman 1980). In this study, the ratio of medium to coarse silt was selected. Profile distribution of the ratio are displayed in Figure 7. The ratios do not differ much from one horizon to another. Correspondingly, coefficients of variation of these ratios were small, characteristic of uniform parent material (11, 13, and 9.7 % for pedon 1, 2, and 3, respectively).

The distribution of medium and coarse silt on a non-fine silt basis is shown in Table 5. The variation from mean for both medium and coarse silt was smaller as compared to the values based on only clay-free fractions (Table 4). The ratios of medium to coarse silt on a non-fine silt basis also have small coefficients of variation of 7.6, 4.2, and 8.7 % for pedon 1, 2, and 3, respectively (Table 5). This may imply that particle size distribution on a non-fine silt basis is a better parameter for evaluation of parent material uniformity.

## 2. Elements in Resistant Minerals

Comparing the ratios of the amount of two resistant minerals between horizons is considered the most common method of assessing the uniformity of parent material (Smeck *et al.* 1968; Evans and Adams 1975; Abder-Ruhman 1980; Puan 1988). Recently, the

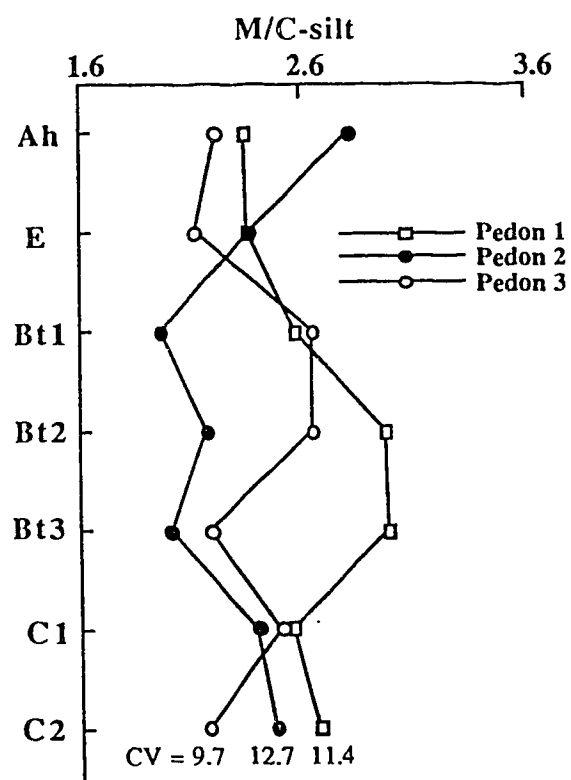


Figure 7. Profile distribution of the ratio of medium to coarse silt (data taken from Table 4).



Table 5. Distribution and ratio of medium and coarse silt fractions (fine silt free basis).

Sample No.	Horizon	Medium silt	Coarse silt	Medium/Coarse
Pedon 1				
11	Ah	72	28	2.6
12	E	70	30	2.3
13	Bt1	72	28	2.6
14	Bt2	74	26	2.8
15	Bt3	74	26	2.9
16	C1	71	29	2.4
17	C2	70	30	2.3
Mean $\pm$ S. D.†		72 $\pm$ 2	28 $\pm$ 2	2.6 $\pm$ 0.2
C V %‡		2.5	6.4	7.6
Pedon 2				
21	Ah	71	30	2.4
22	E	71	29	2.4
23	Bt1	72	28	2.5
24	Bt2	72	28	2.6
25	Bt3	70	30	2.3
26	C1	71	30	2.4
27	C2	71	29	2.5
Mean $\pm$ S. D.		71 $\pm$ 1	30 $\pm$ 1	2.4 $\pm$ 0.1
C V %		1.1	2.8	4.2
Pedon 3				
31	Ah	70	30	2.3
32	E	68	32	2.1
33	Bt1	68	32	2.2
34	Bt2	71	29	2.5
35	Bt3	69	31	2.2
36	C1	71	29	2.4
37	C2	72	28	2.4
Mean $\pm$ S. D.		70 $\pm$ 2	30 $\pm$ 2	2.3 $\pm$ 0.2
C V %		2.4	5.6	8.7

† denotes standard deviation.

‡ denotes coefficient of variation expressed as %.

ratios of amount of chemical elements in one or more size fractions have been used for identifying lithologic breaks, if the chemical element is present exclusively in a resistant mineral, such as Ti in rutile or anatase and Zr in zircon. The likely location of Sr is in the K positions in feldspar minerals (Taylor 1965; Evans 1978). These relatively stable minerals were traditionally used for the evaluation of parent material uniformity in pedology. The contents of Sr, Ti, and Zr in medium plus coarse silt fractions were determined for each horizon and the ratios of Zr/Sr and Ti/Zr were calculated in this study.

The profile distribution of Sr, Ti, and Zr is shown on Table 6. The analytical variability of the three elements by x-ray fluorescence was one percent of the amount present. Contents of Sr, Ti and Zr in the selected silt fraction remained almost constant with profile depth, and the coefficients of variation of the three elements were low (Table 6). The small variation from the mean for Sr, Ti, and Zr contents in the selected silt fraction further indicated that the parent material of white clay soils was uniform.

The ratios of Zr/Sr and Ti/Zr are useful indicators of uniformity (Evans and Adams 1975). Profile distribution of the two ratios and their respective coefficients of variation are displayed in Table 6 and Figure 8. The deviation (CV) from the mean within each profile was low and ranged from 5.0 to 10 % for the Zr:Sr ratios and from 7.4 to 9.2 % for the Ti:Zr ratios. For Zr:Sr ratios, the largest deviation occurred in pedon 3, and for the Ti:Zr ratio the largest deviation occurred in pedon 1. Drees and Wilding (1973) found that percentage deviations of over 22 % were required to detect lithologic discontinuities in a very uniform loess. Evans and Adams (1975) considered that a deviation below 23 % for the Zr:Sr ratio was indicative of parent material uniformity of soils developed on mudstones. In contrast, Chapman and Horn (1968) reported differences in excess of 100 % were required to detect lithologic breaks.

Parent material uniformity was evaluated by classical statistical analysis (LSD and t test). Profile distribution of Ti, Sr, Ti/Zr in silt fractions and of the ratio of medium silt to coarse silt indicated all horizon samples came from a single population. By contrast, profile distribution of Zr, Zr/Sr in silt fractions and of medium silt indicated lithological breaks occurred between the E horizon and the Bt1 horizon. This may throw doubt on the criteria traditionally used for detection of lithologic discontinuities in pedology.

In conclusion, both textural and elemental information indicated lithologic breaks did not occur for white clay soils according to the traditional criteria. Strict statistical

Table 6. Distribution of Sr, Ti, and Zr (mg/kg) in medium silt plus coarse silt and ratios of Zr/Sr and Ti/Zr.

Sample No.	Horizon	Sr	Ti	Zr	Zr/Sr	Ti/Zr
Pedon 1						
11	Ah	190	4500	380	2.0	12
12	E	190	4600	390	2.0	12
13	Bt1	180	4700	360	2.0	13
14	Bt2	170	5200	370	2.2	14
15	Bt3	190	4300	350	1.8	12
16	C1	180	5200	350	1.9	15
17	C2	180	4800	360	2.0	13
Mean $\pm$ S. D.†		180 $\pm$ 10	4700 $\pm$ 300	370 $\pm$ 20	2.0 $\pm$ 0.1	13 $\pm$ 1
C V %‡		4.2	7.2	4.1	5.0	9.2
Pedon 2						
21	Ah	180	4600	370	2.1	12
22	E	180	4500	400	2.2	11
23	Bt1	170	4400	350	2.1	13
24	Bt2	180	4500	330	1.8	13
25	Bt3	180	4200	350	1.9	12
26	C1	170	4600	380	2.2	12
27	C2	170	4200	390	2.3	11
Mean $\pm$ S. D.		180 $\pm$ 10	4400 $\pm$ 200	380 $\pm$ 20	2.1 $\pm$ 0.2	12 $\pm$ 0.9
C V %		3.0	3.8	6.8	9.5	7.4
Pedon 3						
31	Ah	180	4600	380	2.1	12
32	E	180	3900	380	2.1	10
33	Bt1	180	4100	340	1.9	12
34	Bt2	190	4000	340	1.8	12
35	Bt3	190	4500	340	1.8	13
36	C1	170	4000	360	2.1	11
37	C2	170	3900	360	2.1	11
Mean $\pm$ S. D.		180 $\pm$ 10	4100 $\pm$ 300	360 $\pm$ 20	2.0 $\pm$ 0.2	12 $\pm$ 1.0
C V %		4.6	6.9	5.0	10	8.6

† denotes standard deviation.

‡ denotes coefficient of variation expressed as %.

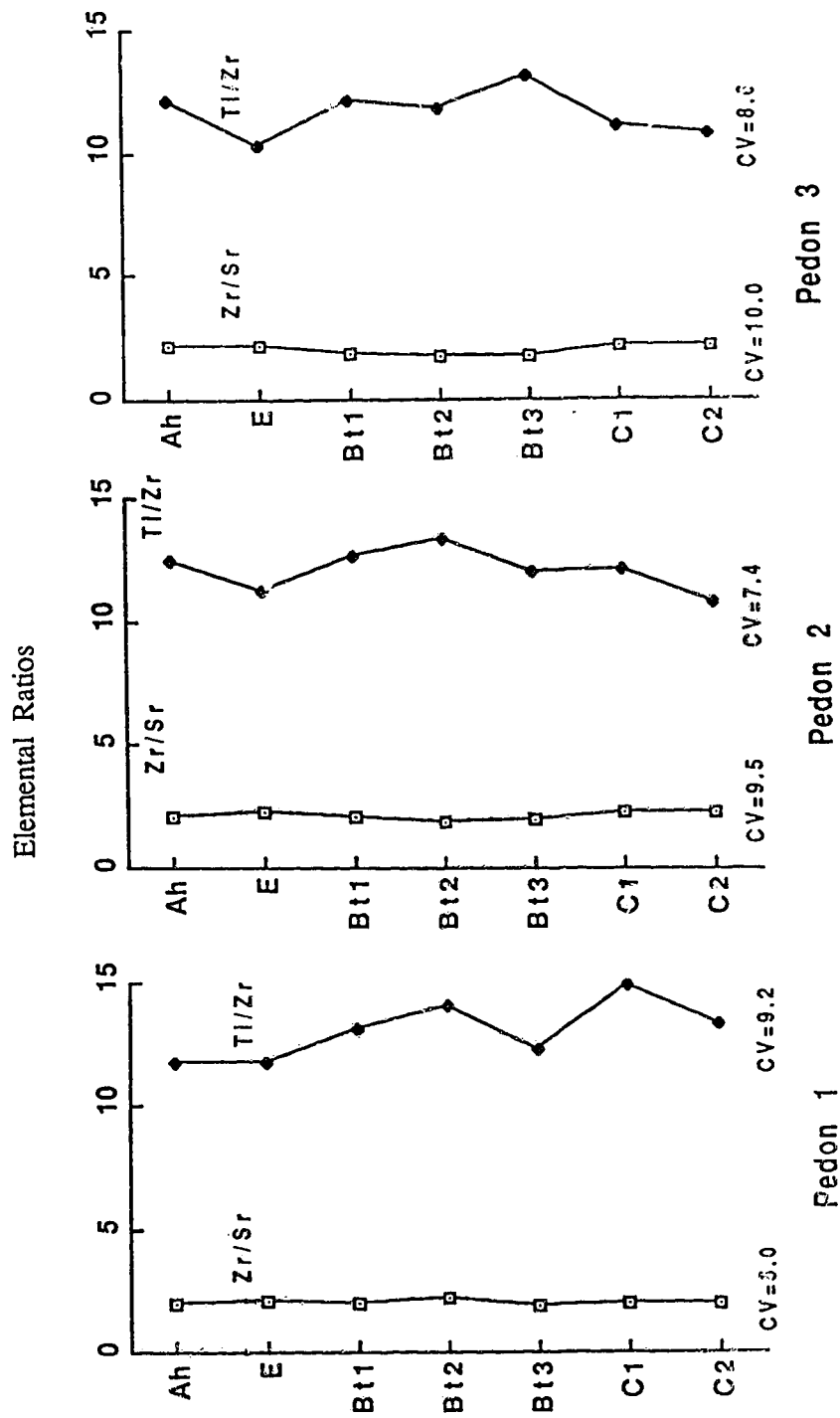


Figure 8. Profile distribution of ratios of Zr/Sr and Ti/Zr in silt fraction (5-50  $\mu\text{m}$ ).

analysis for some parameters reflected geological breaks between the E horizon and the Bt1 horizon. However, The classical criteria in pedology (large variation from means) were accepted in this study. The general trends in changes of soil properties could be interpreted in terms of pedogenic processes.

## **B. Physical, Micromorphological, Chemical, and Mineralogical Properties and Their Pedogenic Implications.**

### **1. Particle Size Distribution and Bulk Density**

The sampled pedons at the two state farms were the typical white clay soils found in Heilongjiang Province. The detailed profile descriptions are given in Table 1, 2, and 3 (in chapter II). Particle size distribution of the soils is presented in Table 7, and profile distribution of clay separates and of the ratio of clay to silt are shown in Figures 9 and 10.

Examination of textural data (Table 7) revealed that particle size distribution was affected by clay translocation. There was a definite accumulation of clay in Bt horizons relative to the Ah and E horizons. The increase in clay content in Bt horizons and decrease in clay content in E horizons meet the criteria, as outlined in the U.S.D.A. 7th Approximation (1978) and the FAO-Unesco system (1988), for textural B horizons (i.e. argillic horizon). The E horizons contained between 15% and 40% clay. Underlying B horizons must contain 1.2 times or more clay than the E horizons to meet the criteria. The white clay soils of this study meet this criteria. The argillation indices (clay content in Bt / clay content in E) are reported in Table 7. All of these indices were greater than 1.2 and the highest values occurred in Bt2 horizons. This reflects the eluviation process. Clay content ranged from 50% to 60% in Bt horizons and averaged 50% in the C horizons. The ratio of the clay content in the Bt to the clay content in the C horizon ranges from 1.0 to 1.2 (Fig. 9). This narrow range suggests illuviation of clay may extend beyond the designated Bt horizons. The presence of argillans (see micromorphological section) at depth illustrated that illuviation occurred in what was designated as C horizons based on field examination. These results suggest that the designated C horizons may be BC horizons transitional to the parent material or still parts of Bt horizons. Deep clay translocation was also reported for certain North America soils (Howitt and Pawluk 1985a).

Migration of clay in youthful soils is more likely to occur subsequent to leaching of soluble salts and carbonates after which wetting will facilitate eluviation and drying of the resultant suspension will cause illuvation of the suspended material at depth (MckKeague

Table 7. Particle size distribution (%), argillation index, and ratio of silt to clay.

Sample No.	Horizon	Sand	Silt	Clay	Argillation	
					Index†	Silt/Clay
Pedon 1						
11	Ah	6.0	69	25		2.8
12	E	13	67	20		3.4
13	Bt1	4.0	50	46	2.3	1.1
14	Bt2	2.0	38	60	3.0	0.63
15	Bt3	2.0	41	57	2.8	0.72
16	C1	3.0	45	52	2.6	0.86
17	C2	3.0	47	50	2.5	0.94
Pedon 2						
21	Ah	12	63	25		2.5
22	E	20	61	19		3.2
23	Bt1	9.0	58	33	1.7	1.8
24	Bt2	5.0	40	55	2.9	0.73
25	Bt3	5.0	42	53	2.8	0.79
26	C1	10	40	50	2.6	0.80
27	C2	9.0	40	51	2.7	0.78
Pedon 3						
31	Ah	8.0	64	28		2.3
32	E	13	65	22		3.0
33	Bt1	6.0	51	43	2.0	1.2
34	Bt2	4.0	44	52	2.4	0.85
35	Bt3	4.0	46	50	2.3	0.92
36	C1	7.0	44	49	2.2	0.90
37	C2	8.0	42	50	2.3	0.84

† denotes the ratio of clay content in Bt horizons to clay content in E horizons.

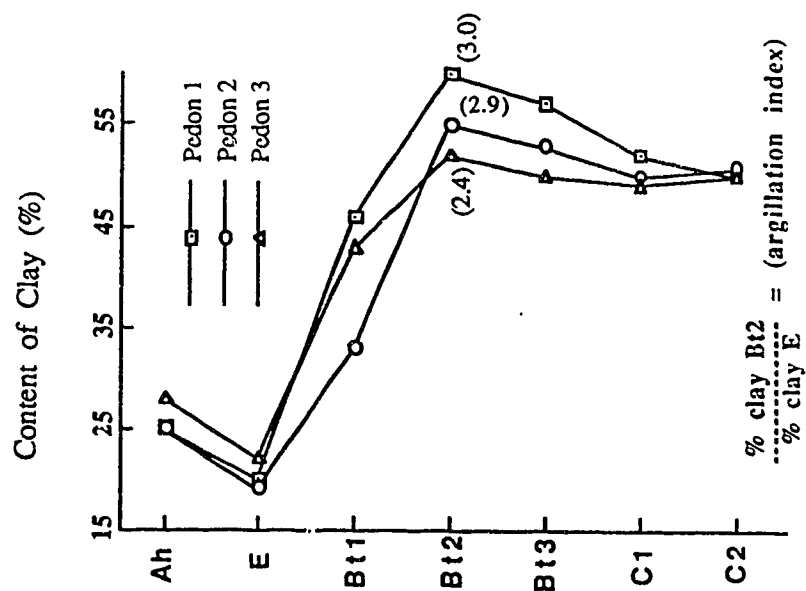


Figure 9. Profile distribution of clay separates (<2.0 μm).

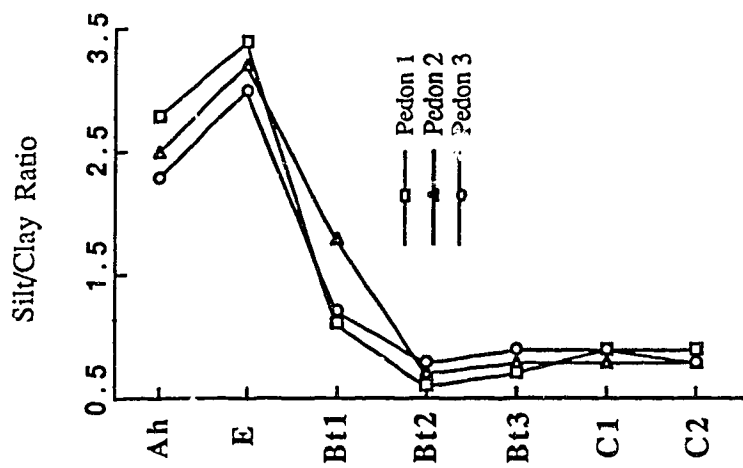


Figure 10. Profile distribution of the ratio of silt to clay.

and St. Arnaud 1969). Zhang (1987) reported that the  $\text{SiO}_2:\text{R}_2\text{O}_3$  ratio of clay separates ranged from 2.79 to 3.31 within profiles of white clay soils. He concluded the migration of clay was mainly lessivage; clay migration without undergoing chemical transformation (Duchaufour, 1970). He also reported in the same study that organic matter participated in clay translocation. Since white clay soils are located on gentle slopes, lateral movement of clay suspensions may occur during wet seasons, especially after the formation of slowly permeable Bt layers. Lateral movement was also thought to be responsible for the depletion of clay in surface horizons (Zheng 1980; Geng *et al.* 1987). The mechanisms of clay migration have been widely discussed by many pedologists (Smith 1934; Bodman and Harradine 1939; Bloomfield 1954; Dijkerman *et al.* 1967; Pettapiece 1969; Mel'Nikova and Kovenya 1974; Rust 1983; Bullock and Thompson 1985; Howitt and Pawluk 1985a; Spiers *et al.* 1985; and Zhang 1987). A detailed discussion of clay translocation will not be presented in this study.

Sand content is very low in white clay soils (Table 7). The variations in the content of sand within profiles were mainly a reflection of clay translocation. A two fold or more increase in the content of sand in the Ah and E horizons (relative to the C horizons) may be explained by the presence of pseudo-sand composed of Fe-Mn nodules. Zheng (1980) recorded that content of Fe-Mn nodules in the E horizon could be as high as 8 % by weight of fine earth fraction (<2.0 mm). Thin sections of this study contained more nodules for the E horizon than the underlying horizons (see micromorphological section). The breakdown of sand to silt and clay particles may also partly account for the low content of sand in B horizons. Bullock (1968) suggests that the clay bulge in a Bt horizon may result partially from weathering in the upper solum.

Silt distribution within profiles is largely a function of the eluviation of clay (Table 7). In other word, there is a negative enrichment of silt in Ah and E horizons. This was a result of clay removal. The ratios of silt to clay (Table 7) also displayed the eluviation process. The ratio ranged from 2.3 to 3.4 for eluviated horizons and were generally less than unity for Bt and C horizons (Fig. 10).

Values of bulk density are displayed in Table 8. The results are comparable to those reported by Zheng (1980). An increase in bulk density in the E horizon and a decrease in the Bt horizon (in comparison with C horizon) were attributed to clay eluviation and illuviation. The enrichment of Fe-Mn nodules could also increase the bulk density of the E horizons. Feijtel *et al.* (1988) reported similar result for Planosols in the Massif central,



France. The bulk density was less than unity in the Ah horizon. This was due to the high content of organic matter, which leads to high porosity through development of granular structure.

Table 8. Bulk density ( $\text{Mg/m}^3$ ) of Pedon 2.

Horizon	Bulk density
Ah	0.98
E	1.5
Bt1	1.4
Bt2	1.3
C	1.4

## 2. Chemical Properties

The total cation exchange capacity is a function of amount and kinds of clay and organic matter content. The total exchange capacity ranged from a low of 14  $\text{cmol (+)/kg}$  in an E horizon to a high of 47  $\text{cmol (+)/kg}$  in a Ah horizon for all 21 soil samples (Tables 9, 10, and 11). The low exchange capacity was always associated with the horizons leached of clay and/or of organic matter. The bulge in total exchange capacity in the Bt horizons parallels the increase in clay content in these horizons. There was a very slight increase in organic carbon (Table 12) in Bt horizons, which also contributed to the high total exchange capacity. The high values of total exchange capacity in Ah horizons was attributed to the high organic matter content (Tables 9, 10, 11, and 12). Base saturation was generally low, and increased with depth.

Exchangeable calcium occupied 23-51 % of the exchange complex in the Bt horizons while in E horizons it occupied only 17-25% of the exchange complex (Table 9, 10, and 11). Again, exchangeable calcium increased with depth. Exchangeable magnesium was second to exchangeable calcium on the exchange complex, but was much less than exchangeable calcium. This reflected that  $\text{Mg}^{2+}$  ions are less strongly adsorbed by clay minerals and are more mobile than  $\text{Ca}^{2+}$  during soil development. Exchangeable magnesium increased with profile depth. The two main exchangeable cations ( $\text{Ca}^{2+}$  and  $\text{Mg}^{2+}$ ) occupied a large proportion of exchangeable base for all horizons. The ratios of exchangeable calcium to magnesium within profiles

Table 9. Cation exchange capacity and exchangeable cations for pedon 1 samples.

Horizon	Exchangeable Cations (expressed as % of total exchange capacity)				Base Saturation %	Total Exchange Capacity	
	Na <sup>+</sup>	K <sup>+</sup>	Ca <sup>2+</sup>	Mg <sup>2+</sup>		Sum of cation† cmol (+) /kg	Determined cmol (+) /kg
Ah	0.91	1.2	45	5.5	52	24	47
E	3.2	1.3	26	6.1	38	6.4	17
Bt1	2.2	1.0	35	11	49	14	28
Bt2	2.8	1.3	44	12	59	19	32
Bt3	2.7	1.3	46	13	63	21	33
C1	2.5	1.1	52	12	68	19	28
C2	3.2	1.4	60	14	78	21	27

† denotes  $\Sigma(\text{Na}^+ + \text{K}^+ + \text{Ca}^{2+} + \text{Mg}^{2+})$

Table 10. Cation exchange capacity and exchangeable cations for pedon 2 samples.

Horizon	Exchangeable Cations (expressed as % of total exchange capacity)				Base Saturation %	Total Exchange Capacity	
	Na <sup>+</sup>	K <sup>+</sup>	Ca <sup>2+</sup>	Mg <sup>2+</sup>		Sum of cations† cmol (+)/kg	Determined cmol (+)/kg
Ah	0.82	1.6	36	6.6	44	14	31
E	1.6	1.0	17	5.6	27	4.0	15
Bt1	2.0	1.1	23	9.6	36	7.0	19
Bt2	2.2	1.3	33	13	49	15	30
Bt3	2.9	1.6	45	17	66	19	29
C1	4.5	2.0	40	15	61	17	28
C2	3.3	1.7	48	18	72	18	26

Table 11. Cation exchange capacity and exchangeable cations for pedon 3 samples.

Horizon	Exchangeable Cations (expressed as % of total exchange capacity)				Base Saturation %	Total Exchange Capacity	
	Na <sup>+</sup>	K <sup>+</sup>	Ca <sup>2+</sup>	Mg <sup>2+</sup>		Sum of cations† cmol (+) /kg	Determined cmol (+) /kg
Ah	0.81	1.9	38	7.0	48	15	31
E	2.7	1.7	25	8.8	38	5.3	14
Bt1	2.8	2.0	31	12	48	11	22
Bt2	3.0	1.7	42	16	63	15	23
Bt3	2.8	1.5	51	17	89	19	22
C1	5.1	2.7	58	21	87	21	24
C2	3.4	2.2	58	21	85	21	25

Table 12. pH and C, N, and P contents of the soils.

Sample No.	Horizon	pH		C	N	P	C/N
		H <sub>2</sub> O	CaCl <sub>2</sub>				
Pedon 1							
1	Ah	5.2	4.9	80	7	1	10
12	E	5.1	4.5	6	0.5	0.5	10
13	Bt1	4.7	4.2	7	0.7	0.2	10
14	Bt2	4.8	4.2	6	0.6	0.4	10
15	Bt3	5.0	4.4	6	0.7	0.3	9
16	C1	5.3	4.8	4	0.6	0.2	7
17	C2	5.4	5.0	3	0.5	0.2	7
Pedon 2							
21	Ah	5.3	4.8	40	4	0.8	10
22	E	5.0	4.3	6	0.5	0.2	10
23	Bt1	4.8	4.2	5	0.6	0.2	8
24	Bt2	4.8	4.1	5	0.8	0.3	8
25	Bt3	5.2	4.4	3	0.5	0.3	5
26	C1	5.4	4.7	4	0.5	0.2	7
27	C2	5.4	4.8	3	0.9	0.2	3
Pedon 3							
31	Ah	5.3	4.7	50	5	0.9	10
32	E	5.0	4.3	5	0.4	0.4	9
33	Bt1	4.9	4.2	5	0.6	0.3	7
34	Bt2	4.9	4.2	4	0.6	0.3	7
35	Bt3	5.2	4.6	6	0.6	0.3	10
36	C1	5.3	4.8	3	0.6	0.2	5
37	C2	5.3	4.8	3	0.5	0.3	6

illustrated the redistribution of these cations resulting from pedogenesis. The high TCEC is due to the presence of organic matter. Biological cycling has enriched Ca in the surface horizon compared to the eluviated horizon and the lower solum.

Exchangeable sodium and potassium were present in very low quantities generally occupying to less than 5 % of the exchange complex. The low values could be due to the ease of displacement and high mobility of these monovalent cations in soil systems. Exchangeable sodium and potassium usually increased with profile depth.

The pH values are displayed in Table 12. Acidic pH values were obtained for all the horizon samples. pH values within profiles were rather uniform and the relatively low values occurred in Bt horizons. Higher values occurred in surface and bottom horizons. The pH values in this study were generally lower than that reported in the literature. The high values of pH for white clay soils in the literature may be caused by a short equilibrium time for pH measurement.

The exchange acidity of white clay soils are shown in Table 13. The high values of exchange acidity in Bt horizons concurred with low pH values in Bt horizons. pH values were more closely related to exchangeable aluminium and hydrogen (Fig. 11). The values of exchange acidity determined by the  $\text{BaCl}_2$ -triethanolamine ( $\text{BaCl}_2$ -TEA) method (Peech *et al.* 1962) were usually higher than that calculated by differences between the total cation exchange capacity and the sum of exchangeable cations determined by the  $\text{NH}_4\text{OAc}$  method. The low values by  $\text{NH}_4\text{OAc}$  method may be due to the fixation of the ammonium ion by micaceous minerals such as vermiculite, to the loss of some ammoniated organic constituents upon washing. Additionally, more proton dissociation occurs for the more alkaline  $\text{BaCl}_2$ -TEA leading to a higher extraction of exchange acidity compared to the near neutral  $\text{NH}_4\text{OAc}$  extractant.

Content of organic matter was high in Ah horizons and declined with profile depth (Table 12). Horizons with clay accumulation also displayed slight enrichment of organic matter compared to the amounts in their respective underlying C horizons. This enrichment in Bt horizons was probably due to translocation of colloidal humus and other simple organic compounds from surface horizons in response to leaching by percolating water. The distribution of the C:N ratio was somewhat erratic but generally lower in the lower solum as compared to the upper parts (Table 12).

Table 13. Exchange acidity (cmol (+)/kg) for horizon samples.

Sample No.	Horizon	Exchange Acidity (by the NH <sub>4</sub> OAc method)	Exchange acidity (by BaCl <sub>2</sub> -triethanolamine method)
Pedon 1			
11	Ah	22	23
12	E	10	10
13	Bt1	14	18
14	Bt2	13	22
15	Bt3	14	19
16	C1	8.7	11
17	C2	5.9	11
Pedon 2			
21	Ah	17	17
22	E	11	11
23	Bt1	12	14
24	Bt2	15	18
25	Bt3	9.7	13
26	C1	11	11
27	C2	7.3	9.7
Pedon 3			
31	Ah	16	17
32	E	8.7	9.5
33	Bt1	12	14
34	Bt2	8.7	16
35	Bt3	5.3	9.3
36	C1	3.2	9.0
37	C2	3.9	9.8

The content of organic carbon in different size fractions is given in Table 14. The content of organic carbon in clay separates was much higher than in the silt fraction. Sand fractions contained almost no organic carbon. The organic carbon in clay separates and silt fractions generally decreased with profile depth. Part of the organic carbon may be associated with clay-organo or silt-organo complexes. The interaction between organic matter and clay minerals has been well documented in the literature (Dudas 1966; Schnitzer 1969; Dudas and Pawluk 1970; Davis 1971; Greenland 1971; Kodama and Schnitzer 1971; Schnitzer and Kodama 1972, 1977; Theng 1976).

The results for pyrophosphate extractable Fe and Al, oxalate extractable Fe and Al, and dithionite-citrate-bicarbonate extractable Fe and Al are given in Table 15. Generally, there was an increase in the amount of pyrophosphate extractable Fe and Al in the Bt horizons. The increase of pyrophosphate extractable Fe and Al in Bt horizons may be a result of the movement of organically complexed weathering products from the upper horizons, i.e., Fe or Al organic compounds. Similarly, there was a slight increase in oxalate extractable Fe and Al in Bt horizons in comparison with Ah and C horizons respectively. These results support the hypothesis of Duchaufour (1970) that lessivage involves the movement of amorphous Fe as well as colloidal clay. Amorphous Al may also accompany lessivage. The high values of dithionite-citrate-bicarbonate extractable Al occurred in Bt horizons while the dithionite-citrate-bicarbonate extractable Fe showed somewhat erratic distribution pattern within profiles. Al oxides may be mobile in the process of physical migration of clay. It should be noted that the highest values of dithionite-citrate-bicarbonate extractable and oxalate extractable Fe appeared in the E horizons. This may be explained by the fact that the E horizons contained abundant Fe-Mn nodules (see micromorphological section). Puan (1988) claimed that soluble Fe and Mn in soil solution of lower horizons may migrate to the E horizon along with capillary rise during dry seasons, and then participate in the formation of nodules.

Table 16 shows the results of total Fe and Al and ratios of these elements for different extractants. There was a definite increase in total Al and Fe in Bt horizons. This was attributed to the clay accumulation, since clay generally possesses low  $\text{SiO}_2\text{:R}_2\text{O}_3$  ratios. The Fe-o:Fe-d ratios revealed that amorphous Fe accounted for more than 50% of free Fe, i.e., dithionite-citrate-bicarbonate extractable Fe, and Fe-d:Fe-t ratios indicated the free Fe occupied, on average, 43 % of total Fe in the white clay soils. The Al-d:Al-t ratios indicated the amorphous Al accounted for only a minor amount of total Al in the soils.



Table 14. Organic carbon content (g/kg) in different size fractions.

Sample No.	Horizon	Clay	Silt	Sand
Pedon 1				
11	Ah	93	66	2
12	E	14	3.2	0.3
13	Bt1	9.7	3.7	0.0
14	Bt2	8.7	3.9	0.0
15	Bt3	8.4	3.7	0.0
16	C1	4.3	2.1	0.3
17	C2	4.2	2.0	0.1
Pedon 2				
21	Ah	67	34	0.4
22	E	11	4.2	0.1
23	Bt1	8.0	2.6	0.1
24	Bt2	7.1	3.2	0.0
25	Bt3	5.3	4.4	0.0
26	C1	4.1	1.9	0.1
27	C2	3.8	2.3	0.0
Pedon 3				
31	Ah	67	34	1
32	E	11	4.4	0.0
33	Bt1	6.5	3.2	0.0
34	Bt2	5.2	3.5	0.0
35	Bt3	7.2	1.8	0.6
36	C1	3.7	2.5	0.0
37	C2	3.8	2.3	0.0

Table 15. Pyrophosphate, oxalate, and dithionite extractable Fe and Al (g/kg).

Sample No.	Horizon	Pyrophosphate		Oxalate		Dithionite	
		Fe	Al	Fe	Al	Fe	Al
Pedon 1							
11	Ah	2.1	2.7	8.3	3.5	11	4.9
12	E	1.1	2.2	16	2.6	19	3.4
13	Bt1	1.6	3.6	9.2	3.7	13	5.5
14	Bt2	2.4	6.0	9.1	4.4	14	6.5
15	Bt3	2.0	3.1	11	3.9	15	6.3
16	C1	1.3	2.6	9.3	3.1	15	4.4
17	C2	1.0	2.0	9.1	3.1	18	4.5
Pedon 2							
21	Ah	1.7	2.4	9.9	3.3	13	4.7
22	E	1.0	1.9	14	2.9	18	3.7
23	Bt1	1.4	2.9	11	3.2	12	5.2
24	Bt2	1.5	3.8	11	4.0	12	6.9
25	Bt3	1.0	3.1	9.9	3.0	13	5.2
26	C1	1.9	3.3	9.8	2.9	14	4.3
27	C2	1.6	3.0	9.7	2.9	14	4.2
Pedon 3							
31	Ah	2.0	2.6	8.6	3.6	13	5.0
32	E	1.1	1.8	15	3.0	23	3.8
33	Bt1	1.3	2.6	11	3.4	15	4.7
34	Bt2	1.8	2.8	9.5	4.0	16	5.2
35	Bt3	1.6	2.2	9.6	3.0	18	4.3
36	C1	1.4	2.7	7.9	3.1	12	4.2
37	C2	1.6	2.7	8.5	3.0	15	4.7

Table 16. Total Fe and Al (g/kg) and selected ratios of Fe and Al based on the average of three pedons.

Horizon	Fe-t†	Fe-o‡/Fe-d§	Fe-d/Fe-t	(Fe-d-Fe-o)/Fe-t	Al-t	Al-o/Al-d	Al-d/Al-t
Ah	26	0.72	0.49	0.13	44	0.71	0.11
E	34	0.76	0.59	0.14	33	0.78	0.12
Bt1	33	0.75	0.41	0.10	72	0.67	0.07
Bt2	39	0.73	0.36	0.10	79	0.68	0.08
Bt3	41	0.67	0.37	0.13	72	0.63	0.07
C1	37	0.67	0.37	0.12	69	0.70	0.06
C2	39	0.59	0.41	0.14	65	0.67	0.07

† denotes total content.

‡ denotes oxalate extractable.

§ denotes dithionite extractable.

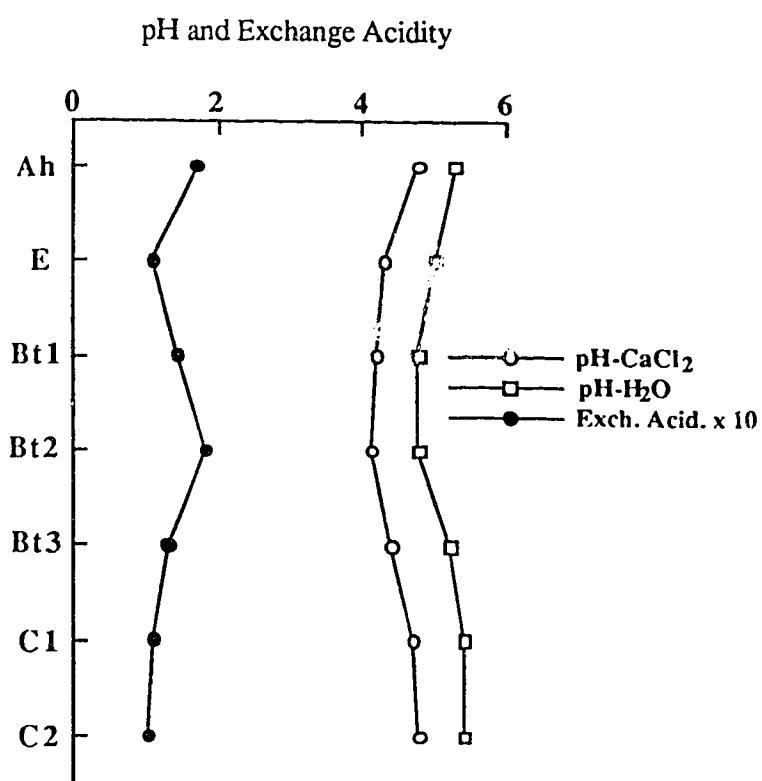


Figure 11. Profile distribution of pH and exchange acidity for pedon 2.

### 3. Micromorphology

Granular aggregates (mull-granoidic fabric), as described by Brewer (1976) were noted in the Ah horizon (Table 17 and Fig. 12). Aggrotubules and fungus mycelia around peds were also present. These features are indicators of soil biological activity. The granular structure in the Ah may also be partly attributed to freeze-thaw actions (Pawluk 1988). There were some partially decomposed and undecomposed plant fragments and Fe-Mn nodules in the Ah horizon.

Isoband fabric, as described by Dumanski and St. Arnaud (1966), was clearly observed in the E horizon. Isolated iron and manganese nodules were abundant in the E horizon. The isobanded fabric was mainly a result of the combination of clay removal and the physical action of ice lenses which forced the soil apart along horizontal planes. Wetting and drying may also be an important process in the development of platy structure and banded fabric (Dumanski and St. Arnaud 1966).

Bt horizons exhibited fragmic and fragmoidic fabric. The fragmic units are well developed and accommodated. There are also few big cracks. These reflect the effects of wetting-drying, shrinking-swelling, and freeze-thaw on the soil fabric. Argillans are common in the Bt horizons. The field designated C horizon showed similar fabric to Bt horizons. This further suggests the sampled C horizon may still be a part of the Bt horizon or BC transitional horizon.

Nodules in which Fe and Mn are concentrated relative to the soil matrix are an important feature in these soils. The presence of Fe-Mn nodules is indicative of weathering with periodic reducing conditions. Most of the nodules in the white clay soil were non-magnetic and exhibited randomly distributed grains of primary minerals (mainly quartz and feldspars). Mineralogical composition of the nodules was similar to the composition of the surrounding soil matrix (see mineralogy section). The internal fabric arrangement within



Figure 12. Mull-granoidic fabric of the Ah horizon. This field of view is primarily composed of fecal pellets and partially decomposed plant material (plane polarized light, mag. 20 X).

Table 17. Micromorphological description of pedon 2.  
(all percentages based on whole thin section area).

Ah 0 to 15 cm	
Sequence:	Fragmic and granic
Type:	Fragmoidic//humic-mullgranoidic
Description:	Dominant fabric type is framoidic with common mixed complex mullgranoidic and humigranoidic fabric. Size of fragmoidic units varies from 0.7 mm to 2.5 mm and the fragmoidic units are composed of soil plasms and few quartz and feldspar grains. Zones of fragmic and iunctic fabric are also present. Voids comprise 55% of the whole thin section area. Some channels of variable size contain intact roots, partially decomposed plant residues and debris.
Pedological feature:	(i) Discrete, spherical, sesquioxidic and manganiferous nodules with sharp boundary are dominant (8%). Average size of nodules is 0.8 mm with a large variability in diameter. (ii) Fecal pellets are frequent, which fuse into humigranoidic fabric. (iii) organic glaeboles and aggroutubules comprising mullgranoidic and humigranoidic fabric are also present. (iv) there are some fungal hyphae.
Plasmic fabric:	Dominant fabric type is silasepic. The nodules and organic glaeboles have isotic fabric type.
E 15 to 41 cm	
Sequence:	Fragmic
Type:	Banded fragmic//banded fragmoidic
Description:	Banded fragmic is very dominant fabric type with common banded fragmoidic fabric. Banding varies from 1 mm to 3 mm, and the horizontal length of fragmic units can be up to 4 cm. Fragmic units are well developed and well accommodated. Voids compose 40% of the area and most of the voids are planar type.

Pedological feature:	Dominant pedological feature is discrete, spherical, sesquioxidic and mangiferous nodules with sharp boundary (15%). These nodules are evenly scattered over thin section and most are associated with voids. Size of nodules ranges from 25 $\mu$ m to 1.8 mm in diameter. Some nodules are coated with a clay skin (15 to 20 $\mu$ m). There are also few irregular nodules and pedodes.
Plasmic fabric:	Silasepic plasmic fabric type is very dominant. Nodules have isotic fabric.

#### Bt1 41 to 53 cm

Sequence	Fragmic
Type:	Fragmic//fragmoidic
Description:	Fragmic fabric is dominant with common fragmoidic fabric at the top and fragmoidic fabric becomes dominant in the lower portion. The horizontal length of fragmic units is much smaller than that of the E horizon. Fragmic units are partially accommodated. A few zones of weakly banded fragmic fabric also occur. Voids comprise 40 % of the area and consist of numerous small planar and a few large planar voids.
Pedological feature:	(i) Dominant pedological feature is plane- and ped-argillans and ferri- argillans with some areas of vugh argillans and embedded grain argillans. Thickness of argillans is up to 0.1 mm. (ii) There are also few microlaminated clay infilling of channels with strong continuous orientation and neoargillans. (iii) Discrete, spherical sesquioxidic nodules with sharp boundaries are still present, but the number and size of nodules decrease dramatically, compared to that in the E horizon.
Plasmic fabric:	Vosepic plasmic fabric type is dominant with few zones of mosepic and masepic fabric.

#### Bt2 53 to 123 cm

Sequence:	Fragmic
Type:	Fragmic//fragmoidic
Description	Dominant fabric type is fragmic with frequent fragmoidic type. Fragmic units are angular blocky, and strongly developed and well accommodated. The average size of the units is 1.4 mm. large fragmic



	units often contain small subunits. Voids make up to 50 % of the area. Most of voids are continuous craze planes and some are large skew planes with variable width.
Pedological feature:	Plane- and ped- argillans and ferri-argillans are common but not ubiquitous. Average thickness is 50 $\mu\text{m}$ but can be up to 200 $\mu\text{m}$ . Sometimes, fine silt grains are embedded in the argillans. Vugh, neo- , and Quasi- argillans can be found, as well. Microlaminated oriented clay is similar to the ones in Bt1 horizon. Clay is present within the soil matrix. Sesquioxidic nodules (impregnated with clay and soil matrix materials) are very few. Silans are also observed on the top of argillans with diffuse boundary.
Plasmic fabric:	Vosepic is very dominant with some skelsepic fabric. The plasmic fabric within the fragmic unit is silasepic.
Bt3 123 to 165 cm	
Sequence:	Fragmic
Type:	Fragmoidic//fragmic
Description:	Dominant fabric type is fragmoidic with common fragmic fabric. Fragmic units are larger than that of Bt2 comparatively, but the width of planes between the units is narrower. Voids comprise 45 % of the area, and voids consist of craze planes and few large skew planes.
Pedological feature:	Plane- and ped- argillans and ferri-argillans are frequent, and they (30 mm, average) are thinner than Bt2. Embedded grain and vugh argillans, neo- and quasi- argillans, and silans also occur. Sesquioxidic nodules are very few and the matrix of nodules is similar to the nodules in Bt2.
Plasmic fabric:	Dominant plasmic fabric type is vosepic with few zones of skel-mosepic type. Sometimes, fragmic units have insepic and silasepic plasmic fabric.
C 165+ cm	
Sequence:	Fragmic
Type:	Fragmoidic//fragmic
Description:	Fragmoidic fabric is the dominant fabric type mixed with common fragmic fabric. The shape and size of fragmic units are similar to that of

Bt3, but there are fragmoidic-porphyric types. Voids occupy 40 % of the area, and they are craze and skew planes and vughs.

Pedological feature:	Plane-, and ped- argillans and ferri-argillans are still common, but occurrence and thickness are less and thinner than that of Bt2 and Bt3. Vugh argillans and embedded argillans increase compared to the Bt3. Neo-argillans and sesquioxidic nodules are present, as well. Silans are very few.
Plasmic fabric:	Vo-masepic is the common plasmic fabric type with some zones of skel-mosepic fabric type.

---

the nodules dominantly reflected the fabric of the s-matrix (Figs. 13 and 14). These results revealed that the nodules may have developed *in situ*. Most nodules are associated with voids and iron enrichment areas. This suggests that soluble Fe and Mn from the lower solum may be brought up by capillary rise and participate in the formation of nodules, which is also supported by the Mn profile distribution (see trace element section).

Nodules separated from the white clay soil contained little organic carbon. This suggests that organic complexed Fe and Mn are not enriched in these nodules. Several other workers (McKenague *et al.* 1968; Childs 1975; Sidhu *et al.* 1977) also reported that only a small fraction of the total Fe, Mn, Co, and Ni in Fe-Mn pans and nodules was associated with organic matter.

Nodules occurred throughout the solum. Nodules were most concentrated in the E horizon where the oxidation-reduction process is very active due to the presence of a temporary perched water table. The amount of nodules decreased with profile depth. The nodules from the E horizon are generally denser and darker, and larger than the nodules from the Bt horizons. This suggests the nodules in the E horizon are more strongly developed than those in the mid-solum.

Well-oriented illuvial argillans were associated with peds and voids. These argillans occupied more than 1 % of the area of the slides from Bt horizons (Table 17). This meets

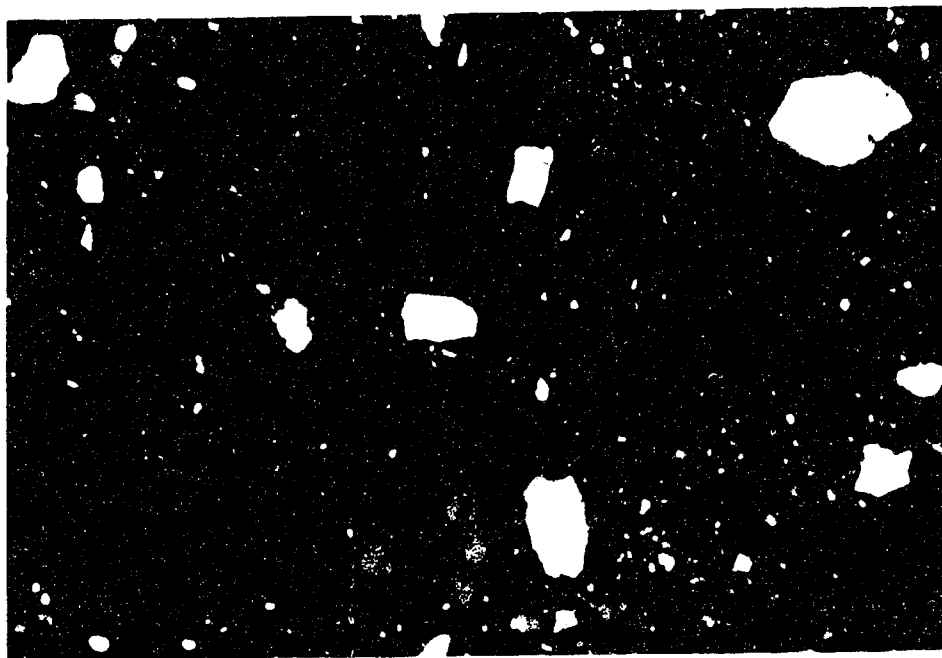


Figure 13. Photomicrograph of a Fe-Mn nodule from the E horizon. The matrix of the nodule is similar to the adjacent soil matrix (cross polarized light, mag. 20 X).

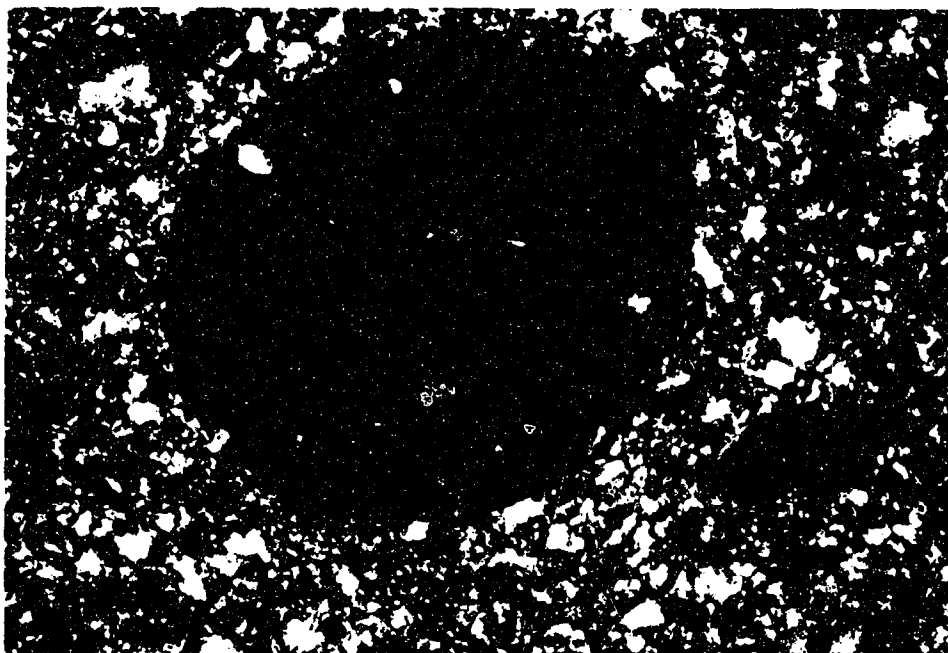


Figure 14. Photomicrograph of a spherical Fe-Mn nodule from the E horizon. The matrix of the nodule is the same as the adjacent soil matrix. The opaque center may contain more Mn than the outer zone (cross polarized light, mag. 80 X).

the requirement for a textural B horizon as defined in the U.S.D.A. 7th Approximation (1975). The thickness and number of the argillans increased with profile depth and reached maximum in the Bt2 horizon at a depth of 0.5 to 1.2 m. Argillans were also common in the field designated C horizon.

The occurrence of argillans in the what was believed to be C horizon at 1.8 m depth indicates illuviation may extend beyond the depth of sampling. This was consistent with the high clay content of the C horizon. Howitt and Pawluk (1985) reported the presence of illuvial argillans to depths of 2.5 m in Alberta Luvisols. Bullock (1968) reported that argillans were present at a depth of 2.3 m in the Langford soil. Argillans at depth in this study were generally associated with large planar voids and cracks, which suggested some clay may have been translocated well beyond 1.8 meter.

The location of maximum argillan concentration parallels the observed maximum clay content in the Bt2 horizon. The well-oriented argillans are illustrated in Figures 15 and 16. The ferrans and ferri-argillans and microlaminated clay infilling of channels were also observed in the Bt horizons (Figs.15-17). The presence of ferrans and ferri-argillans in the Bt horizons indicated the movement of iron during soil development.

Capillary withdrawal of water from moving clay-water suspension at the mid and lower solum upon drying was the main mechanism for the formation of the argillic horizons of white clay soils under this study. Transport of clay was tied to the depth of percolation of infiltrating water. The lack of carbonates and excess salts in the parent material of the soils enhanced the orientation of argillans (Brewer and Hadane 1957). Strong orientation and birefringence of argillans in the thin sections of this study were mostly found along the wall of planar voids and vughs hundreds or thousands of times larger than clay-sized particles. This evidence indicates sieving was not a major process in the formation of the Bt horizons of this study.

The presence of silt particles in argillan matrices, as noted by Howitt and Pawluk (1985), was fairly common in the thin sections of this study. Xiong and Huang (1986) reported whitish silicon powder was frequently seen in field observations on the surface of peds of white clay soils in Jilin Province. They also indicated the powder was composed of silt-size quartz, feldspar, and a small quantity of phytorelicts. They concluded that these silt-sized quartz, feldspars, and phytorelicts were translocated from the upper solum to the lower solum. The mixture of clay and silt coating may be a result of silt moving with clay. Howitt and Pawluk (1985) and Spiers *et al.* (1988) observed the presence of fine quartz

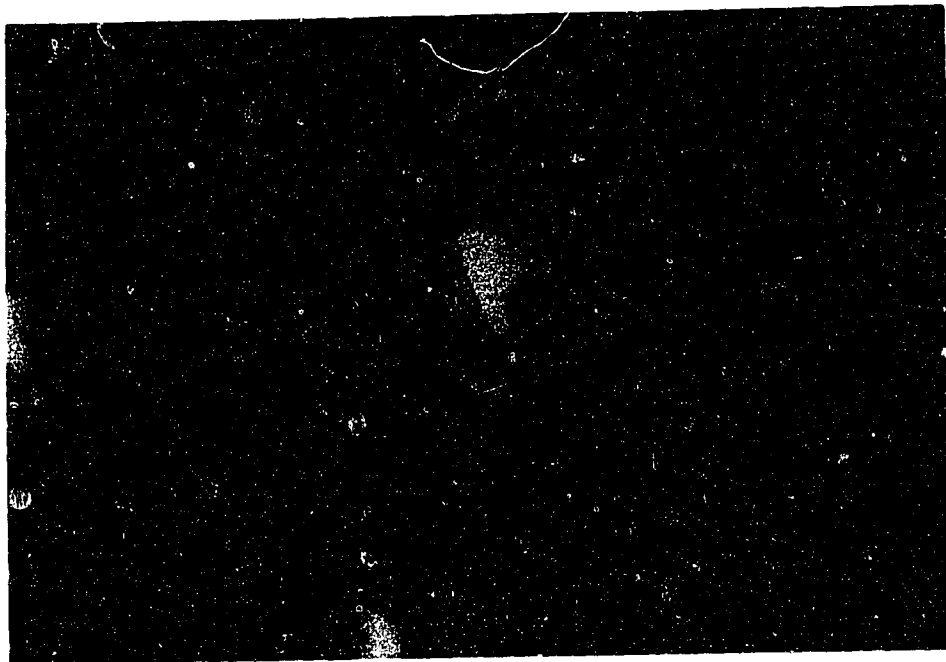


Figure 15. Illuvial argillans, ferrans, and ferri-argillans in the Bt2 horizon. Argillan at upper middle, ferri-argillan at lower right, and ferran on the right.(plane polarized light, mag. 80 X).

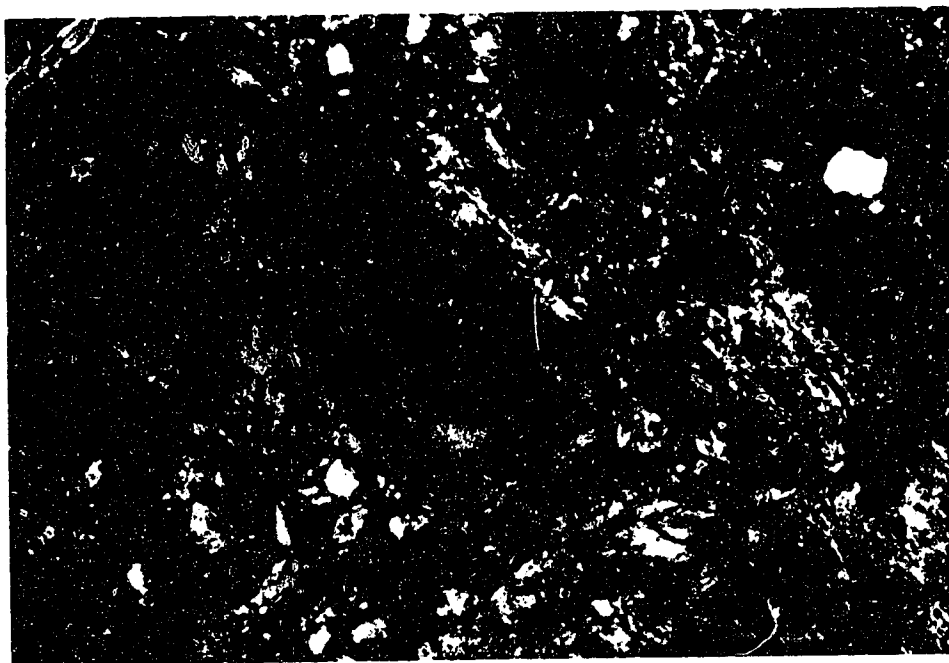


Figure 16. Microlaminated clay infilling of channels in Bt2 horizon. (cross polarized light, mag. 80 X).

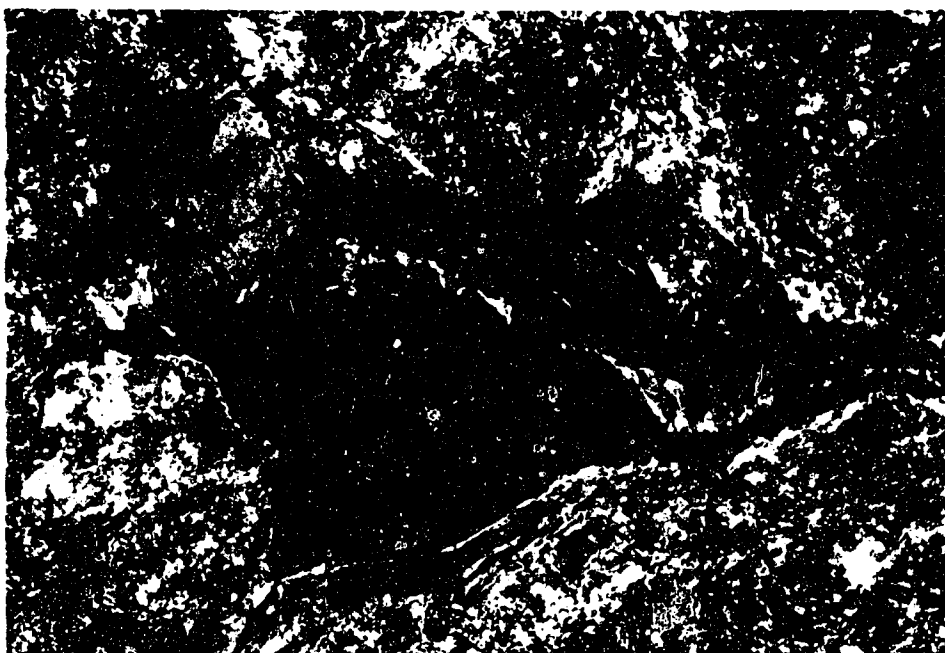


Figure 17. Ferran and ferri-argillan of the Bt2 horizons.  
(Cross polarized light, mag. 80 X).

grains in lysimeter leachates in their study. They suggested that fine grains of quartz and feldspar could move during soil development. However, the presence of quartz may be an artifact of field installation of lysimeters. The mobility of silt-sized quartz and feldspars during pedogenesis needs further investigation.

#### 4. Mineralogy

##### Clay Mineralogy

The purpose of the clay mineralogical analyses was to identify clay mineral assemblages and to investigate the changes in clay mineralogy among horizons. Qualitative, semi-quantitative, and quantitative determinations of clay mineral species were obtained by x-ray diffraction, elemental composition, cation exchange capacity and surface area determinations.

X-ray diffraction patterns of clay separates from pedon 2 are shown in Figures 18 to 24. The x-ray diffraction patterns of clay separates from pedon 1 and 3 are contained in Appendix I. Mineralogy, surface area, cation exchange capacity, and elemental analysis of clays are presented in Tables 18 and 19.

Clay mineral composition of the  $< 2 \mu\text{m}$  fraction was qualitatively similar throughout profiles with a minor variation in quantity. Soil vermiculite (intergrading to smectite, i.e., vermiculite-smectite intergrades), mica, and kaolinite are consistently present in relatively high amounts. Chloritic intergrades, quartz, and feldspar are present in trace amounts.

Soil vermiculite was thought to be depotassified mica. Soil vermiculite appears to have a higher surface area than true vermiculite. Also, soil vermiculite exhibits expansion beyond 1.4 nm on treatment with ethylene glycol unlike geological specimens of vermiculite. The presence of soil vermiculite was confirmed by assessing the degree of rehydration by examining the 1.0 nm and 1.4 nm peak intensities of K-saturated specimens when equilibrated at 0% and 54% relative humidity, respectively. Dehydrated K-saturated vermiculites do not rehydrate. Also, the presence of vermiculite was indicated by well-defined 1.4 nm peaks for glycerol treated samples.

The soil vermiculite-smectite intergrades (VSI) were present in clay separates of this study. The intermediates can be described as a series of 2:1 phyllosilicate clay minerals with charge density between soil vermiculite and smectite. These minerals may have formed *in*

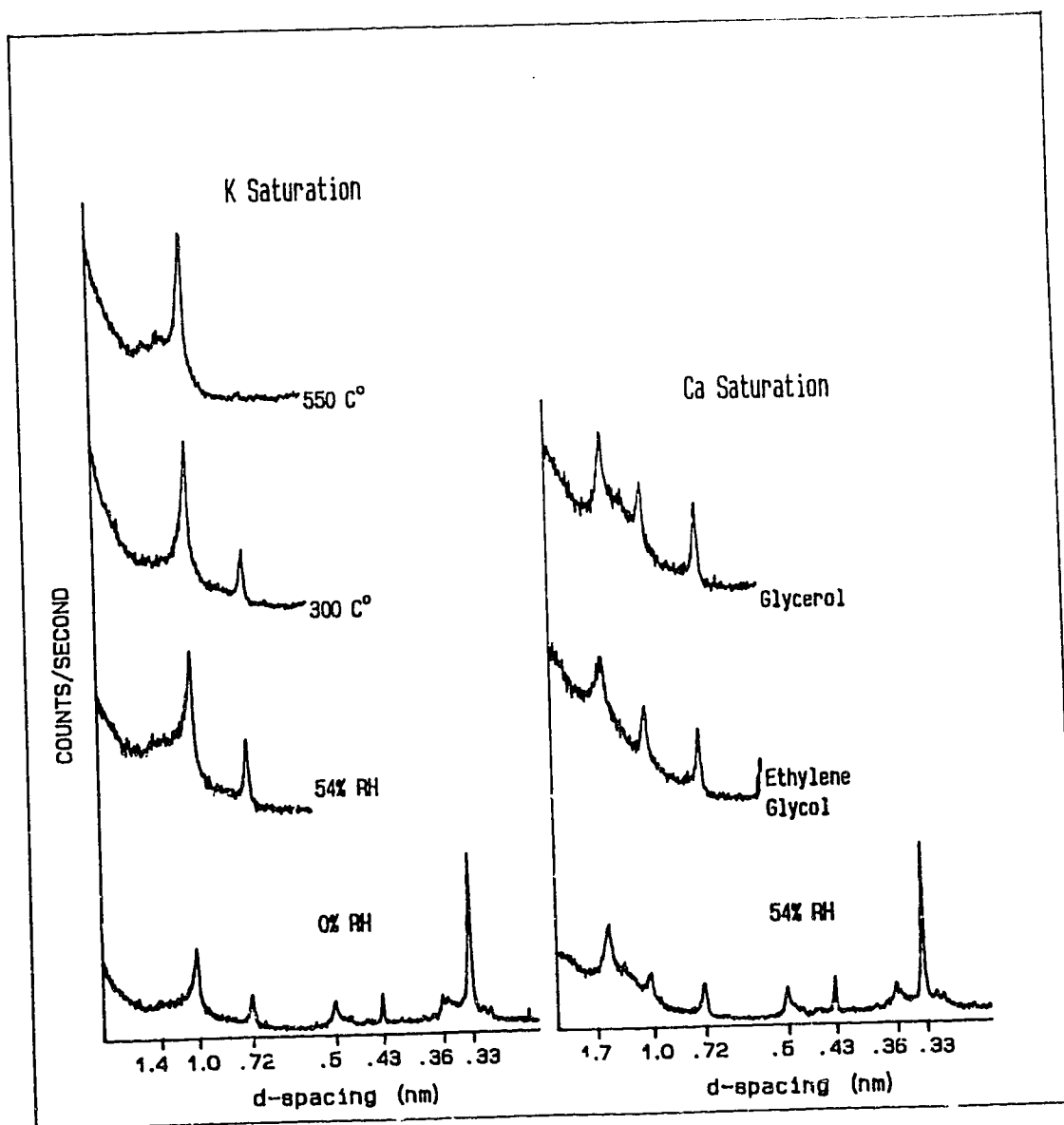


Figure 18. X-ray diffractogram of the clay separates from the Ah horizon of pedon 2.



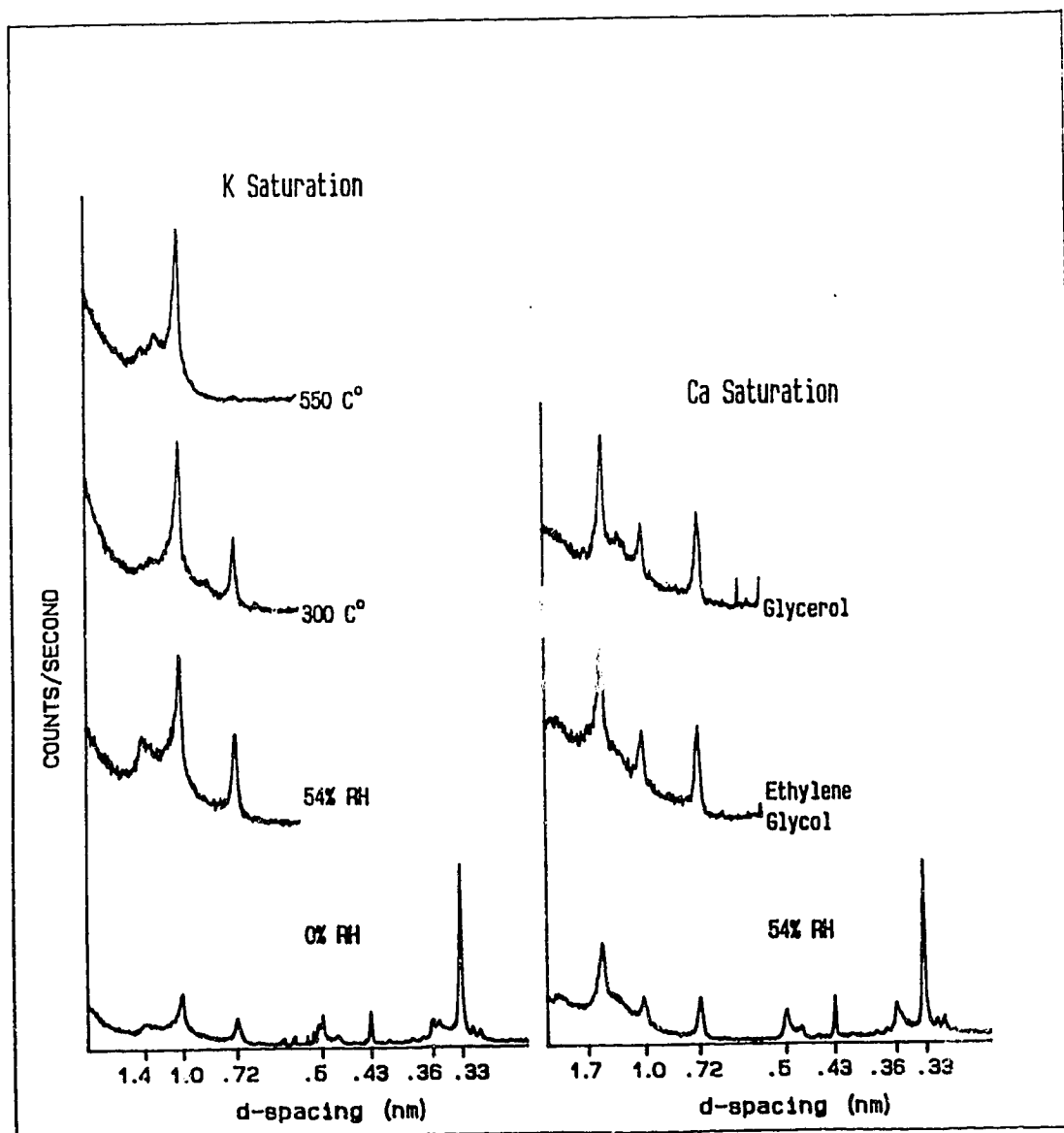


Figure 19. X-ray diffractogram of the clay separates from the E horizon of pedon 2.

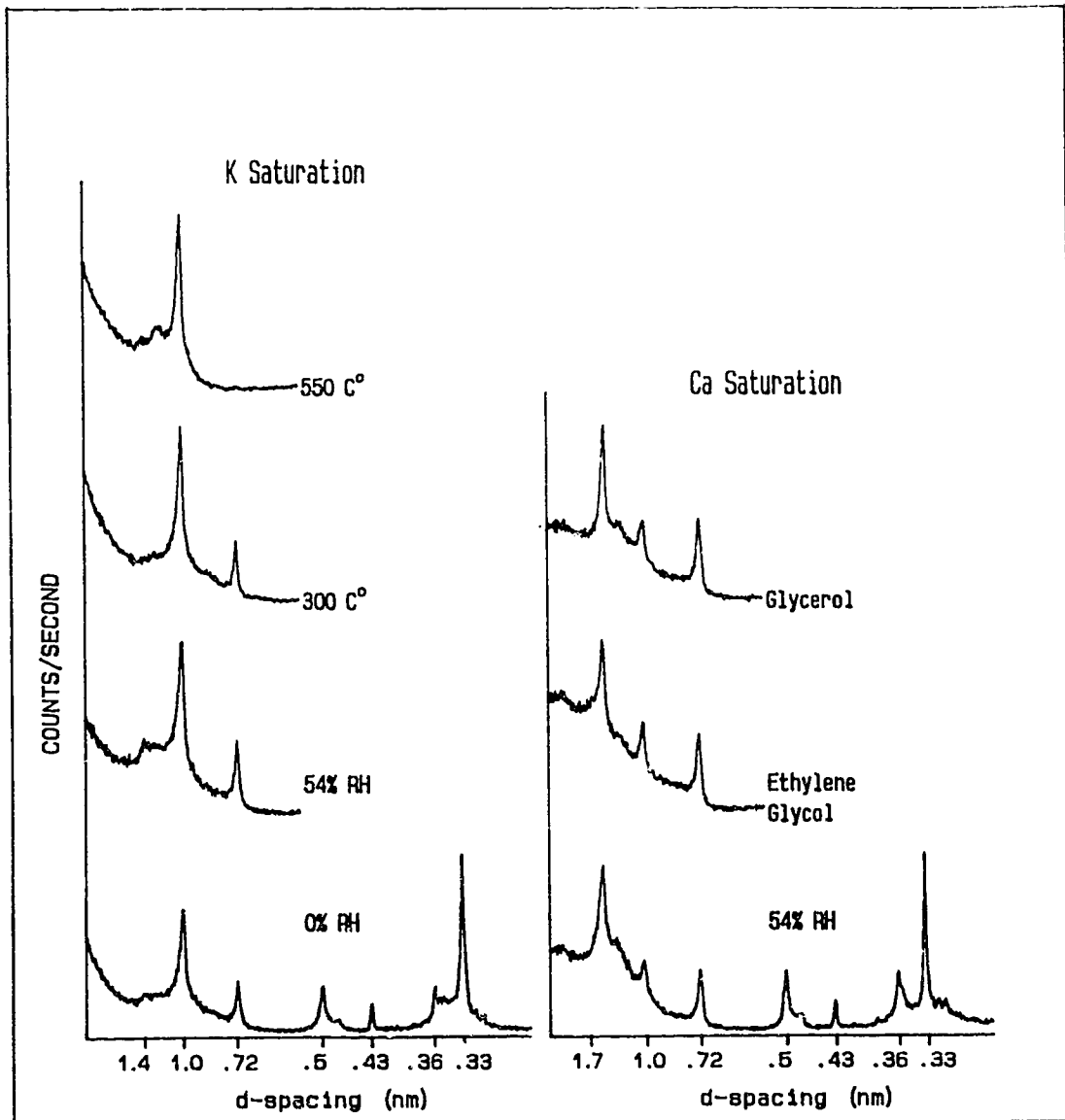


Figure 20. X-ray diffractogram of the clay separates from the Bt1 horizon of pedon 2.

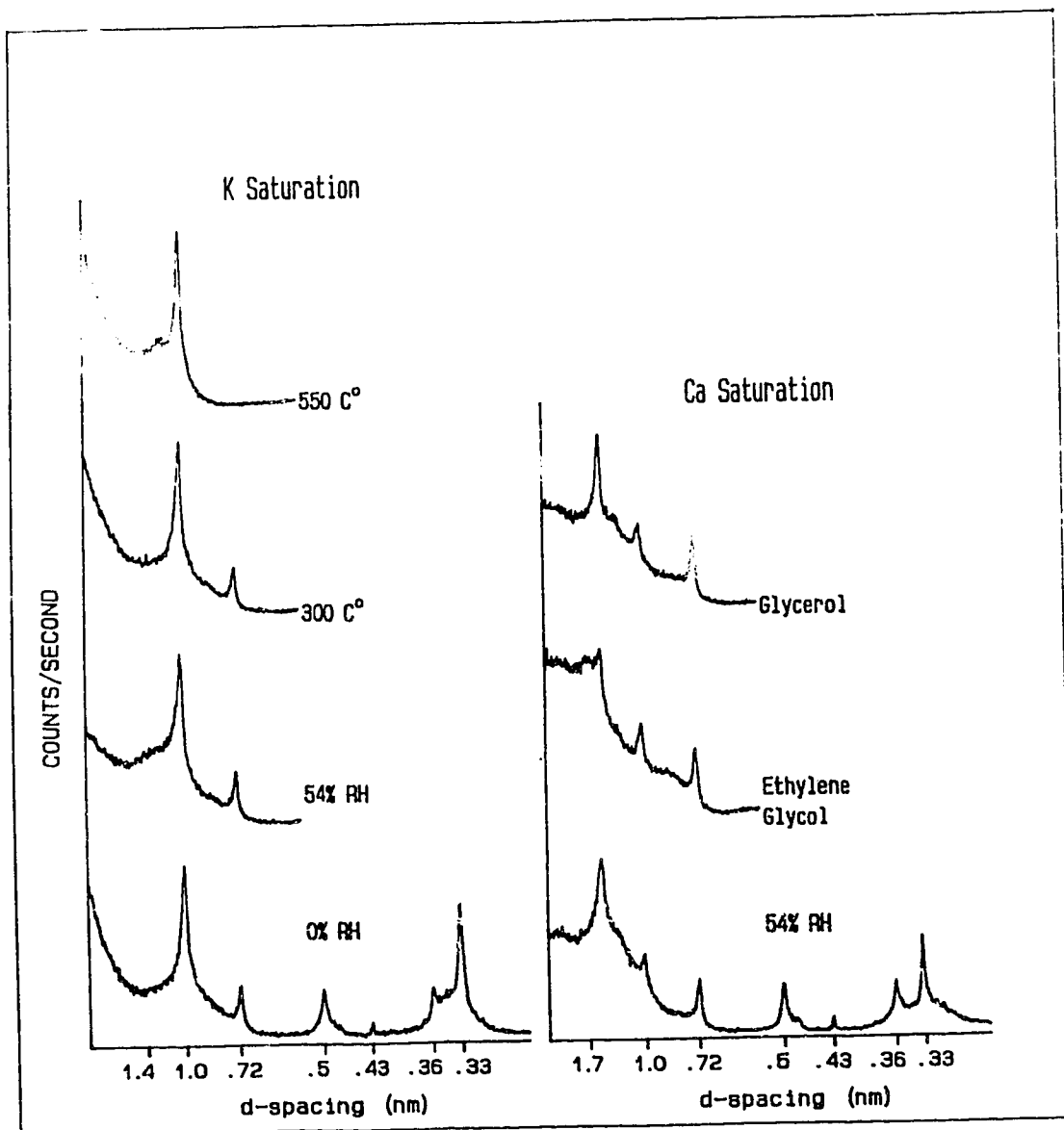


Figure 21. X-ray diffractogram of the clay separates from the Bt2 horizon of pedon 2.

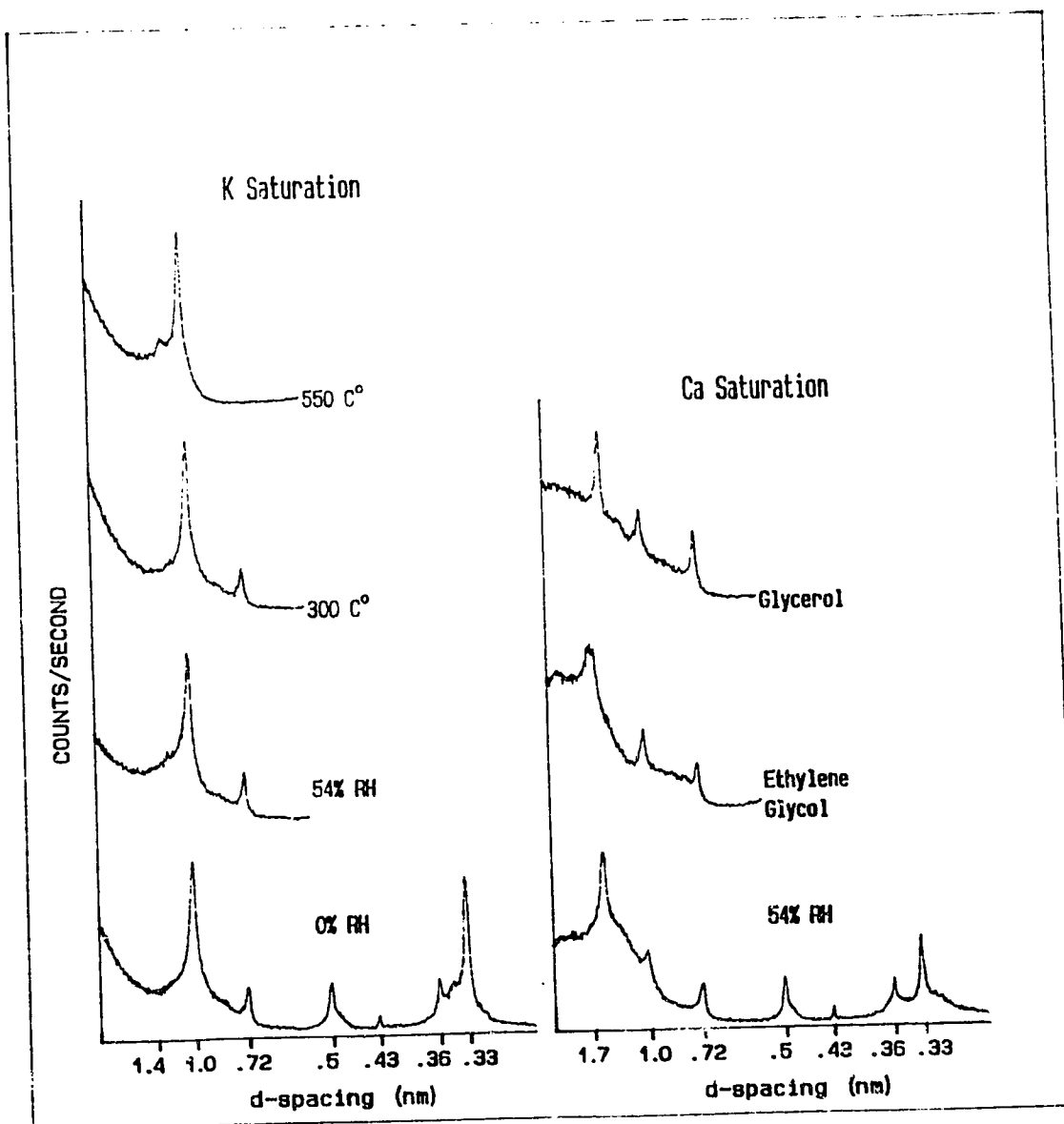


Figure 22. X-ray diffractogram of the clay separates from the Bt3 horizon of pedon 2.

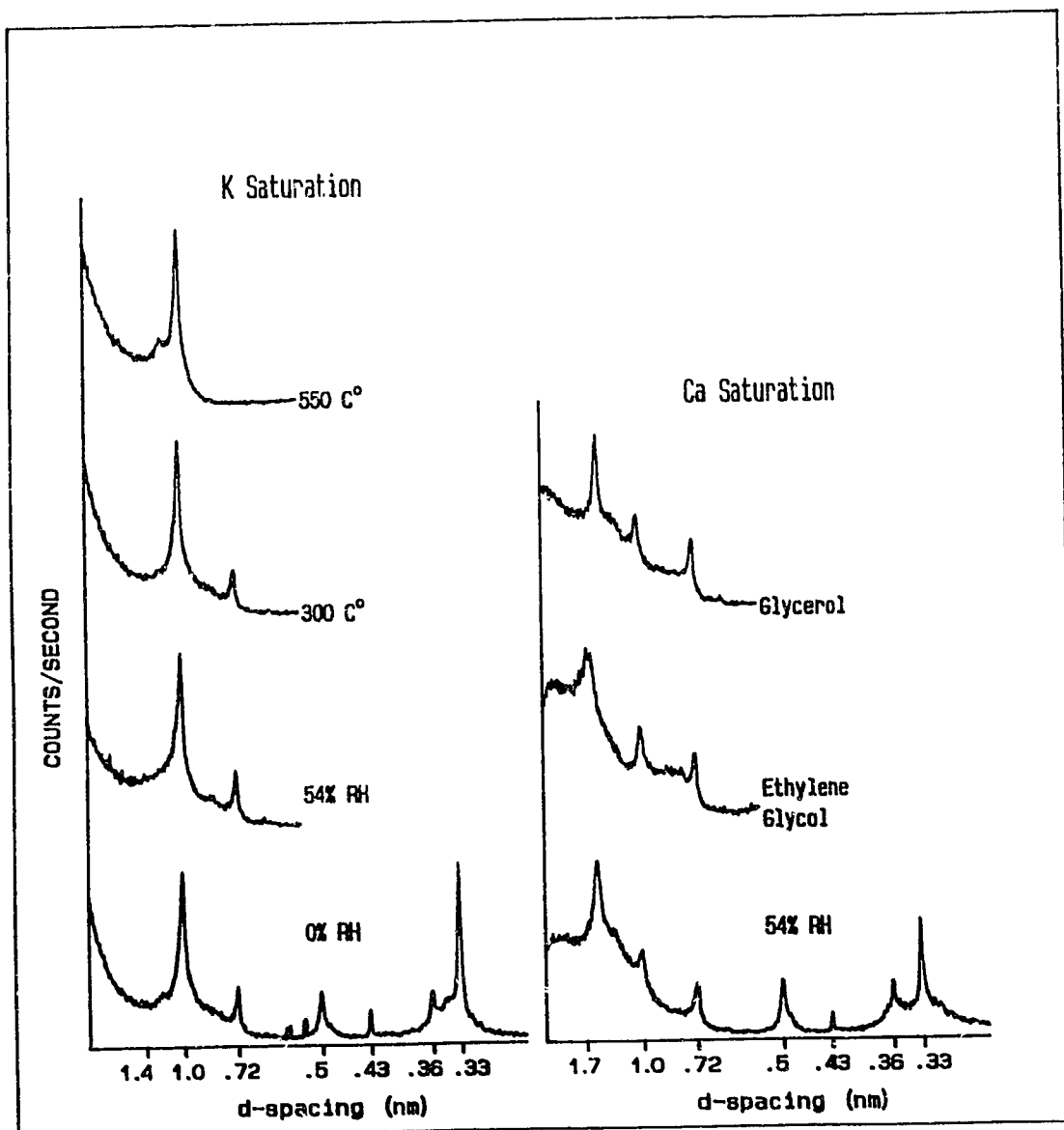


Figure 23. X-ray diffractogram of the clay separates from the C1 horizon of pedon 2.

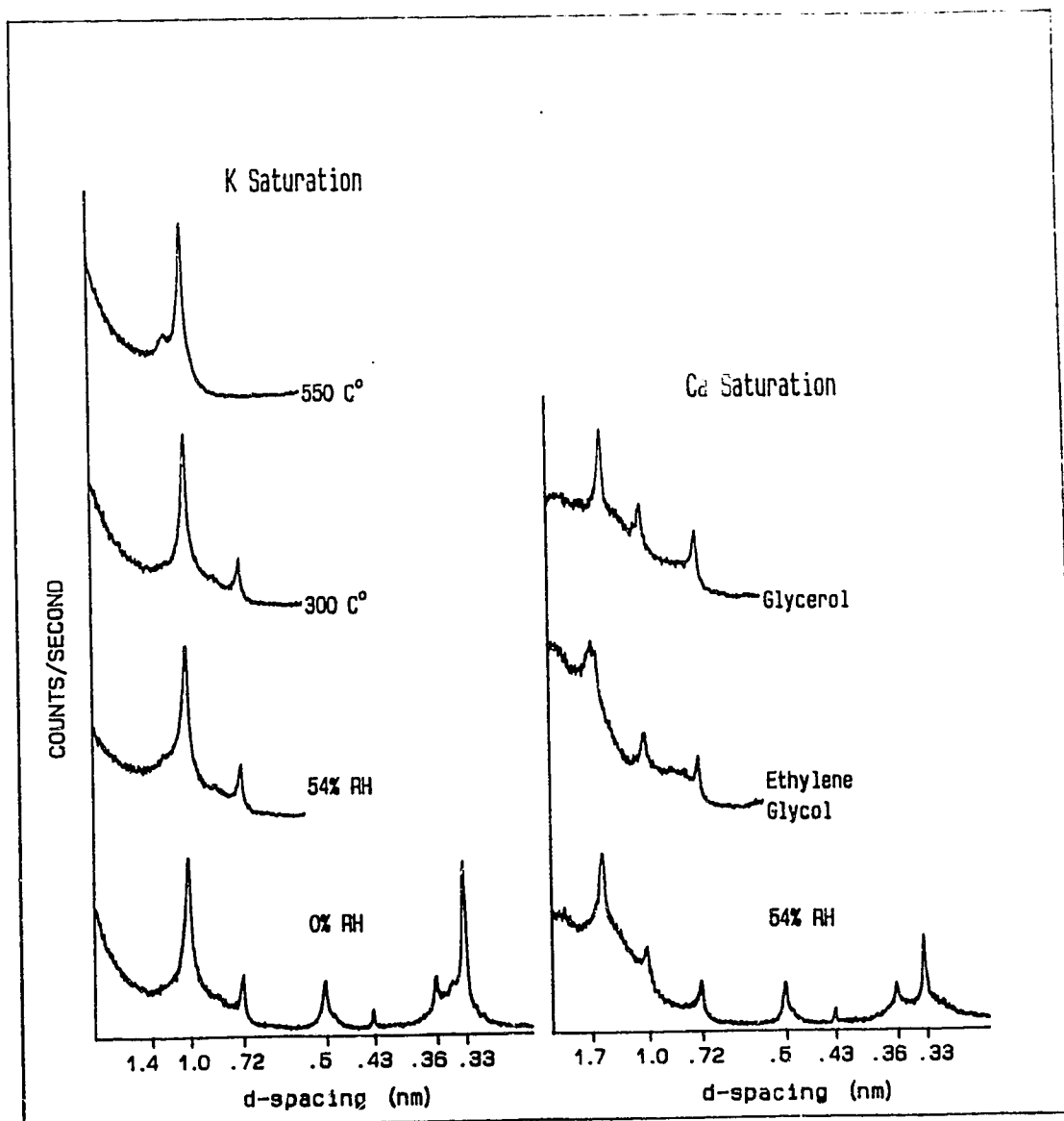


Figure 24. X-ray diffractogram of the clay separates from the C2 horizon of pedon 2.

Table 18. Surface area and chemical analysis of clay separates (average values for three pedons).

Horizon	Surface area m <sup>2</sup> /g	K <sub>2</sub> O	Al <sub>2</sub> O <sub>3</sub>	Fe <sub>2</sub> O <sub>3</sub> (g/kg)	MgO	Na <sub>2</sub> O	CEC cmol (+)/kg	
							Ca-sat.	K-sat.
Ah	270	22	92	61	9.0	3.8	48	35
Ae	240	24	99	69	7.4	5.7	23	11
Bt1	410	21	78	89	11	3.3	30	12
Bt2	490	17	93	97	12	2.3	42	20
Bt3	490	18	92	96	9.2	2.7	41	20
C1	480	17	94	98	9.6	2.0	40	20
C2	470	17	96	94	8.8	2.0	37	17

Table 19. Distribution of clay mineral species within the clay sized fraction.

horizon	(g/kg)			
	Mica	Vermiculite	VSI†	Kaolinite + others
Ah	220	90	310	410
E	240	80	100	580
Bt1	210	120	110	560
Bt2	170	150	180	500
Bt3	180	140	190	490
C1	170	130	180	520
C2	170	130	170	530

† denotes vermiculite-smectite intergrades.

*situ* from weathering of mica and micaceous vermiculite through reduction of layer charge. Mechanisms of decrease in layer charge have been discussed by Borchardt (1989) and Jackson and Luo (1986). K-fixing capacity, surface area determination, and x-ray analysis of clay separates of this study indicated the presence of vermiculite-smectite intermediate (VSI) minerals. The remaining CEC of clay separates, after deducing the amount of soil vermiculite, mica, and kaolinite, was attributed to the vermiculite-smectite intermediates (Table 19).

Mica occurred in all samples. This clay mineral was identified by the consistent presence of the 1.0 nm peak for all the treatments. The 0.50 nm peak for the Ca-saturated samples at 54% relative humidity indicated the mica was dioctahedral, mostly likely muscovite (Fanning *et al.* 1989). The interpretation of biotite was complicated by 0.50 nm peaks. The 060 spacing (0.152-0.154 nm) in XRD patterns of randomly oriented specimen would be required to confirm the presence of trioctahedral mica (biotite). The broad shoulder on the high angle side of the 1.0 nm peak for Ca-saturated samples was indicative of hydrous mica.

Identification of kaolinite was based on the presence of the 0.72 nm peak which disappeared with heating at 550° C. The interpretation of kaolinite was not confounded by chlorite since the latter phyllosilicate was not present in these samples.

The presence of minor amounts of chloritic intergrades was indicated by broad peaks or shoulders between 1.0 nm and 1.4 nm for K-saturated specimens heated at 550° C. Chloritic intergrades can be defined as those 2:1 phyllosilicate clay minerals with partial infilling of hydroxy Al material. Therefore, they could be either hydroxy interlayered vermiculite (HIV) or hydroxy interlayered smectite (HIS). X-ray analyses of K-saturated specimens heated at different temperatures indicated a low degree of interlayer infilling for chloritic intergrades in this study.

Chloritic intergrades observed in this study may have been formed *in situ* from progressive filling of interlayer space of vermiculite or smectite with hydroxy-Al material. Formation of hydroxy interlayered minerals from vermiculite and smectite in acid soil environments was also reported by Barnhisel and Bertsch (1989), Jackson (1963), Kirland and Hajek (1972), and Rich (1968).

Quartz and feldspar were present in very trace amounts as indicated by low intensities of their corresponding diagnostic x-ray diffraction peaks. The presence of quartz



was confirmed by 0.43 nm and 0.33 nm peaks for the Ca-saturated samples at 54% relative humidity. The occurrence of a 0.32 nm peak for the Ca-saturated samples at 54% relative humidity was indicative of the presence of feldspar.

The proportion of each mineral species varied with profile depth (Table 19). It should be noted that profile distribution of mica and soil vermiculite in this study did not show the trend commonly reported in the literature (Allen and Hajek 1989; Howitt and Pawluk 1985). A high content of mica and low content of vermiculite occurred in surface horizons (Ah and E) in this study. This is not consistent with the higher weathering intensity at surface horizons which promotes depotassification. Therefore, there must be some addition of mica onto surface horizons during pedogenesis. It is proposed in this study that addition of mica may be fall-out of tropospheric dust (aerosol).

The Gobi Desert of China and Mongolia, the Takla Makan Desert of extreme western China, and the Loess Plateau of northwestern China could be major sources of aerosolic dust over the Three River Plain. During winter and spring (roughly November through May), Central Asia, western China, and northwestern China are at their driest condition, in response to the cold, dry Siberian high pressure system. The powerful cyclones and anticyclones of this high pressure system could create strong up-down air movements while passing through the Deserts and Loess Plateau. After agitation by strong winds, the sediment of the Deserts and, to lesser extent, of the Loess Plateau was incorporated into the upper westerlies. The sediment was then transported and disseminated, eventually falling over the Loess Plateau and the region to the east and south. The dust incorporated in the upper westerlies could be transported to great distances. For example, dust originating in the Gobi Desert, the Takla Makan Desert, and the Loess Plateau was reportedly found in Alaska (Rahn *et al.* 1981), the Northwest Pacific Ocean (Blank *et al.* 1985; Rea and Leinen 1988), and in Japan (Syers *et al.* 1972). Therefore, aerosolic dust must fall over the the Three River Plain especially upon precipitation and during the Holocene when velocity of westerlies were thought to be less. The high mica content in surface horizons of white clay soils of this study agrees with the analysis which shows mica was a major clay mineral of aerosolic dust (Liu 1985; Syers *et al.* 1972).

Soil vermiculite and VSI were enriched in Bt horizons relative to the E horizons. This may be partly attributed to lessivage since these expandable clay minerals are more susceptible to eluviation compared to mica and kaolinite. Also, the addition of mica from

tropospheric dust relatively lowered percentages of vermiculite and VSI in clay separates in this study.

Elemental data on analysis of clay separates can be found in Table 18. The distribution of elements in clay separates among horizons was nearly constant.

### **Silt Mineralogy**

Silt mineralogy was studied by x-ray powder diffraction and petrographic analysis. The x-ray diffractograms of the silt fractions separated from the three pedons are shown in Appendix I. Quartz and feldspar were dominant minerals. Mica and vermiculite was present in minor amounts. The petrographic examination revealed the presence of amorphous Fe and Mn nodules in addition to quartz and feldspar.

### **Sand Mineralogy**

Content of sands was usually less than six percent. Fe-Mn nodules composed a considerable portion of the sand fraction, especially in the E horizon.

Mineralogical characterization of sands was facilitated by heavy liquid separation, x-ray diffraction, scanning electron microscopic (SEM) and petrographic examination. The heavy fraction was primarily composed of Fe-Mn nodules. The lack of primary ferromagnesian minerals indicates the parent material of white clay soils had experienced intense geochemical weathering. The light mineral fraction consisted of quartz, feldspar, and Fe-Mn nodules as well.

The surface morphology of quartz grains examined by the scanning electron microscope (SEM) was generally characterized by irregular shapes, rounded edges, low to moderate relief, and smooth surfaces (Plate 1). These features may be attributed to edge abrasion caused by fluvial transport (Krinsley and Takahashi 1962; Krinsley and Doornkamp 1973). Chemical dissolution and precipitation of silica may also account for the smooth surfaces (Crook 1968; Krinsley and Doornkamp 1973; Black and Dudas 1986). There were no features indicative of glacial and eolian transport as outlined by Krinsley and Doornkamp (1973).

Samples of white, porous sand grains were selected and examined with the scanning electron microscope (Plate 2). The examination revealed that these grains were extensively weathered feldspars. The feldspars from the surface soil horizons appeared to

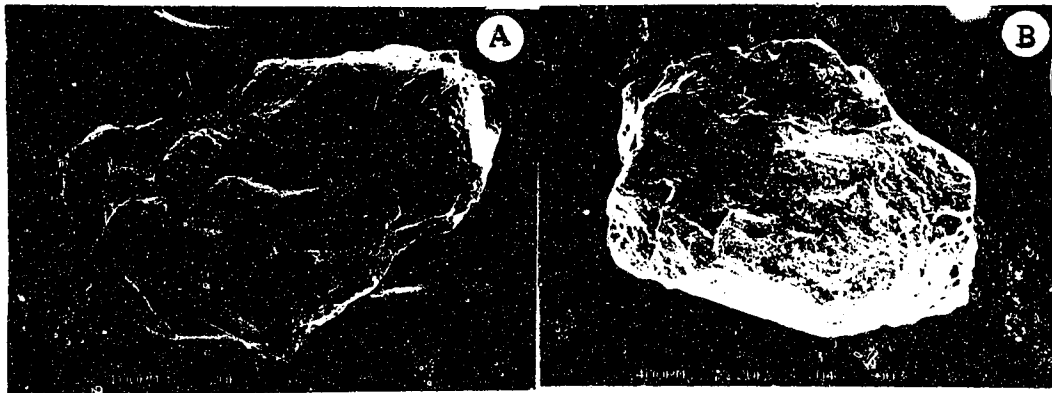


Plate 1. Scanning electron micrographs of quartz grains. A, smooth surfaces of a quartz grain from the E horizon. B, rounded edges of a quartz grain from the C horizon.

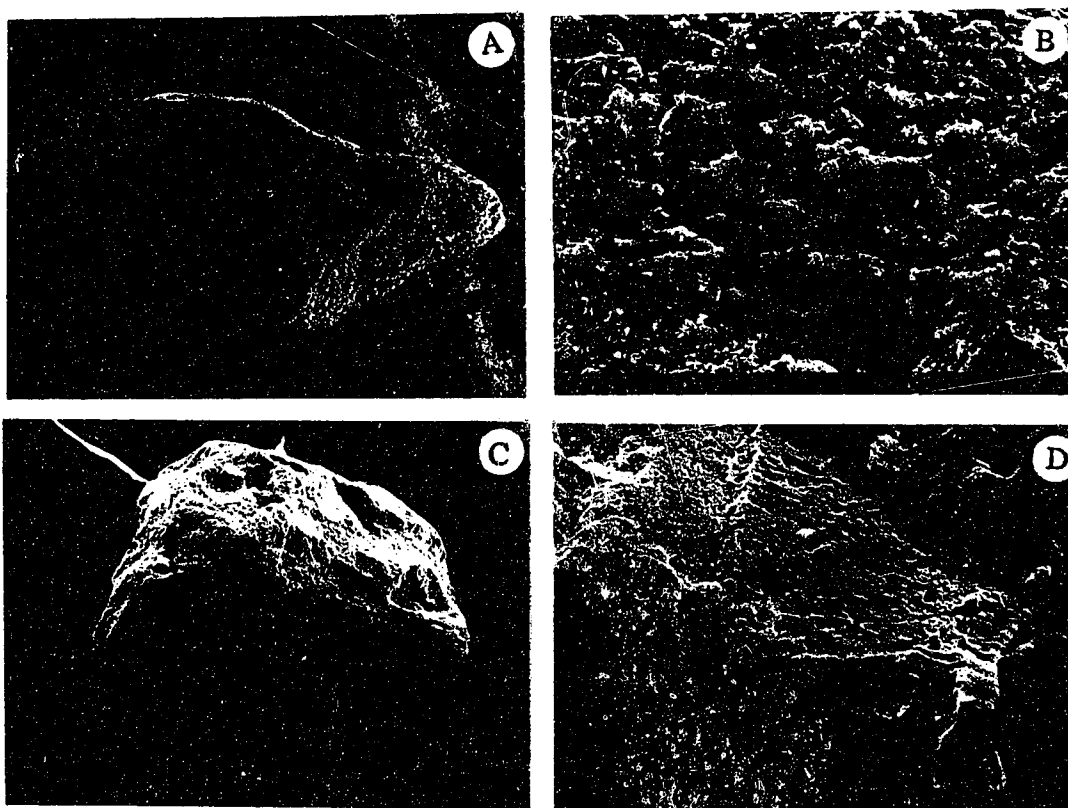


Plate 2. Scanning electron micrographs of feldspar grains. A, highly weathered feldspar grain from the E horizon. B, close-up of A. C, relatively less weathered feldspar grain from the C horizon. D, close-up of C.

be more chemically weathered than the feldspar in the lower horizons. Feldspar grains from the surface horizons exhibited extensive surface dissolution. Cleavage plates were not readily observed, while the feldspar grains from the lower horizons showed less dissolution and some weathering along parallel cleavage plates (Plate 2).

Most nodules in the sand fraction were rounded in shape and some were hollow (Plate 3). Compound nodules were also often observed (Plate 3). While surface topography was generally smooth, the surface pores were fine and numerous (Plate 3, A and D). Quartz and feldspar grains were embedded in Fe-Mn nodules (Plate 4). The elemental composition of nodules determined by energy dispersive x-ray analyses was Si, Al, Mn, Fe, K, and Ca in decreasing order of abundance. It was not uncommon for the content of Fe to be higher than the content of Mn in nodules.

The mineralogy of nodules was determined by powder x-ray diffraction. The x-ray diffraction patterns of the nodules from different horizons were similar. A diffractogram for a typical sample is shown in Figure 25, and others can be found in Appendix I. Only quartz, feldspar, and mica peaks could be identified. None of the peaks could be ascribed to Fe and Mn minerals. Even step scanning did not indicate the presence of any Fe or Mn minerals, suggesting these two elements occurred in amorphous forms. The Fe-Mn compounds may simply form coatings around skeleton grains of quartz and feldspar. Several other researchers were also unable to detect crystalline Fe or Mn compounds in Fe-Mn concretions (Childs 1975; Sidhu *et al.* 1977). The similarity between the nodules and adjacent soil matrix indicates that the nodules may have developed *in situ*. Similar considerations have been used by Wieder and Yaalon (1974) to identify orthic carbonate nodules and by Sidhu *et al.* (1977) to identify orthic Fe-Mn concretions.

### C. Trace Elements

In this section, the background levels of 30 trace elements will be presented. Profile distribution of the trace elements and their pedogenic implications will also be discussed.

A total of 21 horizon samples from three pedons of typical white clay soils were analyzed for total contents of 30 trace elements in bulk soil samples (<2.0 mm, i.e. fine earth fraction, Table 20) and of 26 elements in clay separates (< 2.0  $\mu\text{m}$  Table 21). However, only the results of pedon 2 are presented in this section. The information on

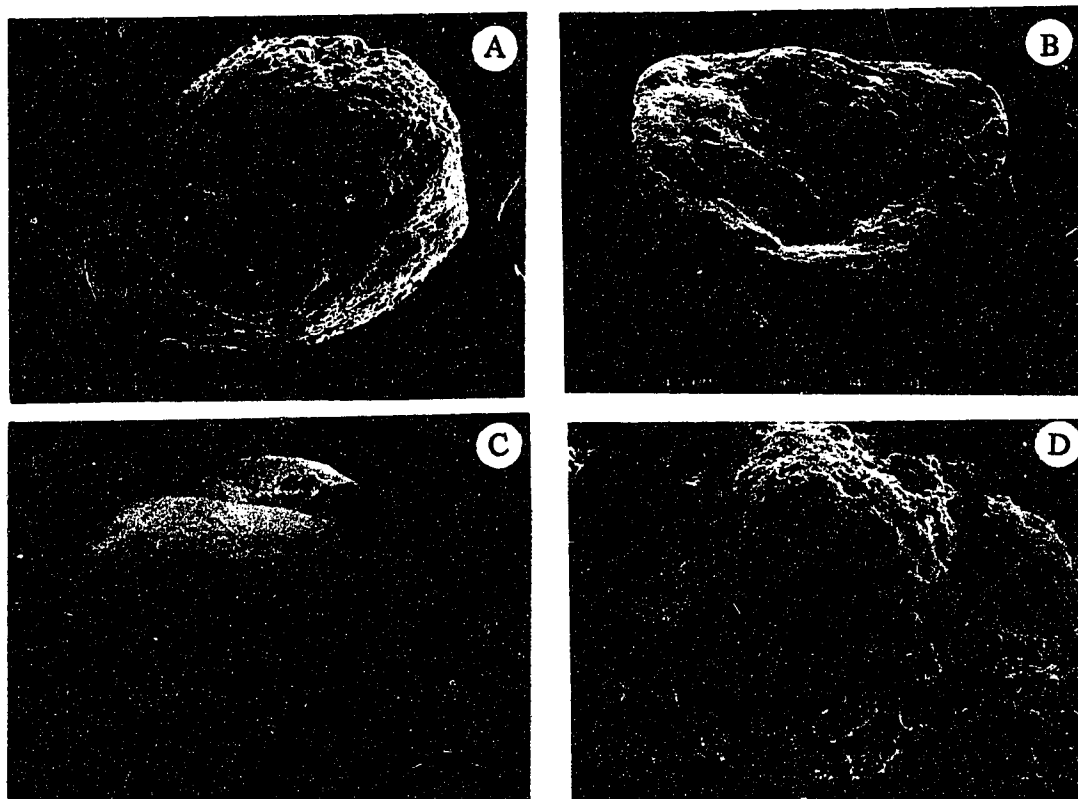


Plate 3. Scanning electron micrographs of Fe-Mn nodules of the E horizon. A, a rounded nodule. B, a hollow nodule. C, a compound nodule. D, close-up of C.

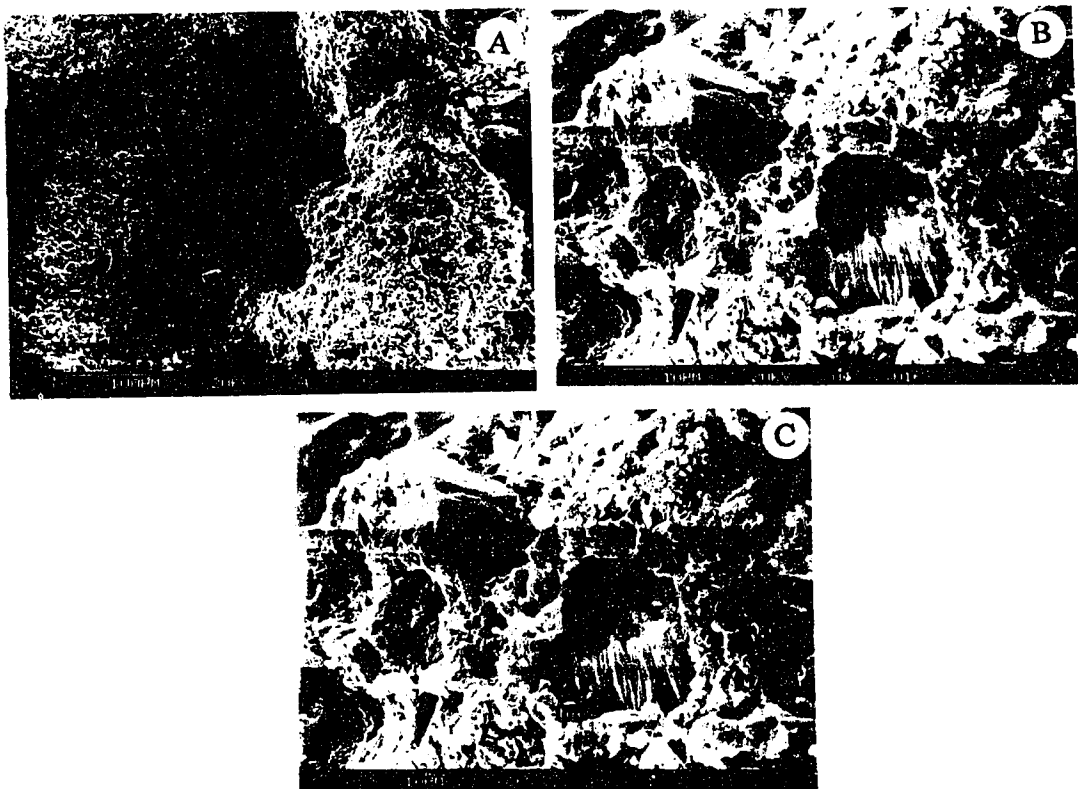


Plate 4. Scanning electron micrographs of an Fe-Mn nodule of the E horizon.  
A, the surface of the nodule. B and C, Close-up of A showing quartz and feldspar grains embedded in the nodule.

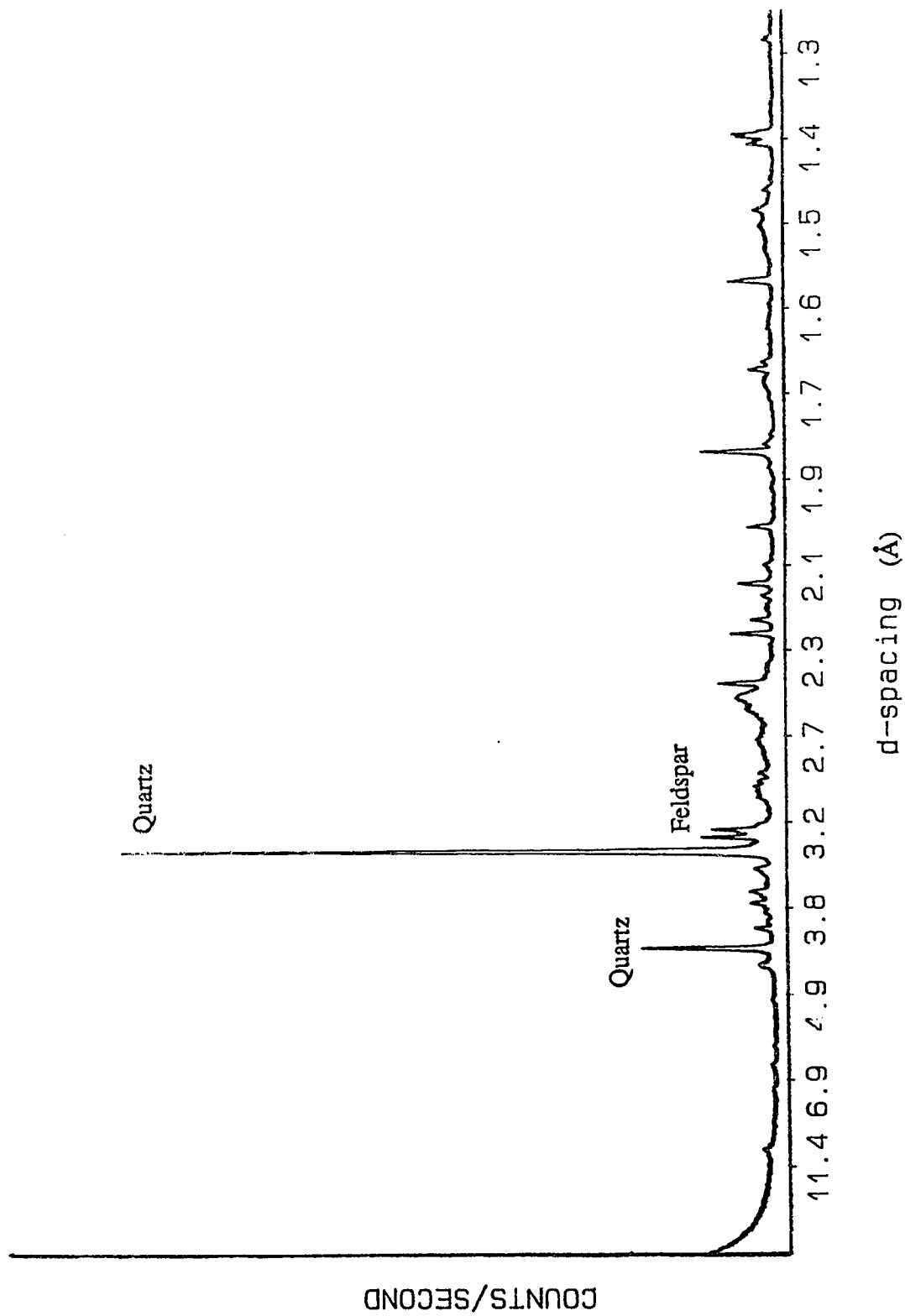


Figure 25. X-ray diffractogram of Fe-Mn nodules from the E horizon of pedon 2.



Table 20. Total content (mg/kg) of trace elements in bulk soil samples and literature values for terrestrial material.

Element	DL†	A	As	Btl	Bt2	Bt3	C1	C2	Granite‡	Shale‡	Crust‡, #	Soil #
Ag	0.2	†	†	†	†	†	†	†	0.04	0.1	0.07	0.05
As	0.2	12	18	9.4	13	12	11	13	1.5	6.6	1.5	7.2
Au(µg/kg)	1.0	1	2	1	†	†	†	†	§	§	§	§
B	0.2	38	42	40	37	40	38	37	15	100	10	33
Ba	20	540	590	520	580	610	610	580	600	580	500	580
Br	0.5	5	1.6	1.1	0.6	0.8	0.5	0.4	1.3	6.0	0.37	0.85
Cl	10	§	§	§	§	§	§	§	200	160	130	100
Co	0.1	11	21	7.7	10	15	14	16	1.0	20	20	9.1
Cr	0.2	28	52	60	71	60	38	44	4.0	100	100	54
Cs	0.1	3.7	4.4	5.3	6.8	7.5	8.4	8.2	5.0	5.0	3.0	4.0
Ga	5.0	†	†	†	†	18	21	†	18	19	18	17
Hf	0.1	6.2	6.8	6.1	5.5	5.6	5.1	5.6	4.0	6.0	3.0	§
Hg(µg/kg)	0.4	53	27	33	50	46	44	44	80	40	50	90
I	0.5	5.5	3.5	†	4.4	4.6	3.4	3.8	0.5	1.0	0.14	1.2
Mn	0.1	1200	1500	330	350	620	480	590	400	850	950	550
Mo	0.4	†	†	†	†	†	†	†	2.0	2.0	1.5	0.97
Ni	50	†	†	†	†	60	†	†	0.5	95	80	19
Rb	5.0	110	120	120	160	150	160	140	150	140	90	67
Sb	0.1	1.0	1.4	0.9	0.7	1.3	1.1	1.3	0.2	1.5	0.2	0.66
Sc	0.05	9.5	8.3	10	14	14	12	13	5.0	10	16	8.9
Se	0.5	†	0.9	1.2	†	2.6	†	†	0.05	0.6	0.05	0.39
Sr	2.0	140	130	130	110	120	110	110	285	450	370	240
Ta	0.1	0.8	1.2	†	1.4	†	1.0	0.9	§	§	§	§
Th	0.1	9.9	13	9.5	10	13	10	11	17	11	12	9.4
Ti	5.0	4800	4800	4800	4500	4600	4500	4600	2300	4500	5600	2900
U	0.01	3.1	3.8	3.1	3.6	3.6	3.5	3.5	4.8	3.2	2.4	2.7
V	0.5	62	90	110	120	100	83	95	20	130	160	80
W	1.0	1.0	1.0	1.0	1.0	†	1.0	1.0	2.0	2.0	1.5	§
Zn	3.0	73	63	73	120	110	66	89	40	80	75	60
Zr	3.0	290	310	280	240	240	260	250	180	200	190	230

† denotes detection limits; ‡ denotes contents below detection limits; § denotes data unavailable.

¶ taken from Krauskopf (1978); # taken from Sposito (1989).

Table 21. Total content (mg/kg) of trace elements in clay separates and literature values for terrestrial material.

Element	DL†	A	As	Btl	Bt2	Bt3	C1	C2	Granite‡	Shale‡	Crust.‡, #	Soil#
Ag	0.2	5.4	4.3	‡	4.1	5.0	5.0	4.9	0.04	0.1	0.07	0.05
As	0.2	16	15	20	22	2.0	21	20	1.5	6.6	1.5	7.2
Au(µg/kg)	1.0	4.0	7.0	5.0	4.0	2.0	8.0	9.0	‡	‡	‡	‡
B	0.2	41	40	42	41	44	36	37	15	100	10	33
Ba	20	540	450	450	450	450	450	480	600	580	500	580
Br	0.5	17	3.8	2.1	2.4	0.7	1.0	1.3	1.3	6.0	0.37	0.85
Cl	10	160	40	30	50	30	40	40	200	160	130	100
Co	0.1	15	15	13	14	17	15	18	1.0	20	20	9.1
Cr	0.2	97	96	110	120	100	100	100	4.0	100	100	54
Cs	0.1	12	13	13	15	16	16	17	5.0	5.0	3.0	4.0
Ca	5.0	26	24	28	39	24	23	52	18	19	18	17
Hf	0.1	4.9	5.5	5.4	5.1	4.1	4.2	5.0	4.0	6.0	3.0	‡
Hg(µg/kg)	0.4	‡	‡	‡	‡	‡	‡	‡	80	40	50	90
I	0.5	190	100	53	63	51	53	49	0.5	1.0	0.14	1.2
Mn	0.1	600	590	200	290	430	430	630	400	850	950	550
Mo	0.4	‡	‡	0.8	0.6	‡	‡	0.9	2.0	2.0	1.5	0.97
Ni	50	‡	‡	‡	110	‡	‡	‡	0.5	95	80	19
Rb	5.0	200	220	200	200	220	210	230	150	140	90	67
Sb	0.1	1.8	1.7	1.9	2.0	1.8	1.9	1.8	0.2	1.5	0.2	0.66
Sc	0.05	22	25	25	25	27	26	27	5.0	10	16	8.9
Se	0.5	‡	5.7	‡	‡	3.2	2.7	5.2	0.05	0.6	0.05	0.39
Sr	50	‡	‡	‡	‡	‡	‡	‡	285	450	370	240
Ta	0.1	0.8	1.2	0.9	0.9	0.9	0.7	0.8	‡	‡	‡	‡
Th	0.1	19	20	22	18	16	17	16	17	11	12	9.4
Ti	20	4100	4600	2800	2700	2600	2500	3000	2300	4500	5600	2900
U	0.01	4.3	4.8	4.4	4.1	4.1	3.8	4.3	4.8	3.2	2.4	2.7
V	0.5	130	140	100	110	99	100	130	20	130	160	80
W	1.0	3.0	3.0	3.0	3.0	2.0	2.0	2.0	2.0	2.0	1.5	‡
Zn	3.0	90	95	100	110	100	95	100	40	80	75	60
Zr	3.0	‡	‡	‡	‡	‡	‡	‡	180	200	190	230

† denotes detection limits; ‡ denotes contents below detection limits; § denotes data unavailable.

¶ taken from Krauskopf (1978); # taken from Sposito (1989).

trace elements for pedon 1 and 3 can be found in Appendix II. Detection limits of each element are displayed in Table 20). Selected elements in bulk soil samples were used to construct graphs (concentrations vs depth, Figs. 26-32).

Contents of Ag, Au, Cl, Ga, Mo, Ni, Ta, and W were generally below their respective detection limits in one or more horizons for bulk soil samples. Profile distribution of these elements will not be discussed individually. The contents of these elements in some horizons are given in Table 20.

Content of arsenic (As) varied from 8.2 to 23 mg/kg for all 21 bulk soil samples with most values in the range of 11 - 13 mg/kg. The element was markedly enriched in the E horizon and slightly depleted in the Bt1 horizon as compared to the C horizon. Arsenic content tended to increase with depth from the Bt1 horizon (Fig. 26). The mean content of Arsenic was 12 mg/kg for all the bulk soil samples. The average content was 18 mg/kg in the clay separates.

Profile distribution of boron (B) appeared uniform within and among pedons. Boron content ranged from 37 to 47 mg/kg with a mean of 40 mg/kg in bulk soil samples. The coefficient of variability for 21 soil samples was 2.1 %. The B content in clay separates was essentially same as that in bulk soil samples.

Content of barium (Ba) ranged from 500 to 650 mg/kg for 21 bulk soil samples. The element was more or less evenly distributed throughout the soil. The mean of Ba was 581 mg/kg. Ba content in bulk soil was slightly higher than in clay separates.

Bromine (Br) displayed a profile distribution pattern characterized by consistently enriched levels in surface horizons compared to amounts in the lower solum. Br content ranged from 0.4 to 9.1 mg/kg for bulk soil samples with an average of 1.7 mg/kg. The same trend was observed for clay separates. The content of Br was higher in the clay separates and the average was 4.7 mg/kg.

Total soil samples from E horizons were generally enriched in cobalt (Co). The lowest Co content occurred in the Bt1 horizon, then, the content of the element increased with depth. The range of cobalt content was between 7.1 and 35 mg/kg with an average of 14 mg/kg. There was no marked difference in Co content between bulk soil and clay separates. Clay separates exhibited uniform Co profile distribution (mean = 13 mg/kg).

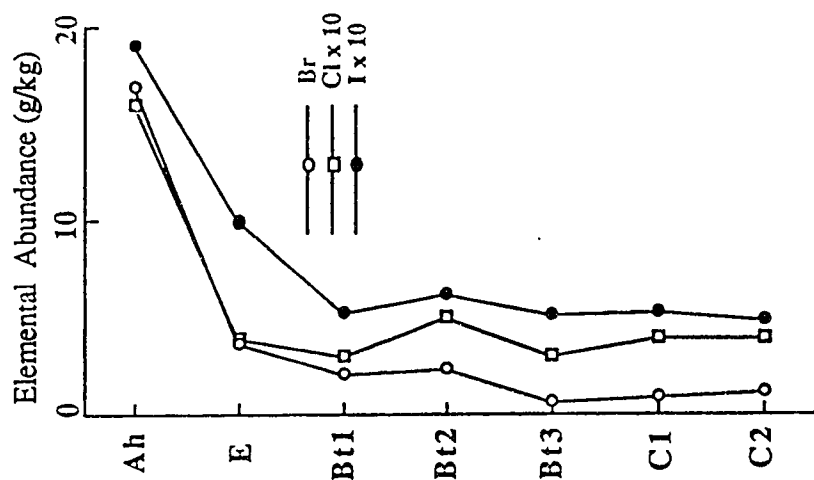


Figure 27. Profile distribution of Br, Cl, and I in the clay separates of Pedon 2.

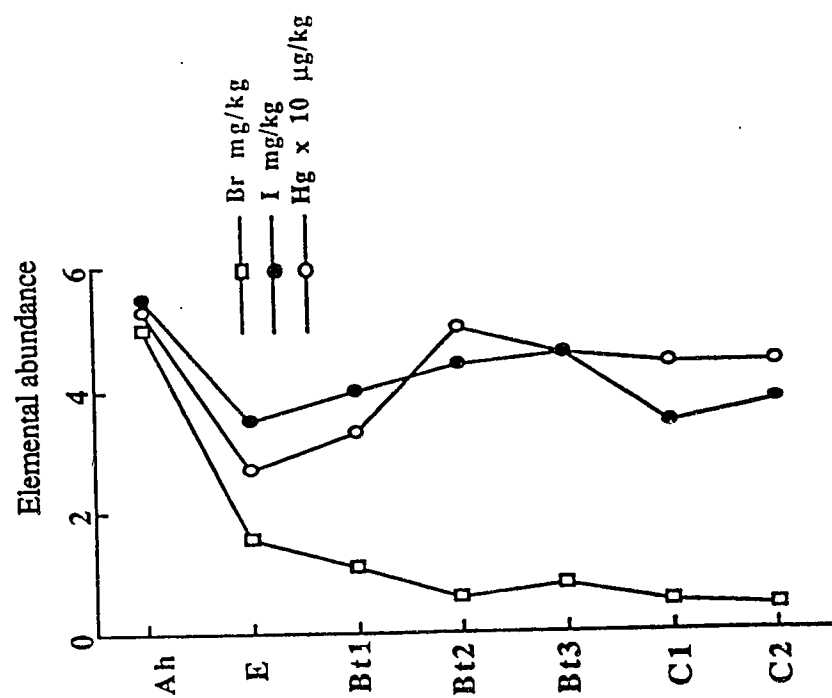


Figure 26. Profile distribution of Br, I, and Hg in the bulk soil of Pedon 2.

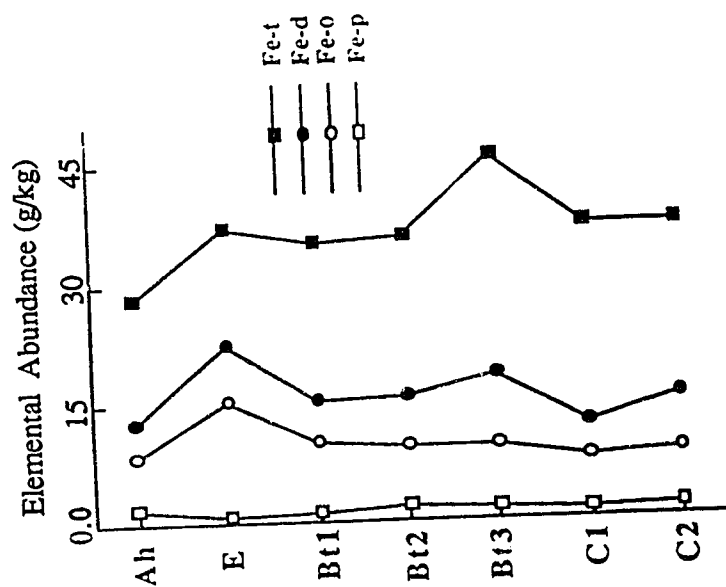


Figure 28. Total and extractable Fe with depth for pedon 3.

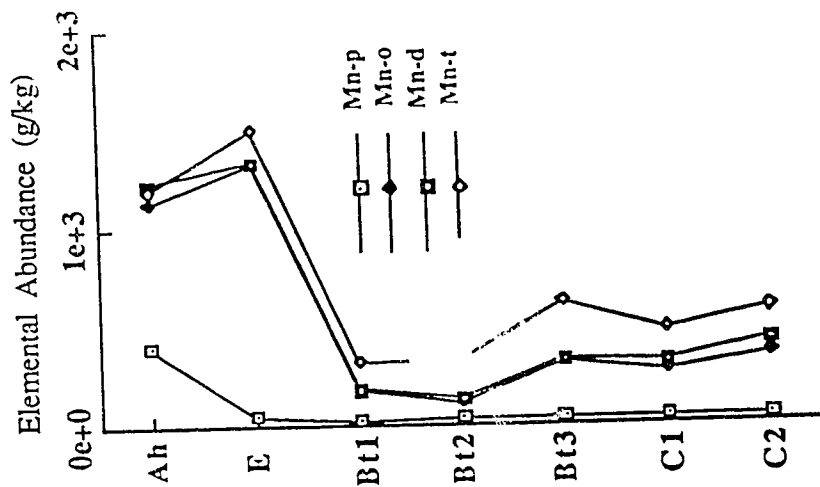


Figure 29. Total and extractable Mn with depth for pedon 2.

t denotes total content of Fe or Al ; d denotes dithionite extractable Fe or Al.  
o denotes oxalate extractable Fe or Al; p denotes pyrophosphate extractable Fe or Al.

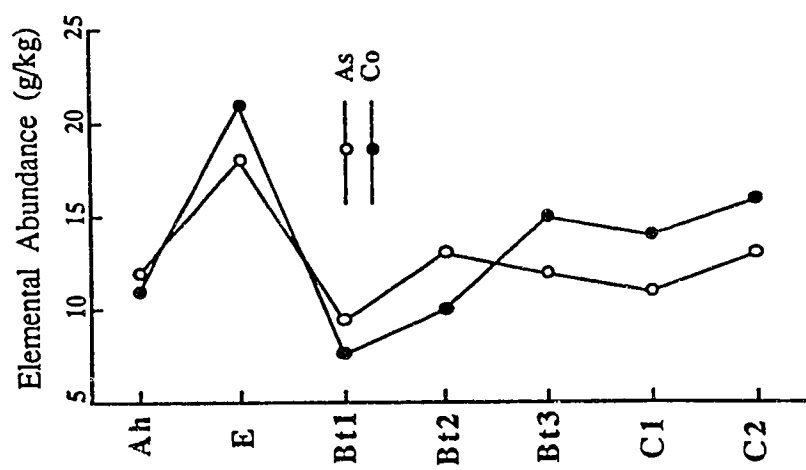


Figure 30. Profile distribution of As and Co in the bulk soil of Pedon 2.

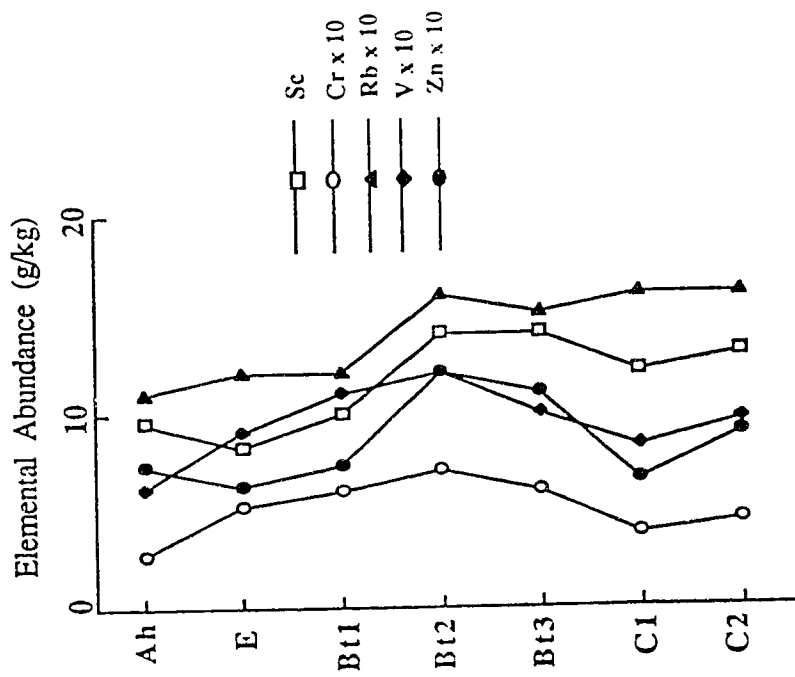


Figure 31. Profile distribution of Cr, Rb, Sc, V, and Zn in the bulk soil of Pedon 2.

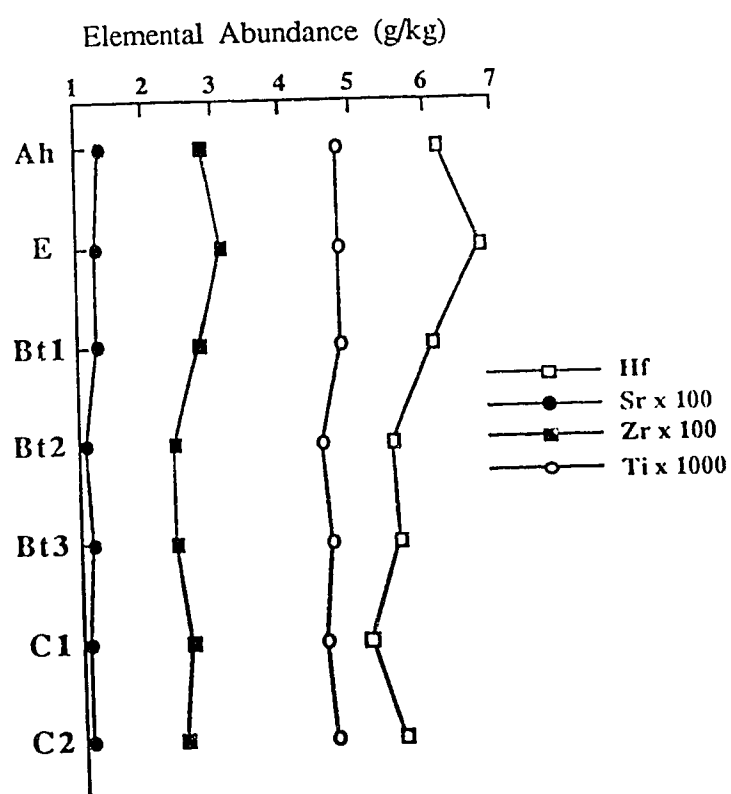


Figure 32. Profile distribution of Hf, Sr, Ti, and Zr in the bulk soil of Pedon 2.

Abundance of chromium (Cr) ranged from 26 to 71 mg/kg with an average of 50 mg/kg. Highest contents of the element usually appeared in Bt2 and Bt3 horizons, and lowest contents appeared in Ah and E horizons. Cr was highly concentrated in clay separates in comparison to bulk soil samples. Clay separates of different horizons have similar concentrations. The mean of Cr content in clay separates was 110 mg/kg.

Content of cesium (Cs) generally increased with profile depth and varied from 3.7 to 9.8 mg/kg with a mean of 7.1 mg/kg for 21 soil samples. The amount of Cs in clay separates was nearly twice as much as the amount in bulk soil. The mean Cs content in clay separates was 13 mg/kg.

Samples of all Ah horizons contained high amounts of mercury. Content of Hg content increased with depth from the E horizon and reached a maximum in the Bt2 horizon. The range of Hg content was from 23 to 64 µg/kg with a mean of 43 µg/kg for all bulk soil samples. The profile distribution pattern is shown in Fig. 21. Hg concentration in clay separates was not determined in this study.

Content of hafnium (Hf) in Ah, E, and Bt1 horizons is slightly higher than that in the other horizons. Profile distribution of the element was rather uniform (Fig. 32). The Hf content ranged from 5.1 to 7.5 mg/kg with a average of 5.9 mg/kg for all 21 bulk soil samples. Hf displayed some depletion in clay separates with regard to bulk soil. However, Hf content in clay separates was uniform throughout profiles.

Like bromine, iodine (I) was concentrated on the Ah horizon. For some horizons, iodine abundance was below the INAA detection limit. Clay separates were largely enriched with iodine. Clay separates from the Ah horizon contained the highest amount of iodine.

There was considerable variation in content of manganese (Mn) within pedons. The content of the element in Ah and E horizons was several fold higher than contents in lower horizons. The range in Mn content was from 330 to 1700 mg/kg with a mean of 773 mg/kg for all 21 bulk soil samples. Mn content in clay separates also showed a large variation, but smaller than the variation in bulk soil samples. The average Mn content in clay separates was 487 mg/kg.

Concentration of rubidium (Rb) increased with profile depth. Rb concentrations varied from 110 to 180 mg/kg with a mean of 142 mg/kg for all 21 bulk soil samples.



Rubidium was enriched in clay separates compared to bulk soil. There was little or no variation of Rb content in clay separates within pedons.

Antimony (Sb) behaved like arsenic. The largest content occurred in the E horizon. Content of the element ranged from 0.7 to 2.1 mg/kg with a mean of 1.3 mg/kg for whole bulk soil samples. Clay separates contained higher amounts of antimony relative to bulk soil. Nevertheless, Sb content in clay separates remained almost constant with depth.

Scandium (Sc) content ranged from 8.3 to 15 mg/kg and the average was 12 mg/kg for all 21 bulk soil samples. Content of the element appeared to be higher in Bt2 and Bt3 horizons for three pedons. The amount of scandium in clay separates (average = 25 mg/kg) was twice higher than in bulk soil. Sc profile distribution for clay separates was quite uniform within and among pedons.

Concentration of strontium (Sr) was analyzed by x-ray fluorescence for bulk soil; the element in clay separates was not determined. Strontium content varied from 110 to 140 mg/kg with a mean of 120 mg/kg in bulk soil. There was a slight accumulation of strontium in Ah and E horizons.

Thorium (Th) was one of the actinide series elements determined in this study. Its content ranged from 9.3 to 17 mg/kg with an average of 12 mg/kg for bulk soil. Like Mn and Co, the E horizon contained the largest amount of thorium. Th concentration in other horizons was uniform. Again, thorium was more concentrated in clay separates (mean = 18 mg/kg). There was no apparent change in Th content in clay separates with depth.

Titanium (Ti) ranged from 4100 to 5000 mg/kg and averaged 4650 mg/kg in bulk soil. Profile distribution of Ti seemed to very uniform within and among pedons except for some high values found for surface horizons. Titanium was significantly depleted in clay separates when compared to their respective bulk soil samples. The average content of titanium in clay separates was 2950 mg/kg.

Content of uranium (U) appeared higher in the E horizon than in other horizons. Also, the Bt2 horizon contained higher levels of uranium than adjacent horizons. The content of the element ranged from 3.1 to 4.0 mg/kg with a mean of 3.5 mg/kg for 21 soil samples. Uranium was enriched in clay separates (mean = 4.2 mg/kg).

Vanadium (V) values varied within pedons. Abundance of V in bulk soil ranged between 60 and 170 mg/kg. The average concentration of the element was 97 mg/kg.

Vanadium level in clay separates was generally higher than in bulk soil except for a few Bt horizons. The average concentration of vanadium in clay separates was 120 mg/kg.

Samples of all Bt2 and Bt3 horizons were noticeably enriched in zinc (Zn), while samples of all Ah and E horizons were depleted in the element. Content of zinc ranged from 57 mg/kg in a sample of an E horizon to 140 mg/kg in a sample of a Bt2 horizon. The average content of the element for 21 soil samples was 98 mg/kg. Like vanadium, zinc was generally concentrated in clay separates except for some Bt horizons. Zn content in clay separates was uniform with depth. The average content of zinc was 100 mg/kg for 21 clay samples.

Zirconium (Zr) in bulk soil was the second element measured by x-ray fluorescence. The element was not determined in clay separates. Zirconium values were similar within and among pedons. Zr concentration ranged from 230 to 340 mg/kg with the mean of 266 mg/kg in bulk soil. Zirconium was slightly enriched in Ah and E horizons and depleted in lower Bt horizons when compared to C horizons (Fig. 32).

Most of the trace elements determined in this study were enriched in clay separates relative to bulk soil samples (Table 20 and 21). The pattern and magnitude of trace element enrichment in clay separates varied according to elements. Some elements, such as Cl and Mn, were enriched in clay separates from surface horizons while elements such as Cs were concentrated in clay separates from the bottom horizons. For the trace metals of the fourth period, the order of enrichment in clay fractions relative to bulk soil was Cr (2.2) > Sc (2.1) > V (1.2) > Zn (1.0) > Co (0.9) > Mn (0.6) = Ti (0.6). The enrichment factors were calculated on basis of the averages for of clay separates and bulk soil samples.

Results of this study (table 20 and 21) indicated that total content of 30 trace elements in these white clay soils closely reflected the geochemical distribution of elements in the rocks which constitute the source of mineral components in the alluvial deposits. The parent material of white clay soils resulted from extensive geochemical weathering of granites in Xiaohinggan and Wandan Mountains during Late Pleistocene and Early Holocene when the climate was warm and humid. The weathered materials were transported and deposited in the Three River Plain by water (Xie 1982). The composition and concentrations of trace elements in different types of rocks, the earth's crust, and soils have been extensively documented by a number of authors (Taylor 1965; Krauskopf 1979; Swaine 1955; Bowen 1979; Shacklette and Boerngen 1984). The average content of elements in granite, shale, the earth's crust, and soils are presented in Tables 20 and 21.

The contents of 30 trace elements analyzed in white clay soils were usually intermediate between the value for granite and shale or were close to the values of shale. Clay minerals have the capacity to adsorb and fix trace elements during weathering processes (Archer and Hodgson 1987; Dudas and Pawluk 1980; Jenne 1977; McKenzie 1957). This may be the reason why most trace elements in the white clay soil were near the values for shale rather than the values for granite. However, some elements (e.g. Cl, Br, Hg, Mo, and W) were even lower than the values for granites. Cl and Br are likely to exist in the form of free anions ( $\text{Cl}^-$  and  $\text{Br}^-$ ) during geochemical weathering. These anions were not attracted by clay minerals and, therefore, they were mobile and subject to leaching loss.  $\text{MoO}_4^{-2}$  and  $\text{WO}_4^{-2}$  (Mo and W) behave similarly.

The geochemically inherited status of trace elements determined in this study appears modified by pedogenesis. Maximum content of arsenic, for instance, occurred in the E horizon, and minimum content of the element in the Bt1 horizon. Otherwise, there should not be such a marked difference in As content among horizons since parent material of the soil under study was relatively uniform throughout profiles.

Thirty trace elements were analyzed in this study. However, the behavior of individual elements will not be discussed. Instead, thirty trace elements will be discussed by groups. Based on pedogenic behavior (profile distribution) discussed at the beginning of this section and on linear correlation analysis of the trace elements in this study, five groups of trace elements were obtained.

The first group of trace elements includes Br, Cl, I, and Hg. These elements had accumulated in the Ah horizon (Table 20, Figs. 26 and 27). This result is comparable to the results reported by Bradley *et al.* (1978). Bradley *et al.* (1978) attributed an affinity of Br, Cl, and I for soil organic matter, which caused positive correlation between the three elements and content of organic matter. However, there are no mechanisms reported in the literature for the retention of these three elements by organic matter. The high contents of Br, Cl, and I in surface horizons (Ah) of this study are believed to be inputs of aerosolic dust. According to enrichment factors relative to aluminium, aerosolic dust contains substantially higher Br, Cl, and I than the earth's crust (Rahn *et al.* 1981). Mercury has generally been reported to be depleted in surface horizons due to volatilization of methyl and elemental mercury (Dudas and Pawluk 1976; Mills and Zwarich 1975). There is no immediate explanation for the elevated level of mercury in Ah horizons of white clay soils.

The second group of trace elements includes As, Co, Mn, and Sb. Elevated levels of these four elements were found in the E horizon where maximum amounts of oxalate and dithionite extractable Fe and Mn occurred (Table 20 and Figs. 28-30). The extractable Fe and Mn largely originate from Fe-Mn nodules. Childs (1975), Childs and Leslie (1977), and Rankin and Childs (1987) reported that Fe-Mn nodules in New Zealand soils were highly enriched in trace elements such as As and Co. Amounts of oxalate and dithionite extractable iron and manganese were positively associated with cobalt, arsenic, and antimony in the soils of this study. This further supports other observations of trace elements associated with Fe and Mn oxyhydroxides (Jenne 1968, 1977; McKenzie 1972; Suarez and Langmuir 1976).

Cobalt may replace Mn in the crystal lattice of Mn oxides (McKenzie 1970, 1972; Loganathan and Bureau 1973). Substitution is attributed to nearly identical ionic radii of  $Mn^{+4}$  and low-spin  $Co^{+3}$  ions, and to a large gain of crystal-field stabilization energy from the exchange of  $Co^{+3}$  for  $Mn^{+4}$  (Means *et al.* 1978). At low soil pH, Fe and Mn amorphous material and oxyhydroxides may develop positive charges by protonation of surface sites. Consequently, As and Sb in oxyanionic form can be strongly retained by specific adsorption. Arsenic was observed to be adsorbed onto iron oxide surfaces after release from pyrite during the genesis of acid sulphate soils in Alberta (Dudas 1987). Arsenic may also form Mn and Fe arsenates in soils with low pH values (Hess and Blanchard 1976). Antimony, in the same family with arsenic in the periodic table, may be expected to behave similarly. Boyle (1975) discovered that hydrous iron oxides fixed antimonite and antimonate ions in soil and sediments at Keno Hill, Canada.

Total concentrations of Mn, Co, As, and Sb in E horizons were substantially higher than the underlying horizons including C horizons (Table 20, Fig. 30). Several possible reasons could account for this observation. First of all, these four elements can be transferred to surface horizons by biological processes. Andersson (1977a) concluded Mn and Co were more available for plant uptake at lower soil pH. Under anaerobic conditions, manganese was reduced to  $Mn^{+2}$  after release from mineralization of organic matter and,  $Mn^{+2}$  ions migrated to E horizons.  $Mn^{+2}$  ions were then oxidized and participated into nodules during aerobic conditions. Secondly, these elements could be brought up by capillary rise from the underlying horizons. The evidence for this was that Fe-Mn nodules in E horizons were generally associated with voids (see micromorphological section) and the contents of the four elements were lowest in the horizons (Bt1) immediately below E

horizons. Thirdly, lateral movement of soil solutes and clay suspension may result in enrichment of these elements, especially after the formation of Bt horizons of low permeability. Finally, addition of aerosolic dust with high contents of As and Sb also could partly contribute to the elevated levels of As and Sb.

Thorium and uranium were two of actinide elements determined in this study. Contents of the two elements are comparable to the value for the earth's crustal abundance and shale (Table 20). Pedogenic behavior of the two elements resembled that of Co and As. Hence, Th and U were classified in the second group. Means *et al.* (1978) reported that Mn oxides are strong absorbents for actinides in soils and sediments.

The third group of trace elements consists of Cr, Rb, Sc, V, and Zn. Levels of these elements increased with profile depth, reached a maximum in Bt<sub>2</sub> horizons, then, decreased slightly with depth (Table 20, Fig. 31). These elements were positively correlated with clay content in this study. The bulge for these trace elements in Bt horizons was attributed to clay translocation within solum.

Numerous workers (McKenzie 1957; Connor *et al.* 1957; LeRiche and Weir 1963; McKeague and Wolynetz 1980) reported very similar trends for profile distributions of Cr, Zn, and V. By contrast, Swaine and Mitchell (1960) found no systematic increase of total trace elements with amount of clay in a wide range of soil materials.

Ionic radii of Cr, Zn, V, and Sc are similar to radii of Mg and Fe (Taylor 1965). Cr, Zn, V, and Sc ions may substitute for Al and Fe in octahedral sites (0.07 nm) to form solid solutions. Cr and Zn were reported to substitute for Al and Mg in clay minerals (Andersson 1977b; Yuan 1983). Scandium could be captured in Fe<sup>+2</sup> positions in iron containing minerals such as biotite. Also, Cr, Zn, V, and Sc may form hydroxy species, for example, Zn(OH)<sup>+1</sup> and Cr(OH)<sub>2</sub><sup>+1</sup>. These charged hydroxy species could be chemisorbed by clay minerals by H-bonding and covalent bonds (King 1988; Ellis and Knezek 1972; Leeper 1970; Hodgson 1963).

Levels of vanadium and zinc in the bulk soil samples of Bt<sub>2</sub> horizons were even higher than in clay separates in this study. Presently, there is no immediate answer.

Rubidium and potassium have very similar ionic radii (Rb = 0.147 nm and K = 0.133 nm), electronegativities, and ionization potential (Taylor 1965). These similar properties lead to a association between the two elements. Accordingly, Rb can enter the

crystal lattice of potassium in micaceous minerals. Bradley *et al.* (1978) obtained similar profile distribution of Rb to this study.

Cs content increased with profile depth in this study. Cesium (0.167 nm) has much larger ionic radius than potassium (0.133 nm), which hinders its preference over Rb for K-lattice positions.  $\text{Cs}^+$  was very mobile due to its large ionic potential. Consequently, Cs ions are subject to leaching during pedogenesis.

Mercury was also relatively enriched in Bt horizons (Table 20, Fig. 26). Dudas and Pawluk (1980) obtained similar results for Luvisolic soils in Canada. Thorium and uranium were also slightly concentrated in Bt2 horizons as compared to immediately adjacent horizons (Table 20). This was the result of lessivage, since the clay separates contained high level of the two elements (Table 21).

The fourth group of the trace elements is composed of B, Ba, Hf, Sr, Ti, and Zr. Profile distribution of these elements has minor variation (Table 20, Fig. 32). In this study, Hf, Ti, Zr, and Sr were depleted in clay separates, B and Ba show no or little depletion in clay separates relative to bulk soil samples. Therefore, clay translocation within solum produced negative enrichment of these elements in surface horizons.

Pedogenic distribution of Sr, Ti, and Zr reflected their occurrence in relatively resistant minerals. Hf and Zr have similar chemical properties. Hf can enter Zr-crystal lattice positions in Zr-containing resistant minerals. For example, hafnium content in zircon was high up to 31 % (Knorring and Hornung 1961).

Barium ( $r = 0.134$  nm) geochemically resembles strontium ( $r = 0.118$  nm). Barium enters K-feldspar more readily than mica due to the nature of charge and spatial arrangement of holes of the three-dimensional network structure of feldspar (Taylor 1965). LeRiche and Weir (1963) reported the distribution of the element in different particle size fractions decreased in the order sand > silt > clay, comparable to the result of this study.

The average content of boron (40 mg/kg) was lower than the average value (60 mg/kg) for Chinese soils studied by Liu *et al.* (1983). This is attributed to the fact that some soil samples developed from marine sediments with high content of boron were selected by Liu *et al.* (1983) in their study. Relative profile distribution of B in this study reflected the fact that B is mainly present in tourmaline.

The last group of the trace elements includes Ag, Au, Ga, Mo, Ni, Se, Ta, and W. These elements were generally below detection limits in some horizons. Thus, trends were not observed for this group of elements. However, these elements (especially Ag, Au, Ga, Ta, and W) appeared enriched in clay separates. Silver ions may enter K-lattice sites in mica and hydrous mica (Taylor 1965). Gold is very inert, like the noble gases. The element may exist in occluded forms within clay minerals. Like aluminium, gallium can exist as hydroxy species. The latter may enter the interlayer space of expandable phyllosilicate minerals at low soil pH conditions. Tantalum was reported to substitute for Al and Fe (III) in muscovite accompanied by partial replacement of  $\text{Si}^{+4}$  by  $\text{Be}^{+2}$  (Vlasov 1966). Further study on the relation between these trace elements and clay minerals is required.

#### D. Rare Earth Elements (REE)

Rare earth elements (REE) are often referred to as a 4f series of elements or as lanthanides (Ln) together with yttrium (Y). REE constitute a group of 15 elements commencing with lanthanum of atomic number 57, and ending with lutetium having an atomic number of 71. The elements are closely related and appear to be mostly undifferentiated in geochemical processes (Moeller *et al.* 1965; Roaldset 1974). This is attributed to the shielding 4f electrons by electrons in the  $5s^2$  and  $5p^6$  sub-shells. The elements from La to Sm are often referred to as light REE and the elements from Gd to Lu as heavy REE.

REE have been used extensively by geochemists in the study of the genesis of rocks or mineral suites (Allegre and Minster 1978; Gast 1968; Minster *et al.* 1977; Haskin 1984). Distribution and fractionation of REE during geochemical weathering, transportation, and sedimentation have also been widely investigated (Balashov *et al.* 1964; Spirn 1965; Ronov *et al.* 1967, 1972, 1974; Roaldset and Rosenqvist 1971; Roaldset 1973; Cullers *et al.* 1975; Schieber 1986). Little literature about rare earth elements is available for soils. In this section, composition of REE in the soils of this study will be presented, and the behavior of REE will also be discussed.

Ten rare earth elements (REE) were measured by instrumental neutron activation analysis (INAA) for both bulk soil samples and clay separates. The data for bulk soils and clay separates for pedon 2 are given in Table 22 and Table 23, respectively, and data for

REE for pedon 1 and pedon 3 can be found in Appendix II. Due to geochemical similarities, REE are often plotted on the same graph for comparison and interpretation. Chondrite and North American shale composites (NASC) were used to normalize the content of REE in the soils. The normalized concentrations of REE were then plotted on a logarithmic scale versus a linear scale of atomic number (Figs. 33 to 38).

Table 22. Profile distribution of rare earth elements (REE) in bulk soil samples of pedon 2 (mg/kg).

Element(Z <sup>†</sup> )	A	Ae	Bt1	Bt2	Bt3	C1	C2	G‡	S§	CB¶
La (57)	34	38	25	41	39	37	35	40	40	25
Ce (58)	62	90	61	55	59	60	58	87	50	67
Nd (60)	11	23	19	15	24	22	23	35	23	28
Sm (62)	4.7	4.8	4.6	4.7	5.4	5.6	5.4	9.4	6.5	7.3
Eu (63)	0.91	0.84	0.90	1.2	1.2	1.0	1.0	1.5	1.0	1.2
Gd (64)	5.6	4.4	4.5	5.3	5.3	6.1	5.2	9.4	6.5	7.3
Th (65)	0.89	0.52	0.79	0.72	0.69	0.61	0.70	1.5	0.90	1.1
Dy (66)	3.4	3.5	3.4	3.8	3.6	3.8	3.6	6.7	4.7	5.2
Yb (70)	1.5	2.4	2.1	1.7	2.4	2.4	2.6	3.8	3.0	3.0
Lu (71)	0.3	0.4	0.3	0.3	0.4	0.4	0.4	1	0.7	0.8
ΣREE	124	168	123	129	141	139	139	195	136	146
ΣLa <sup>#</sup> /ΣLu <sup>††</sup>	9.6	14	11	9.8	9.9	9.3	10	7.7	7.7	7.4

<sup>†</sup> denotes atomic number; <sup>‡</sup> denotes granite; <sup>§</sup> denotes shale; <sup>¶</sup> denotes crustal abundance.

<sup>#</sup> denotes the elements from La to Eu; <sup>††</sup> denotes the elements from Gd to Lu.



Table 23. Profile distribution of rare earth elements (REE) in clay separates for pedon 2 (mg/kg).

Element	A	Ae	Bt1	Bt2	Bt3	C1	C2
La	61	68	66	56	56	55	59
Ce	97.0	105	107	104	100	105	109
Nd	32	34	35	35	30	44	39
Sm	7.3	8.8	7.8	7.2	7.4	7.4	7.3
Eu	1.4	2.3	1.8	1.5	1.6	1.4	1.3
Gd	6.3	7.3	5.3	3.8	5.1	4.9	4.5
Tb	0.83	1.2	1.1	0.81	0.90	1.1	1.1
Dy	5.8	7.1	3.9	5.1	4.1	4.1	5.6
Yb	4.1	4.1	4.0	4.0	3.8	3.8	4.1
Lu	0.6	0.6	0.6	0.7	0.6	0.6	0.6
$\Sigma$ REE	216	238	232	218	209	227	232
$\Sigma$ La/ $\Sigma$ Lu	11	11	15	14	13	15	14

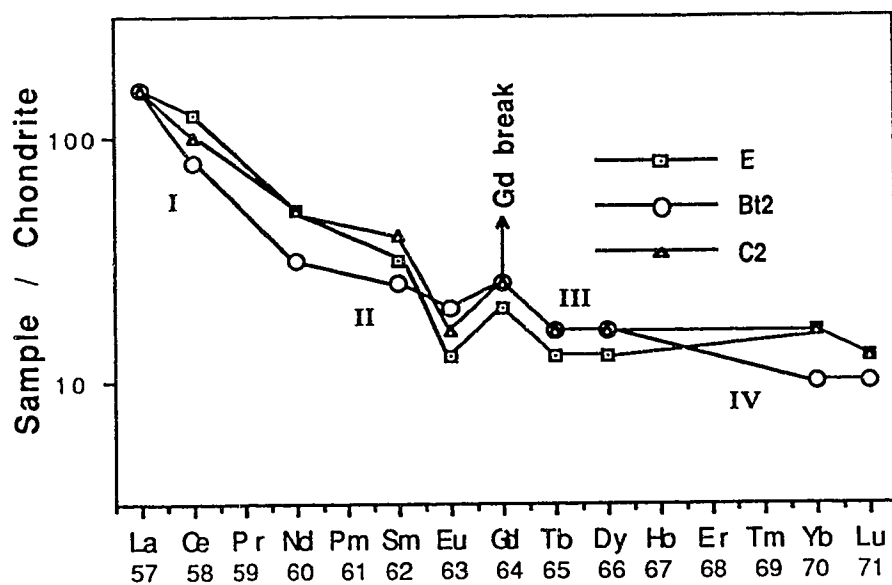


Figure 33. Chondrite-normalized curves of REE in bulk soil of Pedon 2. I, II, III, and IV portray tetrad effect.

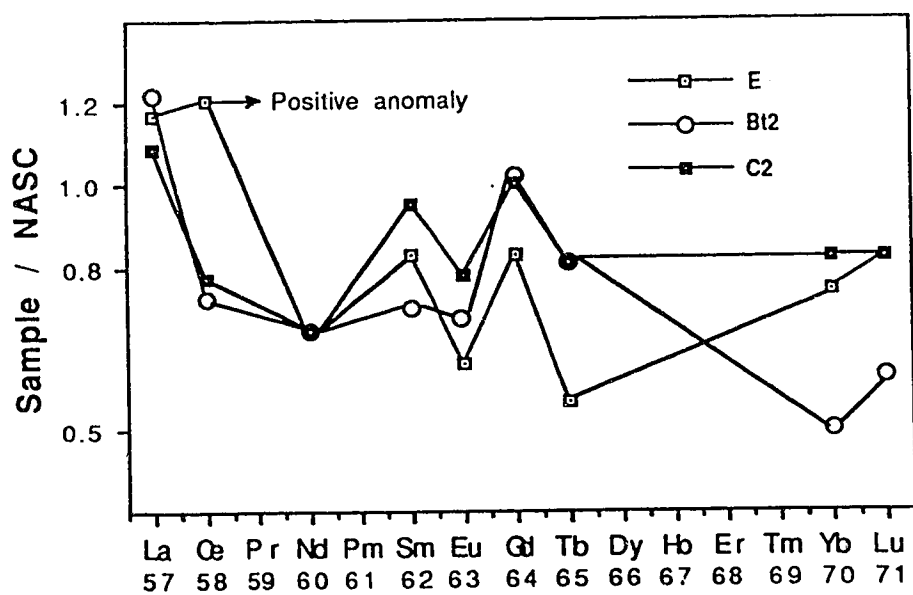


Figure 34. Shale-normalized curves of REE in bulk soil of Pedon 2.

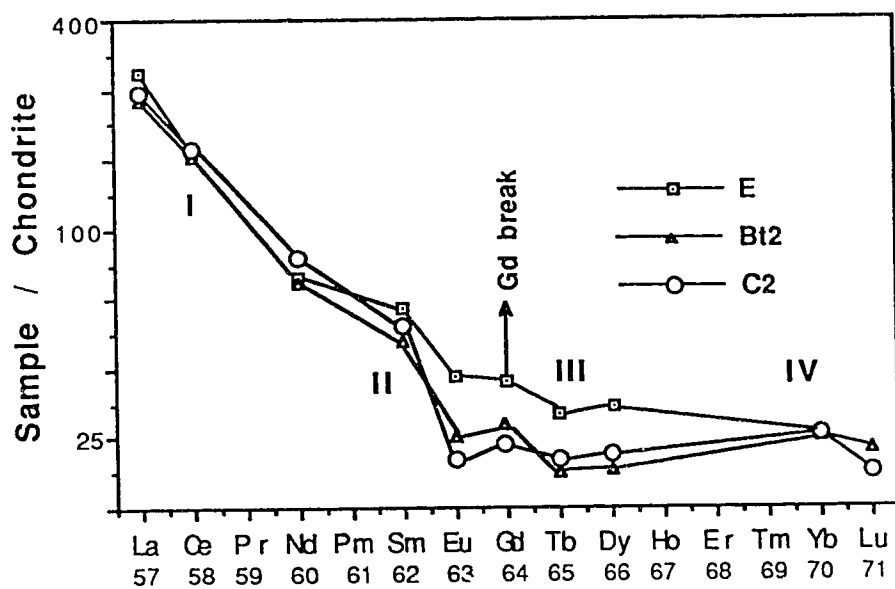


Figure 35. Chondrite-normalized curves of REE in clay separates of Pedon 2. I, II, III, and IV portray tetrad effect.

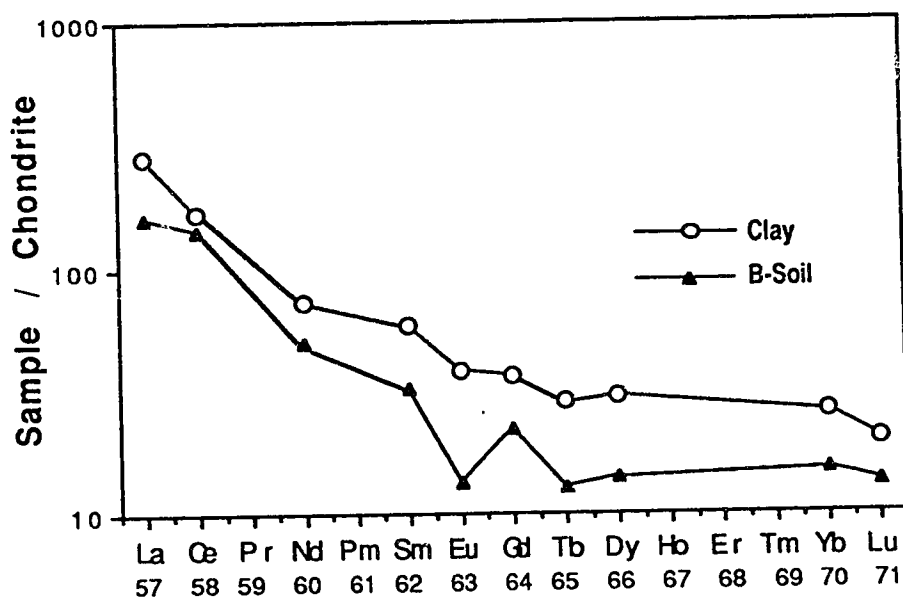


Figure 36. Comparison of REE between the bulk soil and the clay separates in the E horizon for Pedon 2.

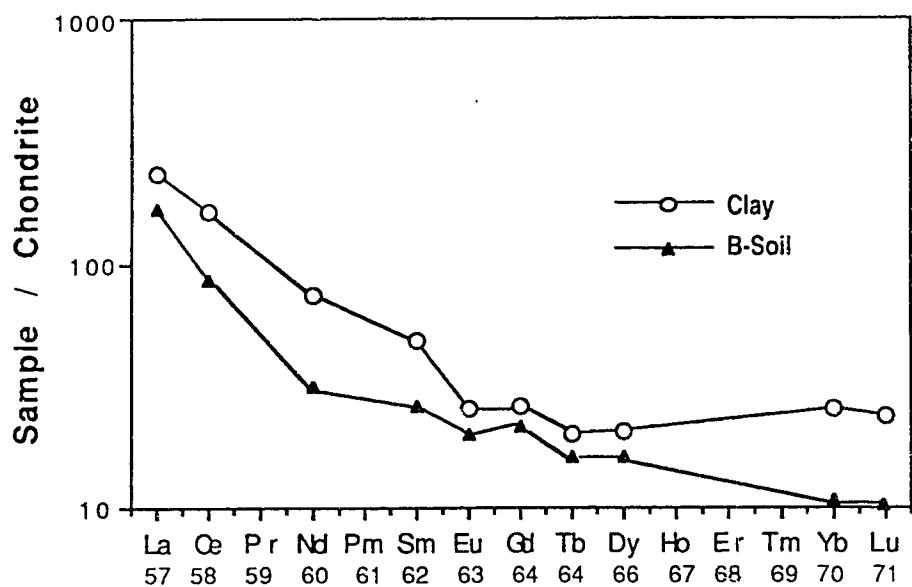


Figure 37. Comparison of REE between the bulk soil and the clay separates in the Bt2 horizon for Pedon 2.

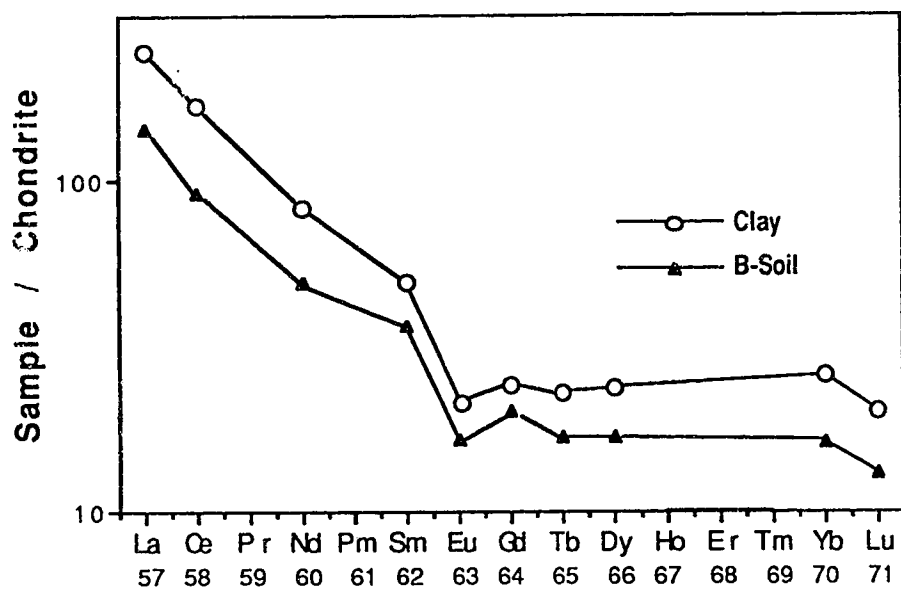


Figure 38. Comparison of REE between the bulk soil and the clay separates in the C2 horizon for Pedon 2.

Table 22 displays the abundance of REE in bulk soil samples, granite, shale, and the earth's crust. REE contents in bulk soil samples were generally lower than the values for granites and shale. Profile distribution of each individual REE was uniform except for cerium (Ce) which was relatively concentrated in E horizons. The ratio of light REE to heavy REE ranged from 9.3 to 14 for all 21 bulk soil samples. These ratios were higher than the ratios calculated for granites and shale (Table 22).

Geochemical weathering appears to have altered the abundance of REE in the parent rock. Granite, which is the source rocks for the parent materials of the white clay soils, had undergone geochemical weathering and transportation, during which the REE were depleted. Several researchers (Topp *et al.* 1985; Duddy 1980; Nesbitt 1979; Cullers *et al.* 1975) reported weathering processes affected distribution and fractionation of REE. REE may form soluble and mobile complexes with organic acids (Cullers *et al.* 1975) and with alkali carbonates (Ronov *et al.* 1967) after release from rocks.

Different degrees of filling of electrons in 4f sub-shells lead to fractionation among REE. Variation in ratio of  $\Sigma\text{La}$  to  $\Sigma\text{Lu}$  indicated fractionation between light and heavy rare earth elements. The ratios of  $\Sigma\text{La}$  to  $\Sigma\text{Lu}$  in the soils of this study were larger than granite and shale (Tables 22 and 23), indicative of enrichment of light REE. Also, high ratios of  $\Sigma\text{La}$  to  $\Sigma\text{Lu}$  in the soils indicates that chemical weathering in warm, humid environments depleted more heavy REE than light REE (Ronov *et al.* 1967; Balashov *et al.* 1964). This pattern of depletion was attributed to higher stability of aqueous inorganic and organic complexes of heavy REE than light REE (Ronov *et al.* 1967; Varshal *et al.* 1975; Duddy 1980).

The REE with even atomic number were more abundant than the adjacent elements with odd atomic number (even-odd effect). This has been explained by the theory that nuclei having both protons and neutrons as even number were inherently more stable than those having odd protons and neutrons (Rankama and Sahama 1950). Surprisingly, on the normalized distribution curves (Figs. 33, 34, and 35), even-odd effect is still shown as a part of the sequence of maxima and minima. The tetrad effect and the Gd break are also observed on the normalized curves (Figs 33-35). These results contrast with the accepted, classic geochemistry that REE do not fractionate in nature (Goldschmidt 1937; Coryell 1950; Haskin and Korotev, 1972). However, the results in this study are consistent with numerous observations in the fields of physical chemistry which were mostly disregarded by geochemists (Marcus and Abrahamer 1961; Yoshida 1962; Fidelis

and Siekierski 1965, 1966, 1967; Hogdahl 1966; Peppard *et al.* 1969; Siekierski 1970, 1971; Nugent 1970). Siekierski (1970) and Nugent (1970) independently discovered the tetrad effect of rare earth elements and they attributed the tetrad effect to quantum mechanical interelectronic repulsion energy of the electrons of the 4f electronic configurations. Presence of the even-odd and tetrad effects and the Gd break in soils of this study agree with the work done by Roaldset (1973, 1974) and Christie and Roaldset (1979).

REE were decidedly concentrated in the clay separates (Tables 22 and 23, Figs. 36-38). Enrichment of REE in clay minerals have been documented by a number of geochemists (Ronov *et al.* 1967; Roaldset 1973; Aagaard 1974; Cullers *et al.* 1975; Laufer *et al.* 1984). Ca-saturated clay was used for the REE determination in this study, thus, the enrichment of REE in clay separates can not be explained by adsorption mechanisms suggested by Brown *et al.* (1955) and Aagaard (1974). Other processes have to be involved or the elements are so strongly adsorbed, calcium is unable to exchange surface adsorbed REE.

Micaeous minerals have higher affinity for REE than for the alkali and earth alkali elements (Amphlett 1958; Roaldset 1973). Duddy (1980) concluded that REE could be fixed by vermiculite. Hydroxy lanthanide cations can migrate into hexagonal holes of the oxygen surface in the interlayer space (Miller *et al.* 1982). Olivera (1986) and Olivera *et al.* (1987) confirmed the presence of hydroxy lanthanide cations in vermiculite interlayer space. Paster *et al.* (1988) also found that uptake of  $\text{Ln}^{+3}$  exceeded the CEC of vermiculite. They detected the presence of  $\text{Ln}^{+3}$  ions in the vermiculite interlayer space by x-ray power diffraction. In the same study, they concluded that strong localization of vermiculite layer charge may catalyze hydrolysis of  $\text{Ln}^{+3}$  ions on the interlayer surface. Lanthanide hydroxyl cations have strong interaction with vermiculite through hydrogen bonds, Van der waal forces, and probably covalent bonds rather than simple electrostatic attraction (Laufer *et al.* 1984).

Patterns of rare earth elements (normalized curves) for clay separates are similar among horizons (Fig. 35). Similar patterns were also observed for bulk soil samples except for the presence of a Ce positive anomaly in E horizons (Figs. 33 and 34), which will be discussed later. These results provide further evidence for the uniformity of parent material

of the soils under study. Therefore, normalized REE patterns may serve as alternative indicators of lithologic discontinuities.

The Ce positive anomaly for E horizons is shown in Figures 33 and 34. The ratio of the measured Ce value to the Ce value obtained by interpolation between La and Nd on the shale-normalized curves was 1.2. Ce enrichment in E horizons was attributed to Fe-Mn nodules. Rankin and Childs (1976, 1987) reported that Ce was highly enriched in Fe-Mn nodules in New Zealand soils. They concluded that Ce positive anomalies were attributable, at least in part, to oxidizing/reducing conditions involved in formation of nodules in soils. In this study, correlation analysis between  $\Sigma$ REE and Fe or Mn and between Ce and Fe or Mn demonstrated that  $\Sigma$ REE and Ce have positive correlations with total Mn, oxalate and dithionite extractable Mn and Fe. The correlation coefficients are shown in Table 24. Oxalate extractable Fe and Mn have large correlation coefficients with Ce and  $\Sigma$ REE.

Table 24. Correlation coefficients among Fe, Mn, Ce, and  $\Sigma$ REE \*.

	Fet	Feo	Fed	Mnt	Mno	Mnd
Ce	-0.37	0.76	0.51	0.67	0.73	0.71
$\Sigma$ REE	-0.18	0.69	0.54	0.63	0.63	0.61

\* denotes  $P < 0.01$  level.

Cerium enrichment in marine manganese nodules attracted the attention of geochemists for two or three decades. Goldberg *et al.* (1963) attributed Ce enrichment to the oxidation of Ce to the tetravalent  $\text{CeO}_2$ . From a consideration of thermodynamics of oxidation of Ce, Glasby (1973) concluded that Ce was precipitated on the surface of nodules as  $\text{Ce}(\text{OH})_3$  and was then spontaneously oxidized to the tetravalent state. Due to a large discrepancy in the ionic radii among  $\text{Ce}^{+3}$  (0.107 nm),  $\text{Ce}^{+4}$  (0.094 nm),  $\text{Mn}^{+4}$  (0.060 nm), and  $\text{Fe}^{+3}$  (0.064 nm), stoichiometric substitution appeared unlikely, and incorporation of Ce into positions between basal layers of Mn/Fe was favored (Glasby 1973; Piper 1974). This mechanism may also be valid for Ce-enrichment in soil Fe-Mn nodules.

## **E. Discussion of the Genesis and Classification**

In this section, possible pedogenic processes responsible for the formation of the soils of this study will be discussed. Classification of the soils will also be proposed based on the physical, micromorphological, mineralogical, and chemical characteristics determined in this study.

Geochemical studies have shown that the sediments in which the soils of this study developed were formerly weathered, alluvial deposits of Late Pleistocene and Early Holocene age (Xie 1982). Parent materials of these soils are fine textured and relatively uniform according to the classical pedogenic criteria (Evans 1978).

Clay translocation is a dominant process in the formation of these white clay soils. This physical movement of clay particles is termed lessivage. Argillation indices and well-developed oriented argillans in Bt horizons are evidences for the lessivage.

As lessivage proceeded, a slowly permeable Bt horizon formed. As the B horizon developed, downward movement of percolation water and clay suspension would be hampered. Consequently, temporary perched water tables and periodic reduction (anaerobic conditions) would develop with precipitation. This characteristic still dominates the soils, today. With the temporary anaerobic conditions, Fe-Mn nodules formed and soil color changed to grayish. Lateral movement of water-clay suspensions may have contributed some Mn and other elements for formation of the nodules. Freeze-thaw coupled with wetting and drying led to the banded fabric in E horizons. In addition to lessivage, accumulation of humus resulted in the formation of a well developed granular structured A horizon composed of mull type humus similar to Chernozemic Ah horizon formed in Canada.

During pedogenesis, the continuous addition of aerosolic dust containing mica onto the Three River Plain resulted in a continuous addition of mica to the surface horizons. However, the amount of aerosolic dust added to the soils is probably small when mixed with 20 to 50 % native clay. Therefore, lithologic discontinuities were not detected.

The soils of this study do not satisfy the criteria for either podzol or solonetz. Table 25 displays selected chemical characteristics of the soils and criteria for podzolic soils. Pyrophosphate extractable Fe and Al, ratio of pyrophosphate extractable Fe plus Al to clay content, and ratio of organic carbon to pyrophosphate extractable Fe in Bt horizons



are smaller than the values required for podzols (Soil Taxonomy, 1975). Color and textures of the soil also do not meet the usual podzol requirements. The ratio of exchangeable Ca to Na in Bt horizons is larger than 10 though hard blocky Bt horizons are present (Tables 9, 10 and 11). However, solonetzic B (natric horizon) requires the ratio to be smaller than 10.

Table 25. Chemical characteristics of Pedon 2 and criteria required for Podzols.

	(Fep†+Alp)	(Fep+Alp)/clay	organic-C/Fep
Ah	0.41	0.02	25
E	0.29	0.02	6.0
Bt1	0.43	0.01	3.3
Bt2	0.53	0.01	3.5
Bt3	0.41	0.01	2.7
C1	0.52	0.01	1.9
C2	0.46	0.01	1.9
Podzolic B	≥0.60	≥0.05	≥20.0

† denotes pyrophosphate extractable Al or Fe

White clay soils of this study might be regarded as intergrades between (gleyic) Greyzems and Planosols. Using FAO-UNESCO key (1988), they are classified as Umbric Planosols (pedon 1 and 2) and Mollic Planosols (pedon 1). According to the U.S.D.A. 7th Approximation (1975), the white clay soil may be treated as intergrades between mollisols (Argialbolls) and Alfisols (Glossoboralfs). Another subgroup should probably be proposed in the Argiaboll great group in order to accommodate soils of this study. This subgroup could be designated as Boralfic Argialbolls (Pawluk<sup>5</sup> 1989, pers. commun.). In the Canadian System of Classification (1987), pedogenic characteristics of these soils are closest to the gleyed Dark Gray Luvisol. Using the Chinese Soil Taxonomy (Zhu 1984), the soils fall into Albic Group within Semi-Hydromorphic Order.

<sup>5</sup> Professor Pawluk, S., Dept. of Soil Science, Univ. of Alberta, Edmonton, Alberta, Canada, T6G 2E3.

## Chapter V

### Summary and Conclusions

White clay soils are widely distributed in Northeast China, especially in Heilongjiang Province. These soils usually occur on the nearly flat lying land (slope = 1 to 5%) within temperate, sub-humid zones. Natural vegetation of the soils consists of trees for upper canopy and shrubs and grasses for the understory. Alluvial deposits characterized by a fine texture are the parent materials.

The results from particle-size distribution of non-clay fractions and ratios of elements in resistant minerals suggest there is no lithologic discontinuity based on traditional criteria used in pedology. Patterns of rare earth elements provide additional evidence for the uniformity of parent material.

Soils of this study are characterized by a platy E horizon overlying a thick Bt horizon. A chernozemic-like A horizon (Ah) is usually present. Samples of E horizons had high bulk densities. Particle size distribution and micromorphology of the soils indicated lessivage was an important pedogenic process. The well-developed oriented argillans coincided with the maximum clay content in the Bt<sub>2</sub> horizon. Capillary withdrawal of moving water-clay suspension upon drying led to the formation of oriented argillans. The presence of argillans in the C horizons suggested clay migration could extend to depth.

Well-developed banded fabric was observed in E horizons. This feature was mainly attributed to the effect of freeze-thaw and wetting and drying. Fe-Mn nodules are common in the E horizon indicative of weathering and periodic reducing conditions. Slowly permeable Bt horizons contribute to anaerobic conditions and temporary perched water tables.

Total CEC averaged 26 cmol (+)/kg with low values in E horizons and high values in Ah horizons. Calcium was the dominant cation on exchangeable complex and exchangeable Na is very low. Differences in ratios of exchangeable cations illustrates redistribution of these major elements during pedogenesis. Exchange acidity accounts for nearly one half of the total exchange capacity. Profile distribution of pH values is rather uniform and moderately acidic (around 5.0). High exchange acidity and low soil pH could be a potential limiting factor for crop production. C/N ratio is around 10.

Highest amounts of oxalate- and dithionite-extractable Fe and Mn occurred in the E horizon where abundant nodules were present. Most of manganese may be in an amorphous form (oxalate-extractable). Amorphous Fe accounts for about 35 % of the total content of iron. Pyrophosphate extractable iron and aluminium reached a maximum in Bt2 horizons. This is thought to be the result of movement of organic complexes of iron and aluminium during pedogenesis. However, the amounts of pyrophosphate extractable Fe and Al are not high enough to meet the requirements for Podzolic soils.

The clay mineral assemblage is qualitatively similar throughout profiles with minor quantitative variation. Soil vermiculite and vermiculite-smectite intergrades (VSI), which had not been recognized before, were the abundant clay minerals in the clay separates of this study. Other clay minerals are mica and kaolinite. Vermiculite likely resulted from depotassification of mica. Chlorite intergrades, quartz, and feldspar are present in trace amounts. Chloritic intergrades may form from Al-hydroxy species entering interlayer spaces of vermiculite and smectite.

High content of mica and low content of vermiculite in surface horizons of the soils of this study were not in agreement with profile distribution of mica reported in the literature. Relatively high content of mica in the surface horizons of the soils was thought to be the result of the continuous addition of tropospheric (aerosolic) dust containing mica as a major clay mineral. Low contents of soil vermiculite and VSI in E horizons were also partly attributed to leaching.

Silt and sand separates consist mainly of quartz and feldspar with trace amounts of mica. The mineral species of silt fraction are almost identical throughout profiles. Sand fractions are composed largely of Fe-Mn nodules. Surface morphology of selected quartz showed no evidence for glacial or eolian transportation. Grains from the surface horizon appeared more weathered than those of the lower solum due to more intense weathering in surface horizons. X-ray powder diffraction analysis of Fe-Mn nodules indicated the presence of quartz and feldspar. The absence of Fe and Mn mineral peaks indicated that Fe and Mn within the nodules occurred mainly in an amorphous form.

The background levels of 30 trace elements were established for soils of this study. These values are useful for future agricultural and environmental studies. Profile distribution of the 30 trace elements determined in this study reflected the influence of

pedogenic processes (e.g., leaching, redox change). Contents of trace elements in clay separates within and among pedons are similar.

Five groups of the trace elements were identified based on geochemical similarities. The first group of trace elements (Br, Cl, I, and Hg) are those with elevated levels occurring in Ah horizons. Br, Cl, and I are reported to have an affinity for soil organic matter. Aerosolic dust is thought to be the source of Br, Cl, and I in the Ah horizons of this study.

The second group of the trace elements was associated with amounts of oxalate and dithionite extractable Mn and Fe. This group includes Mn, As, Sb, Th, and U. Elevated levels of these elements were found in E horizons. The enrichment of these elements is mainly caused by chemisorption onto Mn and Fe materials. Capillary rise, plant uptake, and lateral movement may bring these elements to E horizons from other horizons.

The third group of the trace element consists of Cr, Rb, Sc, V, and Zn. These elements were enriched in clay separates. Bt<sub>2</sub> horizons contained relatively high amounts of these elements. These trace elements were concentrated in clay separates through isomorphic substitution, chemisorption, and occlusion rather than simple electrostatic adsorption.

The fourth group of the trace elements was composed of B, Ba, Hf, Sr, Ti and Zr. They are generally present in resistant minerals. Therefore, profile distributions of these elements exhibited negative enrichment in the E horizon and lower contents in the Bt<sub>2</sub> horizon.

The last group of elements included all of the trace elements which were below their respective detection limits in one or more horizons. Consequently, there is no clear profile distribution observed for this group of the elements. However, some of the elements (e.g. Au, W) were noticeably enriched in clay separates.

Abundances of 10 rare earth elements (REE) were obtained for the soils of this study. The values for REE can be used as background data for future pollution studies. Contents and distribution of rare earth elements in the soils reflect geochemical processes. The gadolinium break, even-odd and tetrad effects were observed on the normalized REE curves. These effects are new information which contrasts with the accepted, classical concept that the REE normalized curves are smooth (i.e. REE do not differentiate among themselves by geological processes). These effects are attributed to the varying degree of

filling of electrons in the 4f orbitals. Specifically, a half of the 4f orbitals are filled with electrons for gadolinium, which is the dividing element between light (La to Eu) and heavy rare earth elements (Gd to Lu). Heavy REE are preferentially leached by natural waters due to a relatively high stability of aqueous complexes with organic and inorganic ligands. The high ratio of  $\Sigma\text{La}$  to  $\Sigma\text{Lu}$  of the soils of this study indicated a warm, humid geochemical weathering environment occurred in the past.

All ten REE were enriched in clay separates. Clay minerals likely retained REE through fixation and chemisorption rather than simply electrostatic attraction. Cerium had a positive correlation with the amounts of oxalate and dithionite extractable manganese and iron and had a positive anomaly on the normalized REE curve of the E horizon. The anomaly was attributed to the two oxidation states of cerium ( $\text{Ce}^{+3}$  and  $\text{Ce}^{+4}$ ).  $\text{Ce}^{+4}$  was expected to participate in the formation of Fe-Mn nodules in the E horizon. Cerium is the most abundant element of REE which contributes to the positive association between  $\Sigma\text{REE}$  and Mn or Fe. Evaluation of the normalized REE patterns among different horizons may serve as an alternative indicator for parent material uniformity.

During the early stages of pedogenesis, percolating water movement along with colloidal clay particles through the profile was relatively unrestricted until a large amount of clay accumulated at depth. After the formation of the Bt horizon, downward water movement through the profile was restricted due to high clay content. Temporary perched water tables and alternating reducing conditions occurred in a cyclic manner as dictated by precipitation. Fe-Mn nodules and grayish colors then developed in E horizons. Mica from aerosolic dust was continuously added on the surface horizons. Accumulation of organic matter in the surface was favored by temperature and moisture conditions. In summary, lessivage, periodic reduction-oxidation change, continuous input of mica, and accumulation of soil organic matter were mainly responsible for pedogenic characteristics observed in this study.

Based on physical, chemical, micromorphological, and mineralogical properties, the pedons of this study were classified as Planosols using the FAO-UNESCO System (1988), as Boralfic Argialbolls using the U.S.D.A. 7th Approximation (1975), as the Gleyed Dark Gray Luvisols by the Canadian Classification System (1987), and as Albic Soils in the Chinese Taxonomy System (1984). They are neither Podzolic nor Solonchic as formerly recognized.

## REFERENCES

- Aagaard, P. 1974. Rare earth elements adsorption on clay minerals. *Bull. Gr. fr. Argiles* 26: 193-199.
- Abder-Ruhman, M. 1980. Mineralogical characteristics of soils from East Central Alberta. M.Sc. Thesis. Univ. of Alberta.
- Adriano, D.C. 1986. Trace elements in the terrestrial environment. Springer-Verlag, New York, Berlin, Tokyo.
- Agriculture Canada Expert Committee on Soil Survey. 1987. The Canadian system of soil classification. 2nd ed., Can. Dep. Agric. Publ. Supply and services Canada. Ottawa, Ont.
- Akhtyrtsev, B.P. 1968. Removal and accumulation of oxides in soils of broadleaf forests in the central Russia Forest Steppe. *Soviet soil Sci.* pp. 1423-1434.
- Allegre, C.J. and J.F. Minster. 1978. Quantitative models of trace elements behavior in magmatic processes. *Earth Planet. Sci. Lett.*, 38: 1 pp..
- Allen, B.L. and B.F. Hajek. 1989. Minerals occurrence in soil environments. In. *Minerals in soil environments*, J.B. Dixon and S.B. Weed (eds.), SSSA, Madison, WI, pp. 200-278.
- Amphlett, C.B. 1958. Ion exchange in clay minerals. *Endeavour* 17:149-155.
- Andersson, A. 1977a. Some aspects of the significance of heavy metals in sewage sludge and related products used as fertilizers. *Swed. J. Agric. Res.* 7: 1-5.
- Andersson, A. 1977b. The distribution of heavy metals in soils and soil material as influenced by the ionic radius. *Swed. J. Agric. Res.* 7: 79-83.
- Archer, F.C. and I.H. Hodgson. 1987. Total and extractable trace element contents of soils in England and Wales. *J. Soil Sci.* 38: 421-431.
- Aubert, H. and M. Pinta. 1977. Trace elements in soils. Elsevier, Amsterdam and New York.
- Balashov, Y.A., A.B. Ronov, A.A. Migdisov, and N.V. Turanskaya. 1964. The effect of climate and facies environment on the fractionation of the rare earths during sedimentation. *Geochemistry*, 5: 951-969.
- Barbour, G.B. 1934. Analysis of the Lushan glaciation problem. *Bull. Geol. Soc. China* 13: 647-656.
- Barnhisel, R.I. and P.M. Bertsch. 1989. Chlorites and hydroxy interlayered vermiculite and smectite. In. *Minerals in soil environments*, J.B. Dixon and S.B. Weed (eds.), SSSA, Madison, WI, pp.729-779.
- Barshad, I. 1964. Chemistry of soil development. In. *Chemistry of the soil*, F.E. Bear (ed.). Chapman and Hall Ltd. London. pp. 1-71.

- Black, J.M.W. and M.J. Dudas 1987. The scanning electron microscopic morphology of quartz in selected soils from Alberta. *Can. J. Soil Sci.* 67: 965-971.
- Blank, M., M. Leinen, and J.M. Prospero. 1985. Major Asian aeolian inputs indicated by the mineralogy of aerosols and sediments in the western North Pacific. *Nature* 314: 84-86.
- Bloomfield, C. 1954. The deflocculation of kaolin by tree leaf leachates. *Trans. 5th Int. Congr. Soil Sci.* 2: 280-283.
- Bodman, G.B. and E.F. Harradine. 1939. Mean effective pore size and clay migration during water percolation in soils. *Soil Sci. Soc. Am. Proc.* 3: 44.
- Borchardt, G. 1989. Smectites. In: *Minerals in soil environments*, J.B. Dixon and S.B. Weed (eds.), SSSA, Madison, WI, pp. 697-699.
- Boul, S.W., F.D. Hole, and R.J. McCracken. 1973. *Soil genesis and classification*. The Iowa State Univ. Press, Ames, Iowa.
- Bowen, H.J.M. 1979. *Environmental chemistry of the elements*. Academic Press, New York, N.Y.
- Boyle, R.W. 1975. The geochemistry of antimony, Keno Hill area, Yukon, Canada. In: *Recent contributions to geochemistry and analytical chemistry*, A.L. Tugarinov (ed.) pp. 354-370.
- Bradley, R.I., C.C. Rudeforth, and C. Wilkins. 1978. Distribution of some chemical elements in the soils of north west Pembrokeshire. *J. Soil Sci.* 29: 258-270.
- Brewer, R. 1976. *Fabric and mineral analysis of soils*, 2nd edition. R.E. Krieger Publ. Co. Huntington, N.Y.
- Brewer, R. 1964. *Fabric and mineral analysis of soils*. Wiley & Sons, New York.
- Brewer, R. and A.D. Haldane. 1957. Preliminary experiments in the development of clay orientation in soils. *Soil Sci.* 84: 301-309.
- Brewer, R. and S. Pawluk. 1975. Investigation of some soils developed in hummocks of the Canadian sub-Arctic and southern Arctic regions. 1. Morphology and micromorphology. *Can. J. Soil Sci.* 55: 301-319.
- Brewer, R., J.R. Sleeman, and R.C. Foster. 1983. The fabric of Australian soils. In: *Soils: an Australian viewpoint*. Division of Soils, CSIRO. pp. 439-476.
- Brierley, J.A. 1988. A comparison of two soils from the Milk River Ridge, southwest Alberta. M.Sc. Thesis. Univ. of Alberta.
- Brown, R.E., H.K. Parker, and J.M. Smith. 1955. Disposal of liquid wastes to the ground. *U.N. Int. Conf. on the peaceful Uses of Atomic energy*, 9: 669-675.
- Bullock, P. 1968. The zone of degradation at the eluvial - illuvial interface of some New York soils. Ph.D. Thesis, Cornell Univ.

- Bullock, P. and M. L. Thompson. 1985. Micromorphology of Alfisols. In. Soil micromorphology and Classification, L. A. Douglas and M.L. Thompson (eds.). SSSA Spec. Publ # 15.
- Canadian Soil Survey Committee. 1981. Manual on soil sampling and methods of analysis. J.A. McKeague (ed), 2nd ed., Can. Soc. Soil. Sci..
- Carter, D.L., M.D. Heilman, and C.L. Gonzalez. 1965. Ethylene glycol monoethyl ether for determining surface area of silicate minerals. *Soil Sci.* 100: 356-360.
- Chapman, S.L. and M.E. Horn. 1968. Parent material uniformity and origin of silty soils in north west Arkansas based on zirconium - titanium ratios. *Soil Sci. Soc. Am. Proc.* 32: 265-271.
- Cheng, Y. 1986. Major regions of igneous rocks in China. In. The geology of China, Z. Yang, Y. Cheng and H. Wang (ed.). Clarendon Press, Oxford. 193 pp.
- Childs, C.W. 1975. Composition of iron-manganese concretions from some New Zealand soils. *Geoderma* 13: 141-152.
- Childs, C.W. and D.M. Leslie. 1977. Interelement relationships in iron-manganese concretions from a catenary sequence of yellow-grey earth soils in loess. *Soil Sci.* 123: 369-376.
- Christie, O.H.J. and E. Roaldset. 1979. Geochemical behavior of lanthanoid elements in some clays and bauxite. *Geoderma. J.* 13: 11-14.
- Coffman, C.B. and D.S. Fanning. 1974. "Vermiculite" determination on whole soils by cation exchange capacity method. *Clays Clay Miner.* 22: 271-283.
- Connor, J., N.F. Shimp, and J.C.F. Tedrow. 1957. A spectrographic study of the distribution of trace elements in some podzolic soils. *Soil Sci.* 83: 65-73.
- Coryell, C.D., J.W. Chase, and J.W. Winchester. 1963. A procedure for geochemical interpretation of terrestrial, rare-earth abundance pattern. *J. Geophys. Res.* 68: 559-566.
- Crook, K.A.W. 1968. Weathering and roundness of quartz sand grains. *Sedimentology* 11: 171-182.
- Cullers, R.L., S. Chaudhuri, and B. Arnold. 1975. Rare earth distribution in clay minerals and in the clay-sized fraction of the Lower Permian Havensville and Eskridge shales of Kansas and Oklahoma. *Geochim. Cosmochim. Acta.* 39: 1691-1703.
- Davis, R.I. 1971. Relation of polyphenols to decomposition of organic matter and to pedogenic processes. *Soil Sci.* 111: 80-85.
- Dawson, B.S.W., J.E. Fergusson, A.S. Campbell, and E.J.B. Cutler. 1985. Distribution of elements in some Fe-Mn nodules and an iron-pan in some gley soils of New Zealand. *Geoderma* 35: 127-143.
- Derbyshire, D. 1987. A history of glacial stratigraphy in China. *Quaternary Sci. Rev.* 6: 301-314.



- Derbyshire, D. 1983. The Lushan dilemma: Pleistocene glaciation south of the Chang Jiang (Yangtze River). *Zeitschrift für Geomorphologie*, N.F. 27: 445-471.
- Derbyshire, D. 1982. Lushan: Status of phenomena used to support the glacial hypothesis. In. *Problems of the Quaternary glacial deposits and landforms in China*, Academia Sinica, Lanzhou pp. 93-95.
- Dijkerman, H.J., M.G. Cline and G.W. Olson. 1967. Properties and genesis of textural subsoil lamellae. *Soil Sci.* 102: 7.
- Drees, L.R. and L.P. Wilding. 1973. Elemental variability within a sampling unit. *Soil Sci. Soc. Am. Proc.* 37: 82-87.
- Duchaufour, Ph. 1970. *Précis de pedologie*. 3rd ed. Masson et Cie, Paris.
- Dudas, M.J. 1987. Accumulation of native arsenic in acid sulphate soils in Alberta. *Can. J. Soil Sci.* 67: 317-331.
- Dudas, M.J. 1987. *Soils 415 Lab Manual*. Dept. of Soil Sci., Univ. of Alberta.
- Dudas, M. J. 1966. Clay-organo studies of selected Chernozems. M.Sc. Thesis, Univ. of Alberta.
- Dudas, M.J. and S. Pawluk. 1980. Natural abundances and mineralogical Partitioning of trace elements in selected Alberta soils. *Can. J. soil Sci.* 60: 76-771.
- Dudas, M.J. and S. Pawluk. 1976. The nature of mercury in Chernozemic and Luvisolic soils in Alberta. *Can. J. Soil Sci.* 56: 413-423.
- Dudas, M.J. and S. Pawluk. 1970. Chernozem soils of the Alberta parklands *Geoderma* 3: 19-36.
- Duddy, I.R. 1980. Redistribution and fractionation of rare earth and other elements in a weathering profile. *Chem. Geol.* 30: 363-381.
- Dumanski, J. and R.J. St. Arnaud. 1966. A micromorphological study of eluvial soil horizons. *Can. J. Soil Sci.* 46: 287-292.
- Edwards, A.P. and J.M. Bremner, 1967. Dispersion of soil particles by sonic vibration. *J. Soil Sci.* 18:47-63.
- Ellis, B.G. and B.D. Knezek. 1972. Sorption reactions of micronutrients in soils. In. *Micronutrients in agriculture*, J.J. Mortvedt *et al.* (eds.). SSSA, Madison, WI.
- Evans, L.J. 1978. Quantification and pedological processes. In. *Quaternary soils*, W.C. Mahaney (ed.). Geo Abstract, Norwich, England pp. 361-377.
- Evans, L.J. and W.A. Adams. 1975. Quantitative pedological studies on soils derived from Silurian mudstones. IV. Uniformity of the parent material and evaluation of internal standards. *J. Soil Sci.* 26: 319-326.

- Fanning, D.S., V.Z. Keramidas, and M.A. El-Desoky. 1977. Micas. In *Minerals in soil environments*, J.B. Dixon and S.B. Weed (eds.), SSSA, Madison, WI, pp. 527-550.
- FAO-Unesco. 1988. *Soil map of the world*. FAO of the United Nations, Rome.
- Fallner, V.C., B.F. Smith, M.J. Wilson, P.J. Loveland, and R.W. Payton. 1988. Readily-extractable hydroxyaluminium interlayers in clay- and silt-sized vermiculite. *Clay Miner.* 23: 271-277.
- Feijtel, T.C., A.G. Jongmans, N. Vanbreemen, and R. Miedema. 1988. Genesis of two Planosols in the Massif Central, France. *Geoderma* 43: 249-269.
- Fidelis, I. and S. Siekierski. 1965. Use of 2-ethylhexylphynylphosphonic acid in reversed phase partition chromatography. *J. Chromatog.* 17: 542-548.
- Fidelis, I. and S. Siekierski. 1966. The regularities instability constants of some rare earth complexes. I. *Inorg. Nucl. Chem.* 28: 185-188.
- Fidelis, I. and S. Siekierski. 1967. The influence of enthalpy and entropy on the separation factor of lathanides in the HEHOP-HNO<sub>3</sub> system. I. *Inorg. Nucl. Chem.* 29: 2629-2635.
- Fox, C.A. and R. Protz. 1981. Definition of fabric distributions to characterize the rearrangement of soil particles in the Turbic Cryosols. *Can. J. Soil Sci.* 61: 29-34.
- Gao, Z., Y. Song, and X. Guan. 1988. Study on the physical and chemical properties of Albic soils in the forming processes. *Acta. Pedol. Sinica.* 25: 13-21.
- Gary, M., R.Jr. McArfee, and C.L. Wolf. 1972. *Glossary of geology*. Am. Geol. Inst., Washington, D.C. 805 pp.
- Gast, P.W. 1968. Trace element fractionation and the origin of tholeiitic and alkaline magma types. *Geochim. Cosmochim. Acta*, 32: 1057 pp.
- Geng, G., Q. Xu, and Y. Hseung. 1987. The relationship between geneses of Lime concretion black soil and Albic soil and ecological environment. *Acta Pedol. Sinica* 24: 369-377.
- Glasby, G.P. 1973. Mechanisms of enrichment of the rarer elements in marine manganese nodules. *Mar. Chem.* 1: 105-125.
- Goldberg, E.D., M. Koide, R.A. Schmitt and R.H. Smith. 1963. Rare earth distribution in the marine environment. *J. Geophys. Res.* 68: 4209-4217.
- Goldschmidt, V.M. 1954. *Geochemistry*, Corr. and revised 1958-1962. Alex, Muri., Oxford.
- Goldschmidt, V.M. 1937. *Geochemische Verteilungsgesetze der Elemente. IX. Die Mengenverhältnisse Elemente und der Atom Arten*. Skr. Norske Videnskaps-Aksdemi i Oslo I, Mat. Naturv, Kl. No. 4.

- Gombeer, R. and J. D'Hoore. 1971. Induced migration of clay and other moderately mobile constituents. III. critical soil/water dispersion ratio colloid stability and electrophoretic mobility. *Pedologie* XXI: 311-342.
- Greenland, D.J. 1971. Interactions between humic and fulvic acids and clays. *Soil Sci.* 111: 34-41.
- Hall, R.B. 1988. The effects of chromium loading on earthworms in an amended soil. M.Sc. Thesis, Dept. of Soil Sci., Univ. of Alberta.
- Haskin, L.A. 1984. Petrogenetic modelling - use of rare earth elements. In: *Rare earth element geochemistry*. P. Henderson (ed.), Elsevier, Amsterdam-Oxford-New York-Tokyo. pp. 115.
- Hasina, L.A. and R.L. Korotev. 1972. Determination of rare earths in geological samples and raw materials in Analysis and Application of rare earth materials. Paper presented at the NATO advanced Study Institute, Kjeller, Norway, 23rd-29th August, 1972.
- Hess, R.E. and R.W. Blanchar. 1976. Arsenic stability in contaminated soils. *Soil Sci. Soc. Am. J.* 40: 847-852.
- Hodgson, J.F. 1963. Chemistry of the micronutrient elements in soils. In: *Adv. Agron.*, A.G. Norman (ed.), 15: 119-159.
- Hogdahl, O. 1966. Distribution of the rare elements in sea water. Semiannual report No. 2, NATO Research Grant No. 203, Central Institute of Industrial Research. Oslo, Norway.
- Howitt, R.W. 1981. Dynamics of a Gray Luvisol. M.Sc. Thesis. Univ. of Alberta.
- Howitt, R.W. and S. Pawluk. 1985a. The genesis of a gray luvisol within the boreal forest region. I. Static pedology. *Can. J. Soil Sci.* 65: 1-8.
- Howitt, R.W. and S. Pawluk. 1985b. The genesis of a gray luvisol within the boreal forest region. II. Dynamic pedology. *Can. J. Soil Sci.* 65: 9-19.
- Huang, P.M. and S.Y. Lee. 1969. Effect of drainage on weathering transformations of mineral colloids of some Canadian Prairie soils. In: *Proceedings of the Int. Clay Conf.*, Tokyo, 1: 541-551.
- Innes, R.P. and D.J. Pluth. 1970. Thin section preparation using an epoxy impregnation for petrographic and microprobe analysis. *Soil Sci. Soc. Amer. Proc.* 34: 483-485.
- Jackson, M.L. and J.L. Luo. 1986. Potassium-release mechanism on drying soils: Nonexchangeable to exchangeable potassium by protonation of micas. *Soil Sci.* 141: 225-229.
- Jackson, M.L. 1975. Soil chemical analysis - advanced course. (6th printing). Published by M.L. Jackson, Dept. of Soil Sci., Univ. of Wisconsin, Madison. WI.

- Jackson, M.L. 1962. Interlayering of expandable layer silicates in soil chemical weathering. *Clays Clay Miner.* 11: 29-46.
- Jackson, M.L. 1963. Aluminium bonding in soils: A unifying principle in soil science. *Soil Sci. Soc. Am. Proc.* 27: 74-78.
- Jenne, E.A. 1977. Trace element sorption by sediments and soils--sites and process. In. *Molybdenum in the environment*, Vol. 2, W.R. Chappell and K.K. Peterson (eds.) pp. 425-553.
- Jenne, E.A. 1968. Controls on Mn, Fe, Co, Ni, Cu and Zn concentrations in soils and water: The significant role of hydrous Mn and Fe oxides. In. *Trace inorganics in water*, R.F. Gould (ed.). *Advances in Chemistry Series*. Am. Chem. Soc., Washington, D.C.
- Kabata-Pendias, A. and H. Pendias. 1984. *Trace elements in soils and plants*. CRC Press, Inc. Boca Raton, Florida.
- Khan, D.H. 1959. Studies in translocations of chemical constituents in some red-brown soils, terra rosas and rendzinas using zirconium as a weathering index. *Soil Sci.* 88: 196-200.
- Khargarot, A.S., L.P. Wilding, and G. F. Hall. 1971. Composition and weathering of loess mantled Wisconsin- and Illinoian- age terraces in Central Ohio. *Soil Sci. Soc. Am. proc.* 35: 621-626.
- King, L.D. 1988. Retention of metals by several soils of the Southeastern United States. *J. Environ. Qual.* 17: 239-246.
- Kirkland, D.L. and B.F. Hajek. 1972. formula derivation of Al-interlayered vermiculite in selected soil clays. *Soil Sci.* 114: 317-322.
- Kittrick, J.A. 1973. Mica-derived vermiculites as unstable intermediates. *Clays Clay Miner.* 21:479-488.
- Knorring, O. and G. Hornung. 1961. Hafnium zircons. *Nature* 190:1098-1099.
- Kodama, H. and M. Schnitzer. 1971. Evidence for interlamellar adsorption of organic matter by clay in a Podzol soil. *Can. J. Soil Sci.* 51: 509-512.
- Krauskopf, K.B. 1979. *Introduction to geochemistry*, McGraw-Hill Co., New York, N.Y.
- Krinsley, D. and J.C. Doornkamp. 1973. *Atlas of quartz sand surface textures*: Cambridge Univ. Press, London, UK.
- Krinsley, D. and T. Takahashi. 1962. The surface textures of sand grains, an application of electron microscopy: *Science* 138: 1262-1264.
- Kukla, G. 1987. Loess stratigraphy in central China. *Quaternary Sci. Rev.* 6: 191-219.
- Laufer, F., S. Yarid, and M. Steinberg. 1984. The adsorption of quadrivalent cerium by kaolinite. *Clay Miner.* 15: 137-149.

- Lavkulich, A.M. 1969. Soil dynamics in the interpretation of Paleosol. In. *Pedology and Quaternary research*, S. Pawluk (ed.). National Res. Council of Canada.
- Lee, J.S. 1947. Quaternary glaciations in the Lushan area, central China. *Memoirs of the institute of geology, Academia Sinica*, B2:1-70.
- Lee, J.S. 1933. Quaternary glaciation in the Yangtze valley. *Bull. Geol. Soc. China* 13: 15-62.
- Lee, J.S. 1922. Notes on traces of recent ice-action in Northern China. *Geological Magazine* 59: 14-21.
- Leeper, G.W. 1970. *Six trace elements in soils*. Melbourne Univ. Press, Carlton, Victoria, Australia.
- LeRiche, H.H. and A.H. Weir. 1963. A method of studying trace elements in soil fractions. *J. Soil Sci.* 14: 225-235.
- Lewis, G.C., M.A. Fosberg, R.E. McDole, and J.C. Chugg. 1975. Distribution and some properties of loess in southcentral and southeastern Idaho. *Soil Sci. Soc. Am. Proc.* 39: 1165-1168.
- Liu, D. 1986. Stratigraphy and paleoenvironmental changes in the loess of central China. *Quaternary Sci. Rev.* 5: 489-495.
- Liu, D. *et al.* 1985. *Loess and the environment*. China Ocean Press, Beijing, pp. 221-228.
- Liu, D., Z. Ding, M. Chen, and Z. An. 1989. The global surface energy system and the geological role of wind stress. *Quaternary International*, 1: 43-55.
- Liu, K. 1988. Quaternary history of the temperate forests of China. *Quaternary Sci. Rev.* 7: 1-20.
- Liu, Z., Q. Zhu, and L. Tang. 1983. Microelements in the main soils of China. *Soil Sci.* 135: 40-46.
- Loganathan, P. and R.G. Bureau. 1973. Sorption of heavy metal ions by a hydrous manganese oxide. *Geochim. Cosmochim. Acta* 37: 1277-1294.
- Marcus, Y. and J. Abrahamer. 1961. Anion exchange of metal complexes. VII. The lanthanides - Nitrate system. Israel Atomic Energy Commission, pp. 608.
- McKeague, J.A. 1978. *Manual on soil sampling and methods of analysis*. Canada Soil Survey Committee. Can. Soc. Soil Sci.
- McKeague, J.A. and J.E. Brydon. 1970. Mineralogical properties of ten reddish brown soils from the Atlantic provinces in relation to parent materials and pedogenesis. *Can. J. Soil Sci.* 50: 47-55.
- McKeague, J.A., W.H. Damman, and P.K. Heringa. 1968. Iron-manganese and other pans in some soils of Newfoundland. *Can. J. Soil Sci.* 48: 243-253.

- McKeague, J.A., N.M. Miles, T.W. Peters, and D.W. Hoffman. 1972. A comparison of luvisolic soils from three regions in Canada. *Geoderma* 7: 49-69.
- McKeague, J.A. and R.J. St. Arnaud. 1969. Pedotranslocation: eluviation-illuviation in soils during the Quaternary. *Soil Sci.* 107: 428-434.
- McKeague, J.A. and M.S. Wolynetz. 1980. Background levels of minor elements in some Canadian soils. *Geoderma* 24: 299-307.
- McKenzie, R.M. 1972. The sorption of some heavy metals by the lower oxides of manganese. *Geoderma* 8: 29-35.
- McKenzie, R.M. 1970. The sorption of cobalt with manganese dioxide minerals. *Aust. J. Soil. Res.* 8: 97-106.
- McKenzie, R.M. 1957. The distribution of trace elements in some Australian red-brown earths. *Aust. J. Agric. Res.* 8: 246-252.
- Means, J.L., D.A. Crerar, and M.P. Borcsik. 1978. Adsorption of Co and selected actinides by Mn and Fe oxides. *Geochim. Cosmochim. Acta* 42: 1763-1773.
- Mehra, O.P. and M.L. Jackson. 1960. Iron oxide removal from soils and clays by dithionite-citrate system buffered with bicarbonate. *Clays Clay Miner.* 7: 317-327.
- Mel'Nikova, M.K. and S.V. Kovenya. 1974. Simulation studies of lessivage. 10th Int. Soil Sci. Conf. Moscow. VI: 600-608.
- Miller, F.P., N. Holowaychuk, and L.P. Wilding. 1971a. Canfield Silt Loam, a Fragiudalf: I. Macromorphological, physical and chemical properties. *Soil Sci. Soc. Am. Proc.* 35: 319-324.
- Miller, F.P., N. Holowaychuk, and L.P. Wilding. 1971b. Canfield Silt Loam, a Fragiudalf: II. Micromorphological, physical and chemical properties. *Soil Sci. Soc. Am. Proc.* 35: 325-331.
- Miller, S.E., G.R. Heat, and R.D. González. 1982. Effects of temperature on the the sorption of lanthanides by montmorillonite. *Clays Clay Miner.* 16: 393-398.
- Mills, J.G. and M.A. Zwarich. 1975. Heavy metal content of agricultural soils in Manitoba. *Can. J. Soil Sci.* 55: 295-300.
- Minster, J.F., J.B. Minster, M. Treuil, and C.J. Allegre. 1977. Systematic use of trace elements in igneous processes. II. Inverse problem of the fractional crystallization process in volcanic suite. *Contrib. Mineral. Petrol.*, 61: 49 pp.
- Mitchell, R.L. 1964. Trace elements. In. *Chemistry of the soil*, F.E. Bear (ed.), 2nd. N.Y. Reinhold Publ. Corp. 323 pp.
- Moeller, T., D.F. Martin, L.C. Thompson, R. Ferrus, G.R. Feistel, and W.J. Randall. 1965. The coordination chemistry of yttrium and the rare earth metal ions. *Chem. Rev.* 65: 1-50.

- Nan, Y. and Y. Huang. 1965. A study on regional plants at Yaohe, Heilongjiang. In. Proceedings of Chinese For. Soil Inst. Papers. Vol. 2, Science Press.
- Nesbitt, H.W. 1979. Mobility and fractionation of rare earth elements during weathering of a granodiorite. *Nature* 279: 206-210.
- Nugent, L.J. 1970. Theory of the tetrad effect in the lanthanide (III) and the actinide (III) series. *Inorg. Nucl. Chem.* 32: 3485-3491.
- Olivera, P. 1986. Cambio ionico de lantanides en vermiculita y sorcion de sustancias organicas por vermiculitas lantanidas: Tesis Doctoral, Universidad de Málaga, Spain.
- Ovilera, P., E. Rodríguez-Castellón, and E. Rodríguez. 1987. Ionic exchange and characterization of lanthanide vermiculite. *Bol. Soc. Esp. Mineral.* 9: 170-173.
- Pastor, P.O., E. Rodríguez-Castellón, and A.R. García. 1988. Uptake of lanthanides by vermiculite. *Clays Clay Miner.* 36: 68-72.
- Pawluk, S. 1988. Freeze-thaw effects on granular structure reorganization for soil materials of varying texture and moisture content. *Can. J. Soil Sci.* 68: 495-494.
- Pawluk, S. 1987. Faunal micromorphological features in moder humus of some Western Canadian soils. *Geoderma* 40: 3-16.
- Pawluk, S. 1967. Soil analysis by atomic absorption spectroscopy. *Atomic Absorption Newsletter* 6: No. 3.
- Pawluk, S. and L. Bal. 1985. Micromorphology of selected Mollic Epipedons. In *Soil micromorphology and soil classification*, SSSA (ed.), Segoe Road, Madison, WI 53711. pp. 63-83.
- Peech, M., R.L. Cowan, and J.H. Baker. 1962. A critical study of the  $\text{BaCl}_2$ -triethanolamine and ammonium acetate methods for determining the exchangeable hydrogen content of soils. *Soil Sci. Soc. Am. Proc.* 26: 37-40.
- Penck, A. and E. Brückner. 1909. *Die Alpen im Eiszeitalter*. Vol. 3, Leipzig.
- Peppard, D.F., G.W. Mason, and S. Lewey. 1969. A tetrad effect in the liquid-liquid extraction ordering of lanthanides (III). *J. Inorg. Nucl. Chem.* 31: 2271-2272.
- Pettapiece, W.W. 1969. The forest - grassland transition. In. *Pedology and Quaternary Research*, S. Pawluk (ed.)
- Pettapiece, W.W. 1970. Pedological investigations in the front range of the Rocky Mountains along the North Saskatchewan River Valley. Ph.D. Thesis, Univ. of Alberta.
- Piper, D.Z. 1974. Rare earth elements in ferromanganese nodules and other marine phases. *Geochim. Cosmochim. Acta.* 38: 1007-1022.

- Price, T.W., R.L. Blevins, R.I. Barnhisel, and H.H. Baily. 1975. Lithological discontinuity in loessial soils of southwestern Kentucky. *Soil Sci. Soc. Am. Proc.* 39: 94-97.
- Puan, X. 1988. White clay soils on the border between Shandong and Jiandshu Provinces. Ph. D. Thesis, Nanjing Agric. Univ. Jiangshu, P.R. China.
- Pye, K. 1983. Loess. In: *Progress in physical geography* 8: 176-217.
- Raad, A.T. and R. Protz. 1971. A new method for the identification of sediment stratification in soils of the Blue Springs Basin, Ontario. *Geoderma* 6: 23-41.
- Raesian, J.D. 1959. Stability of index minerals in soils with particular reference to quartz, zircon and garnet. *J. Sed. Pet.* 29: 493-502.
- Rahn, K.A., R.D. Borys, and G.E. Shaw. 1981. Asian desert dust over Alaska: Anatomy of an arctic haze episode. *Geol. Soc. Amer. Special Paper*, 186: 37-70.
- Rai, D. and L.E. Eary. 1986. Solubility - controlling solids of Cr(III) and Cr(III)/Cr(VI) transformation reactions. In: *Proceedings, Chromium symposium 1986: an update*. D.M. Serrone, (ed.) Industrial Health Foundation, Inc. Pittsburg PA. pp. 331-341.
- Rai, D., J.M. Zachara, L.E. Eary, C.C. Ainsworth, J.E. Amonette, C.E. Cowan, R.W. Szelmeckza, C.T. Resch, R.L. Schmidt, D.C. Girvin, and S.C. Smith. 1988. Chromium reactions in geologic materials. Electric Power Research Institute, Palo Alto, CA. EPRI report EA-5741. pp. 291.
- Rankama, D.F. and T.G. Sahama. 1950. *Geochemistry*, The University of Chicago Press, Chicago.
- Rankin, P.C. and C.W. Childs. 1976. Rare-earth elements in iron-manganese concretions from some New Zealand soils. *Chem. Geol.* 18: 55-64.
- Rankin, P.C. and C.W. Childs. 1987. Rare earths and other trace elements in iron-manganese concretions from a catenary sequence of yellow-grey earth soils, New Zealand. *New Zealand J. Geol. Geophys.* 30: 199-202.
- Rea, D.K. and M. Leinen. 1988. Asian aridity and the zonal westerlies: Late Pleistocene and Holocene record of eolian deposition in the Northwest Pacific Ocean. *Palaeogeogr., Palaeoclimatol., Palaeoecol.*, 66: 1-8.
- Rich, C.I. 1968. Hydroxy interlayers in expandable layer silicates. *Clays Clay Miner.* 16: 15-30.
- Ritchie, A., L.P. Wilding, G.F. Hall, and C.F. Stahnke. 1974. Genetic implications of B horizons in aquifers of northeastern Ohio. *Soil Sci. Soc. Am. Proc.* 38: 351-358.
- Roaldset, E. 1973. Rare earth elements in Quaternary clays of the Numedal area, southern Norway. *Lithos.* 6: 349-372.
- Roaldset, E. 1974. Lanthanide distributions in clays. *Bull. Gr. fr. Argiles.* 26: 201-209.



- Roaldset, E. and I.T. Rosenqvist. 1971. Unusual lanthanide distribution. *Nature Phys. Sci.* 231: 153-154.
- Rode, A.A. 1961. The soil forming process and soil evolution. Isreal Program for Scientific Translations, Jerusalem.
- Ronov, A.B., Y.A. Balashov, and A.A. Migdisov. 1967. Geochemistry of the rare earths in the sedimentary cycle. *Geochem. Int.* 4: 1-17.
- Ronov, A.B., Y.A. Balashov, Y.P. Girin, P.K. Bratishko, and G.A. Kazakov. 1972. Trends in rare-earth distribution in the sedimentary shell in the earth's crust. *Geoderma. Int.* 9: 987-1016.
- Ronov, A.B., Y.A. Balashov, Y.P. Girin, P.K. Bratishko, and G.A. Kazakov. 1974. Regularities of rare earth distribution in the sedimentary shell and in the crust of the earth. *Sedimentology* 21: 171-193.
- Roonwall, G.S. and D.R. Bhumbra. 1969. Contributions to the mineralogy of the sand fraction and geochemistry of the soils developed over gneissic rocks in the Kulu area (central Himalayas, India). *Geoderma* 2: 309-319.
- Runge, E.C.A., T.W. Walker, and D.T. Howarth. 1974. A study of Late Pleistocene loess deposits, south Canterbury, New Zealand. I. Forms and amounts of phosphorus compared with other techniques for identifying paleosols, *Quaternary Res.* 4: 76-84.
- Rust, R.H. 1983. Alfisols. In: *Pedogenesis and taxonomy. II. Soil Orders*, L.P. Wilding, N. Smeck and G.F. Hall, (eds.). Elsevier, Scientific Publ. Amst.
- Rutledge, E.M., N. Holowaychuk, G.F. Hall, and L.P. Wilding. 1975. Loess in Ohio in relation to several possible source areas: I. Physical chemical properties. *Soil Sci. Soc. Am. Proc.* 39: 1125-1132.
- Schieber, J. 1986. Stratigraphic control of rare-earth pattern types in Mid-Proterozoic sediments of the belt supergroup, Montana, U.S.A.: implications for basin analysis. *Chem. Geol.* 54: 135-148.
- Schnitzer, M. 1969. Reactions between fulvic acid, a soil humic compound and inorganic constituents. *Soil Sci. Soc. Am. Proc.* 33: 75-81.
- Schnitzer, M. and H. Kodama. 1972. Reactions between fulvic acid and Cu-montmorillonite. *Clays clay miner.* 20:359-367.
- Schnitzer, M. and H. Kodama. 1977. Reactions of minerals with soil humic substances. In: *Minerals in soil environments*, SSSA, Madison, WI.
- Shacklette, H.T. and J.G. Boerngen. 1984. Element concentration in soils and other surficial materials of the conterminous United States. USGS Prof Paper 1270, US Govt. Printing Office, Washington D.C.
- Shi, Y., B. Ren, and J. Wang. 1986. Quaternary glaciation in China. *Quaternary Sci. Rev.* 5: 503-507.

- Shi, Y. and Y. Deng. 1982. Concrete evidence of Quaternary debris flow deposits at the foot of Lushan. *Kexue Tongbao* 28: 798-806.
- Sidhu, P.S., J.L. Sehgal, M.K. Sinha, and N.S. Randhawa. 1977. Composition and mineralogy of iron manganese concretions from some soils of the Indo-Gangetic Plain in northwest India. *Geoderma* 18: 241-249.
- Siekierski, S. 1970. Further observations on the regularities associated with the formation the lathanides and actinide complexes. *J. Inorg. Nucl. Chem.* 32: 519-529.
- Siekierski, S. 1971. The shape of the lanthanide contraction as reflected in the changes of unit cell volumes, lanthanides radius and the free energy of complex formation. *J. Inorg. Nucl. Chem.* 33: 377-386.
- Smeck, N. E. and E.C.A. Runge. 1971. Phosphorus availability and redistribution in relation to profile development in an Illinois landscape segment. *Soil Sci. Soc. Am. Proc.* 35: 808-815.
- Smeck, N.E. and L.P. Wilding. 1980. Quantitative evaluation of pedon formation in Calcareous glacial deposits in Ohio. *Geoderma* 24: 1-16.
- Smeck, N.E., L.P. Wilding, and N. Holowaychuk. 1968. Genesis of argillic horizons in Celina and Morely soils of western Ohio. *Soil Sci. Soc. Am. Proc.* 32: 550-556.
- Smith, G. D. 1934. Experimental studies on the development of heavy clay pan in soils. *Missouri Agric. Exp. Stn. Res. Bull.* 210.
- Sneddon, J.I., L.M. Lavkulich, and L. Farstad. 1972. The morphology and genesis of some Alpine soils in British Columbia, Canada. II. Physical, chemical and mineralogical determination and genesis. *Soil Sci. Soc. Am. Proc.* 36: 104-110.
- Soil Survey Office. 1960. Soil Survey of Jinlin Province.
- Spiers, G.A., M.J. Dudas, and K. Muehlenbachs. 1985. Isotopic evidences for clay mineral weathering and authigenesis in Cryboralfs. *Soil Sci. Soc. Am. J.* 49: 467-474.
- Spiers, G.A., S. Pawluk, and M.J. Dudas. 1988. The mobile phase in luvisolic soils. Poster presented in the annual Can. Soc. Soil Sci. Mtg. Calgary, Alberta, Canada.
- Spirn, R.V. 1965. Rare earth distributions in the marine environment - Ph. D. Thesis. M.I.T.
- St. Arnaud, R.J. and M.M. Mortland. 1963. Characteristics of the clay fraction on a Chernozemic to Podzol sequence of soil profiles in Saskatchewan. *Can. J. Soil Sci.* 44: 88-99.
- St. Arnaud, R.J. and E.P. Whiteside. 1963. Physical breakdown in relation to soil development. *J. Soil Sci.* 14: 267-281.
- Su, Z. 1984. A view on Quaternary glaciation in Lushan from the result of some modern glacial researches. *J. Glaciology and Cryopedology* 61: 83-88.

- Suarez, D.L. and D. Langmuir. 1976. Heavy metal relationships in a Pennsylvania soil. *Geochim. Cosmochim. Acta* 40: 589-598.
- Sudom, M.D. and R.W. St. Arnaud. 1971. Use of quartz, zirconium and titanium in pedological studies. *Can. J. Soil Sci.* 51: 385-396.
- Sun, T. and H. Yang. 1961. The great ice age glaciation in China. *Acta Geol. Sinica* 41: 234-244.
- Swaine, D.J. 1955. The trace-element contents of soils. *Commonw. Bur. Soil Sci. Tech. Commun.* No. 48.
- Swaine, D.J. and R.L. Mitchell. 1960. Trace-element distribution in soil profiles. *J. Soil Sci.* 11: 347-368.
- Syers, J.K., D.L. Mokma, M.L. Jackson, D.L. Dolcater, and R.W. Rex. 1972. Mineralogical composition and cesium-137 retention properties of continental aerosolic dusts. *Soil Sci.* 113: 116-123.
- Taylor, S.T. 1965. The application of trace element data to problems in petrology. In. *Physics and chemistry of the earth*, L.H. Aherns, F. Press, S.K. Runcorn and H.C. Urey (eds.), Pergamon Press, New York, N.Y. pp. 133-213.
- Theisen, A.A. and M.E. Harward. 1962. A paste method for preparation of slides for clay mineral identification by x-ray diffraction. *Soil Sci. Soc. Am. Proc.* 26: 90-91.
- Theng, B.K.G. 1976. Interactions between montmorillonite and fulvic acid. *Geoderma*. 15: 243-251.
- Topp, S.E., B. Salbu, E. Roaldset, and P. Jørgensen. 1985. Vertical distribution of trace elements in laterite soil. *Chem. Geol.* 47: 159-174.
- Ugolini, F.C. H. Dawson, and J. Zachara. 1977. Direct evidence of particle migration in the soil solution of podzol. *Science* 198: 603-605.
- U.S.D.A. 1975. Soil taxonomy. Soil Conservation Service, Washington, D.C.
- Varshal, G.M., M.M. Senyavin, and R.D. Yaryseva. 1975. Forms of calcium and REE in river water. In. *Recent contributions to geochemistry and analytical chemistry*. A.I. Tugarinov (ed.), Wiley, New York, N.Y., pp. 597-603.
- Vlasov, K.A. 1966. Geochemistry and mineralogy of rare elements and genetic type of their deposits, Vol. I, pp. 368-396.
- Wang, C. and R.W. Arnold 1973. Quantifying pedogenesis for soils with discontinuities. *Soil Sci. Soc. Am. Proc.* 37: 271-278.
- Warren, J.C., B. Xing, and M.J. Dudas, 1990. Simple microwave digestion technique for elemental analysis of mineral soil samples. *Dept. of Soil Sci., Univ. of Alberta*.
- Wieder, M. and D.H. Yaalon. 1974. Effect of matrix composition on carbonate nodule crystallization. *Geoderma* 11: 95-121.

- Wright, W.R. and J.E. Foss. 1968. Movement of silt-sized particles in sand columns. *Soil Sci. Soc. Am. Proc.* 32: 446-448.
- Wu, Z. 1980. *The vegetation of China*. Science Press, Beijing.
- Xia, R. and Z. Shang. 1981. Annual fluctuation of soil moisture of white clay soil and problems of soil reclamation. *Acta. Agric. Univ. Pekinensis* 7: 59-70.
- Xie, Y., 1982. A study on formation of heavy textured material in the Three River Plain, Heilongjiang. In: *Proceedings of the third conference of Quaternary Science, Chinese Quaternary Res. Association (ed.)*, Science Press, Beijing, pp. 130-133.
- Xiong, D. and R. Huang. 1986. A comparative study on the micromorphology of Baijiang soils of Jinlin Province and Huaibei region in China. In *Current progress in soil research in P.R. China*, Soil Sci. Soc. China, (ed.), Jiang shu Sci. & Tech. Publ. House. pp. 543-550.
- Xu, Q. 1979. Study on podzols and white clay soils. *Progress in Soil Sci.* 1: 21-38.
- Yang, Z. 1986. The problem of Quaternary glaciation in China. In *the Geology of China*, Z. Yang, Y. Cheng and H. Wang (eds.). Clarendon Press, Oxford. 173 pp.
- Ye, Y., F. Yan, and X. Mai. 1983. The sporo-pollen assemblages in three well logs from Three-River Plain, north-east China and their geological significance. *Scientia Geol. Sinica* 3: 459-266.
- Yoe, J.H. and H.J. Koch. 1957. *Trace element analysis*, J. Wiley and Sons, New York.
- Yoshida, H. 1962. Solvent extraction studies of thiocyanate complex of the lanthanides. *J. Inorg. Nucl. Chem.* 24: 1257-1265.
- Yu, Z. 1986. *Soil formation, identification, and classification*. Dept. of Soil Science, Zhejiang Agric. Univ., Zhejiang, P.R. China.
- Yuan, K. 1983. *Nutrient element chemistry of plants*. Science Press, Beijing.
- Zeng, Z. 1963. Problems about the formation and classification of white clay soils. *Acta. Pedol. Sinica*. 11: 111-129.
- Zeng, Z. 1980. White clay soils, In: *Soils in Northeast China*, Shenyang Soil and For. Res. Inst. (ed.), Science Press, Beijing. pp. 193-218.
- Zhao. Y., J. Wang, R. Xia, Z. Shang, and S. Zhao. 1984. Comparison on several properties between white clay soils of terrace and alluvial plain. *Acta. Agric. Univ. Pekinensis* 10: 275-284.
- Zhang, Z. 1987. Some mechanisms of white clay soils in Heilongjiang and the methods of reclamation and improvement. Dept. of Agronomy, HALRU.
- Zhang, L.Y. and Y.Z. Mou. 1982. Features and geneses of the diamictos in Lushan region. In: *Quaternary Geology and Environment in China*, T.S. Liu (ed.), China Ocean Press, Beijing pp. 89-93.

Zhang, Z, and Y. Zhang. 1983. Seasonal change on redox potential (Eh) of white clay soils. HALRU. J. 9: 1-11.

Zhu, Z. 1984. Soil science, II. Agricultural Press, Beijing.

## APPENDIX I

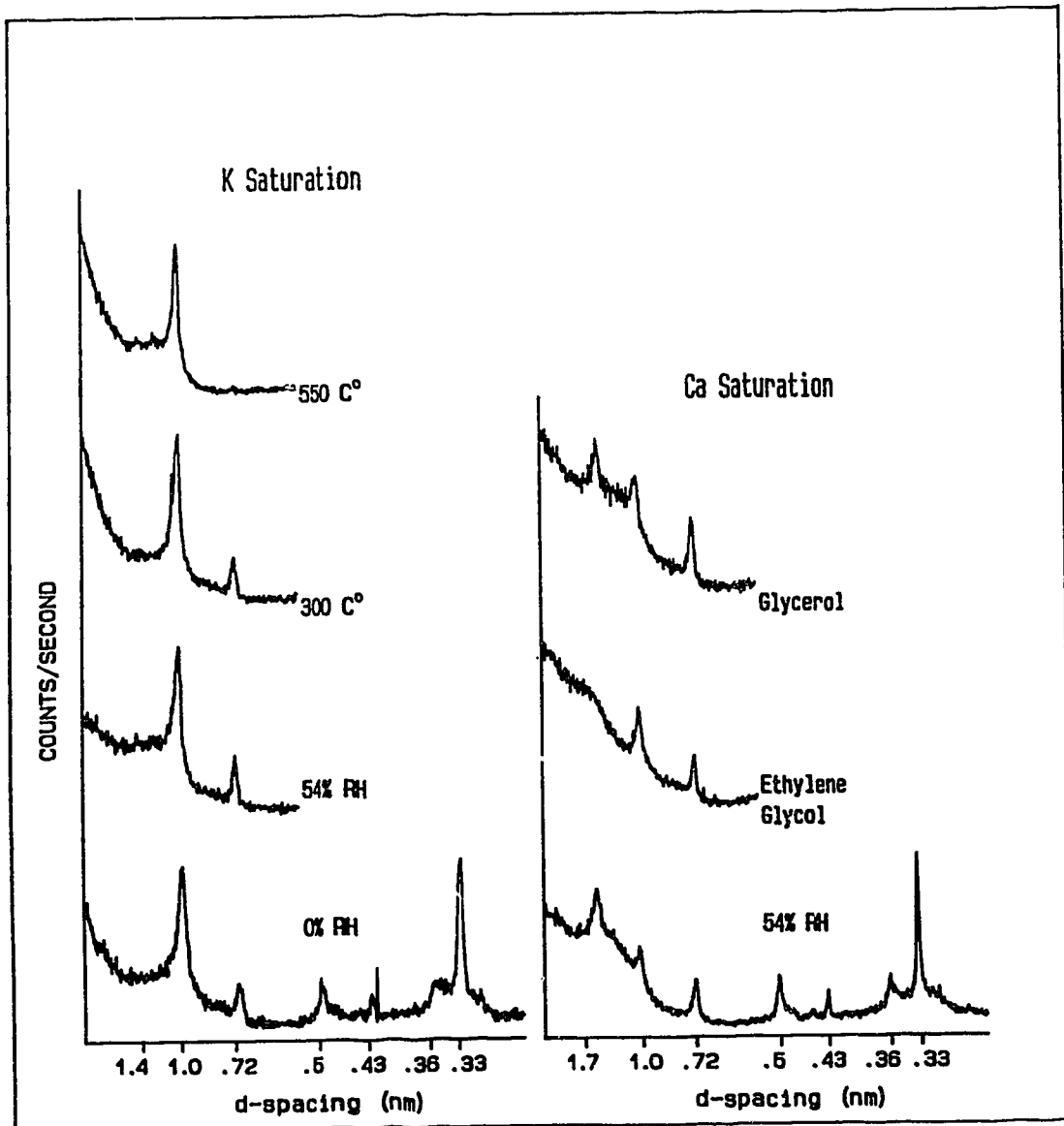


Figure 1. X-ray diffractogram of the clay separates from the Ah horizon of pedon 1.

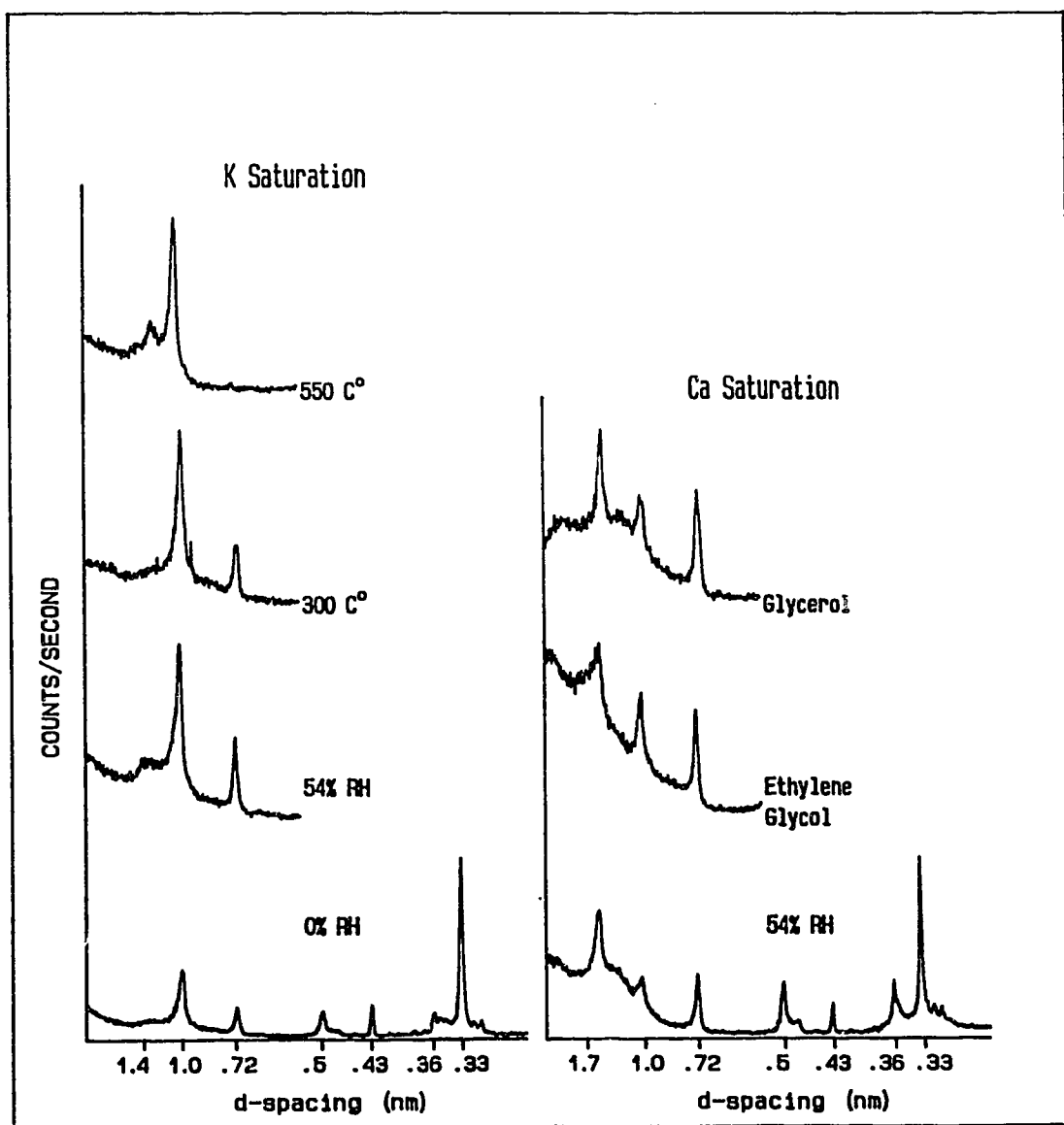


Figure 2. X-ray diffractogram of the clay separates from the E horizon of pedon 1.

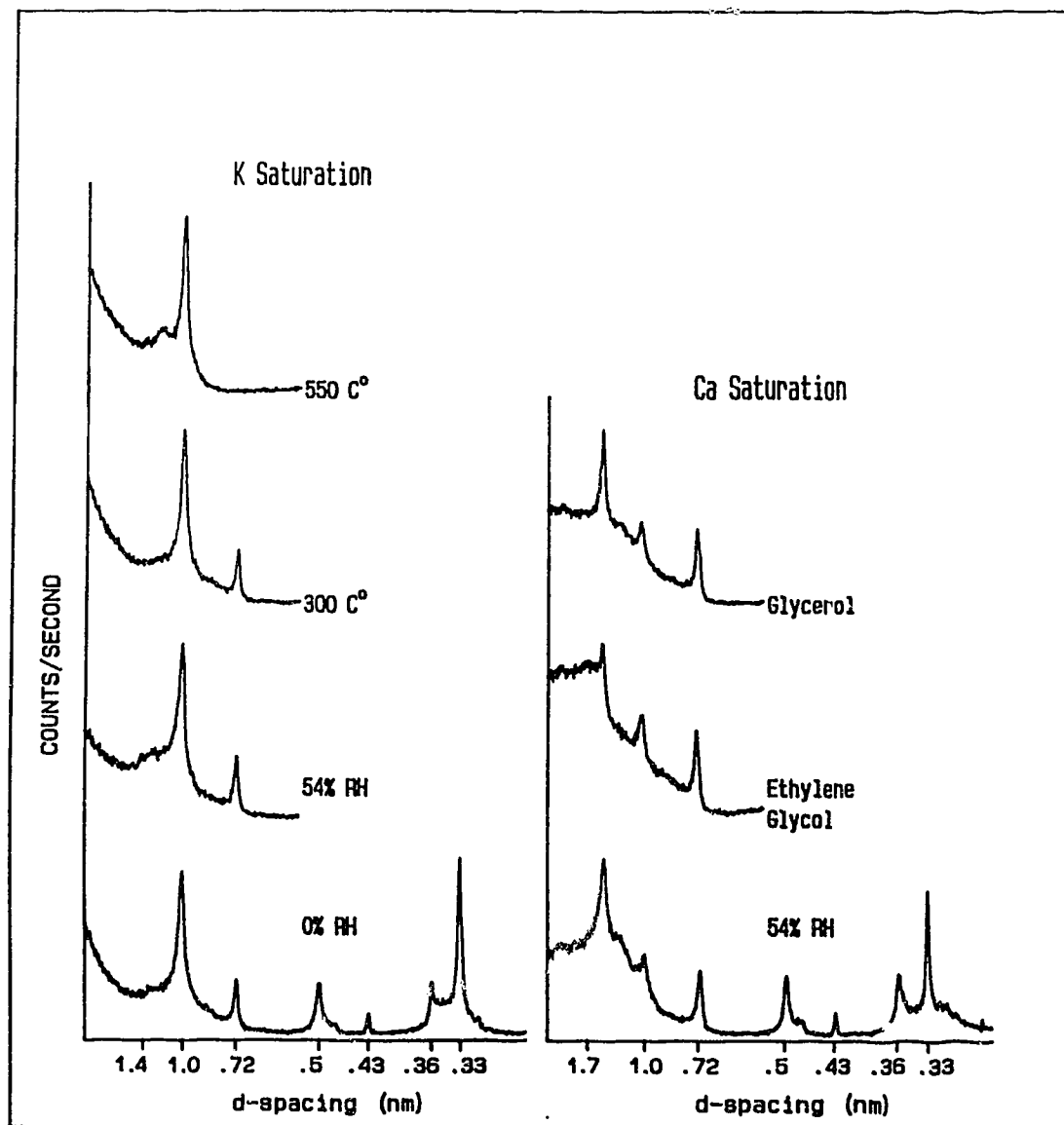


Figure 3. X-ray diffractogram of the clay separates from the Bt1 horizon of pedon 1.



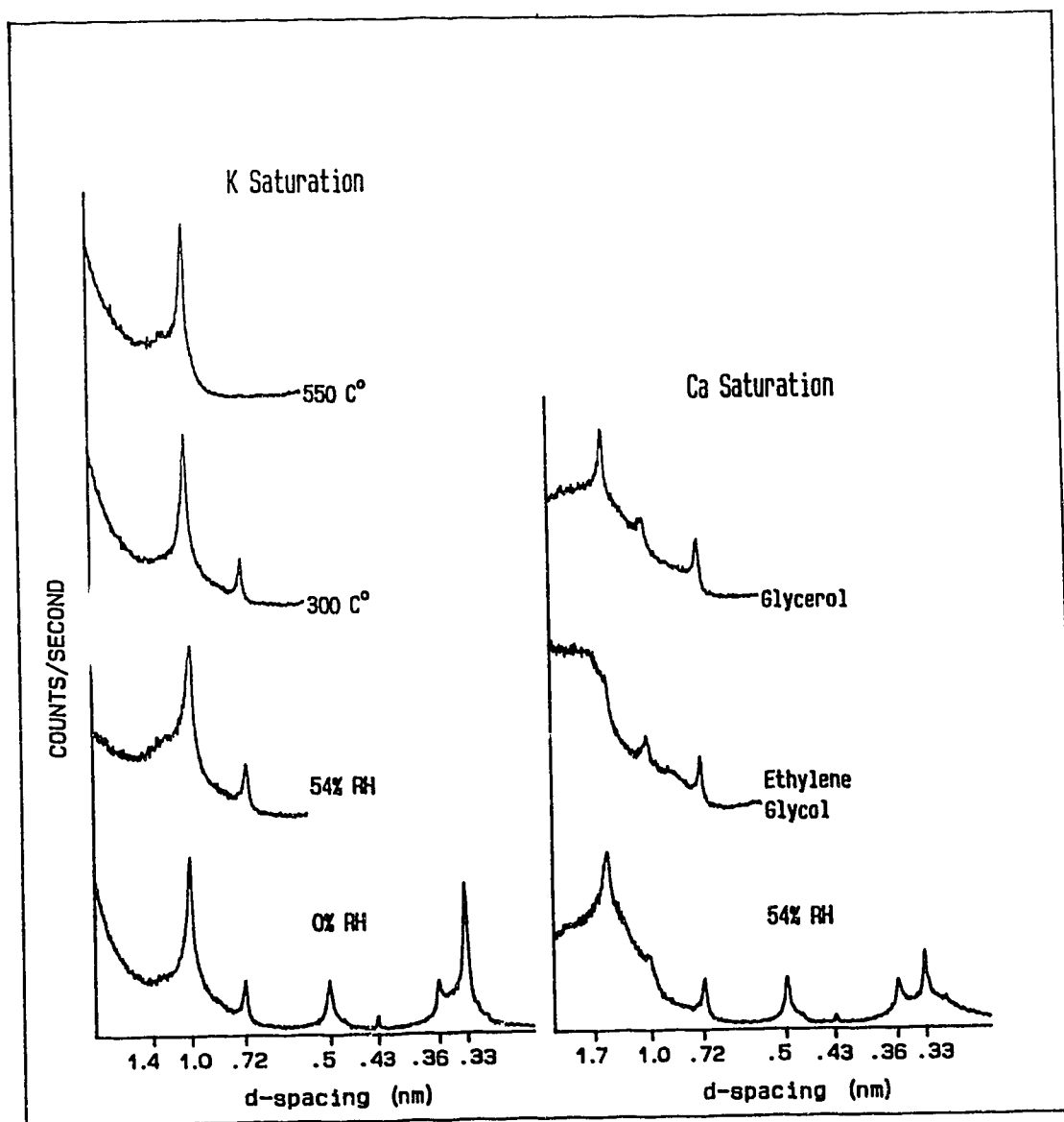


Figure 4. X-ray diffractogram of the clay separates from the Bt2 horizon of pedon 1.

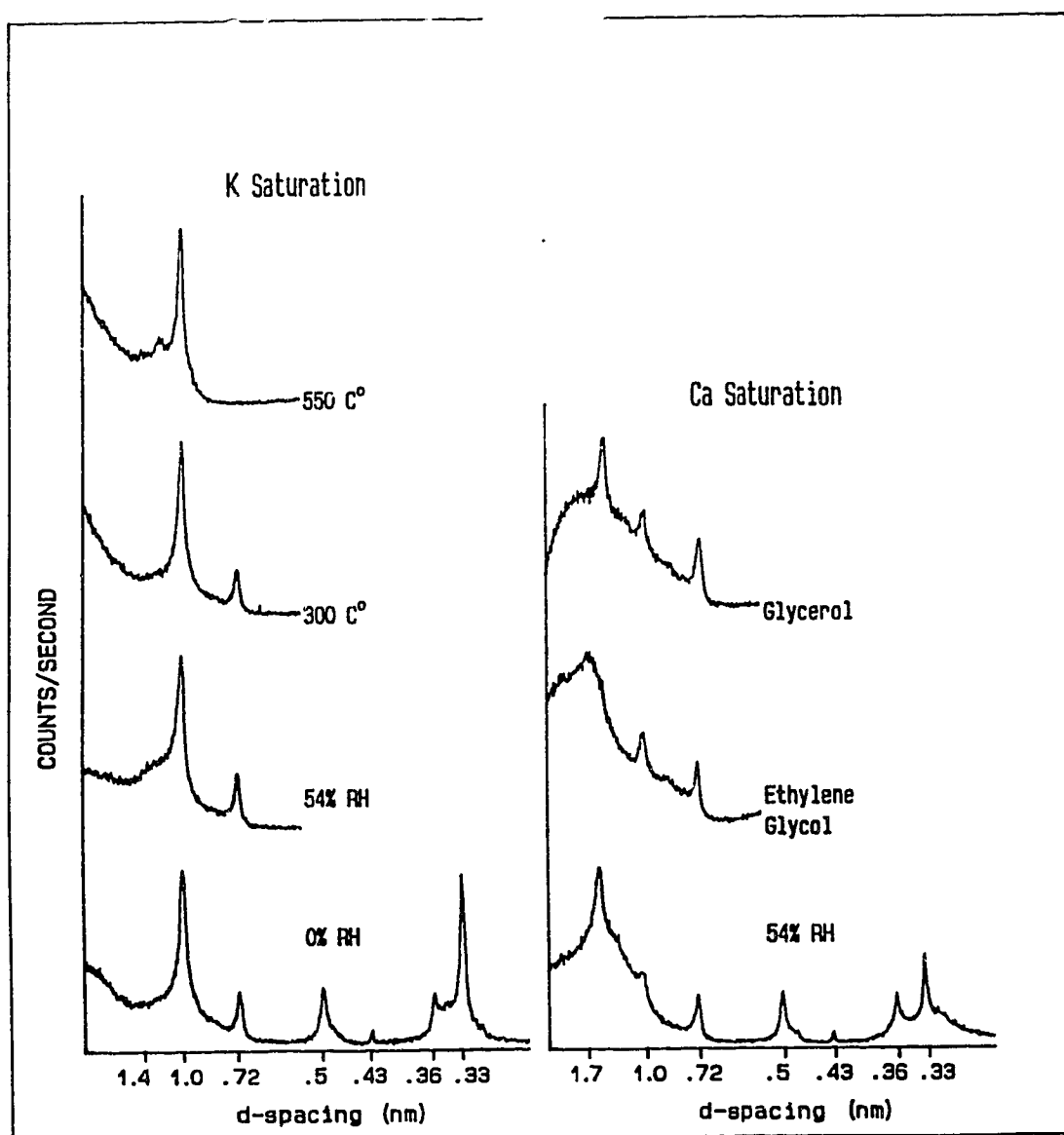


Figure 5. X-ray diffractogram of the clay separates from the Bt3 horizon of pedon 1.

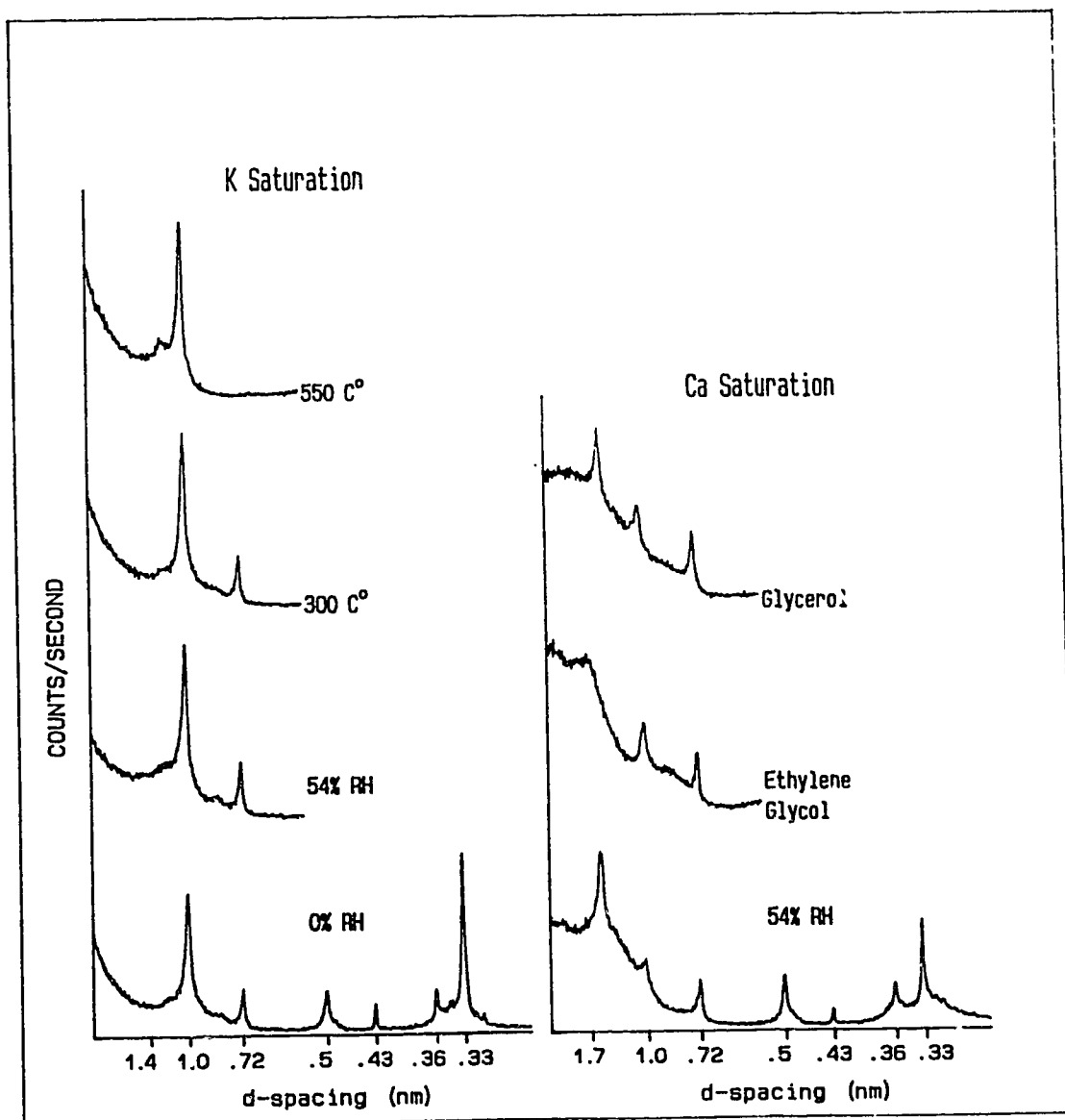


Figure 6. X-ray diffractogram of the clay separates from the C1 horizon of pedon 1.

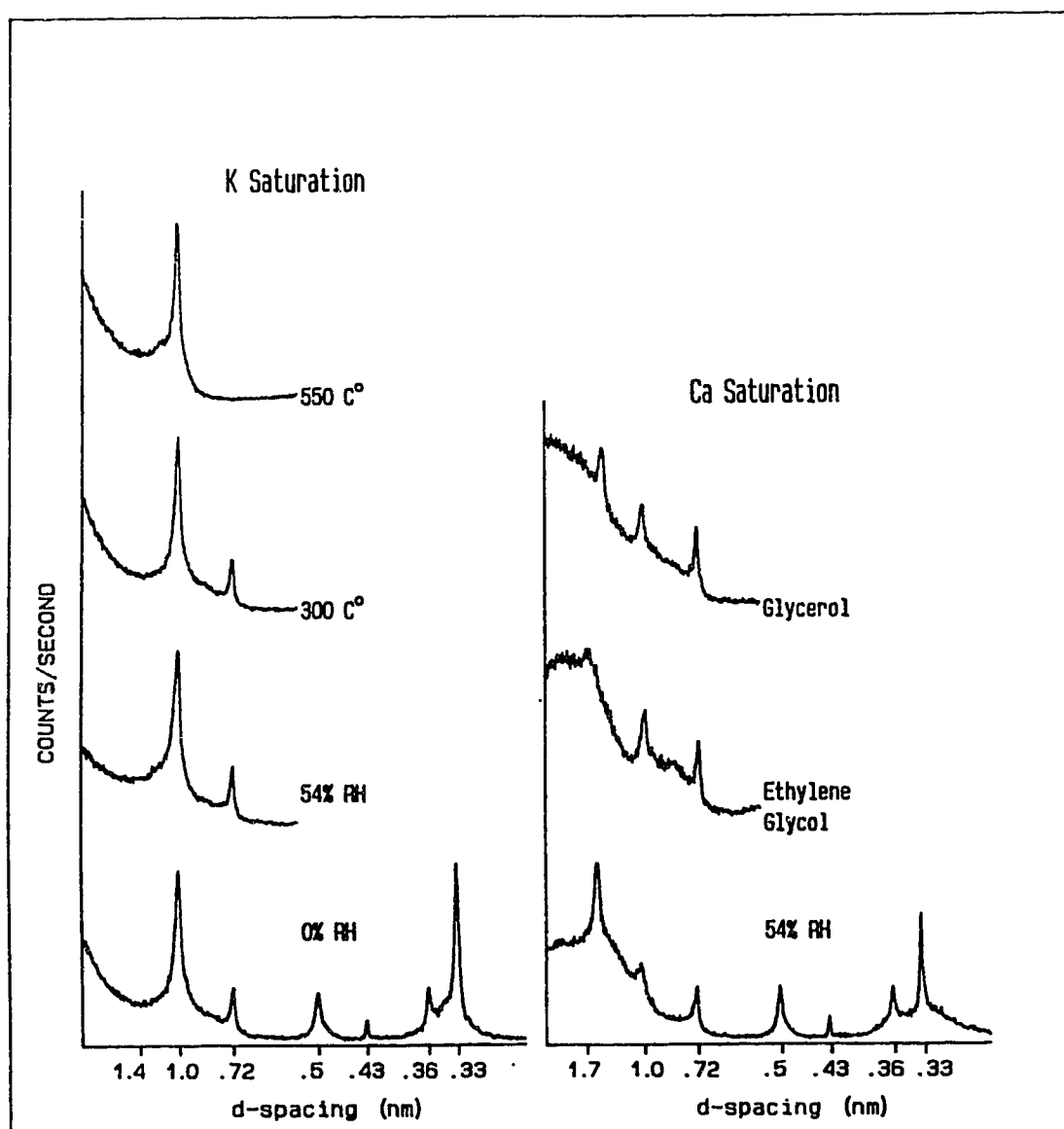


Figure 7. X-ray diffractogram of the clay separates from the C2 horizon of pedon 1.

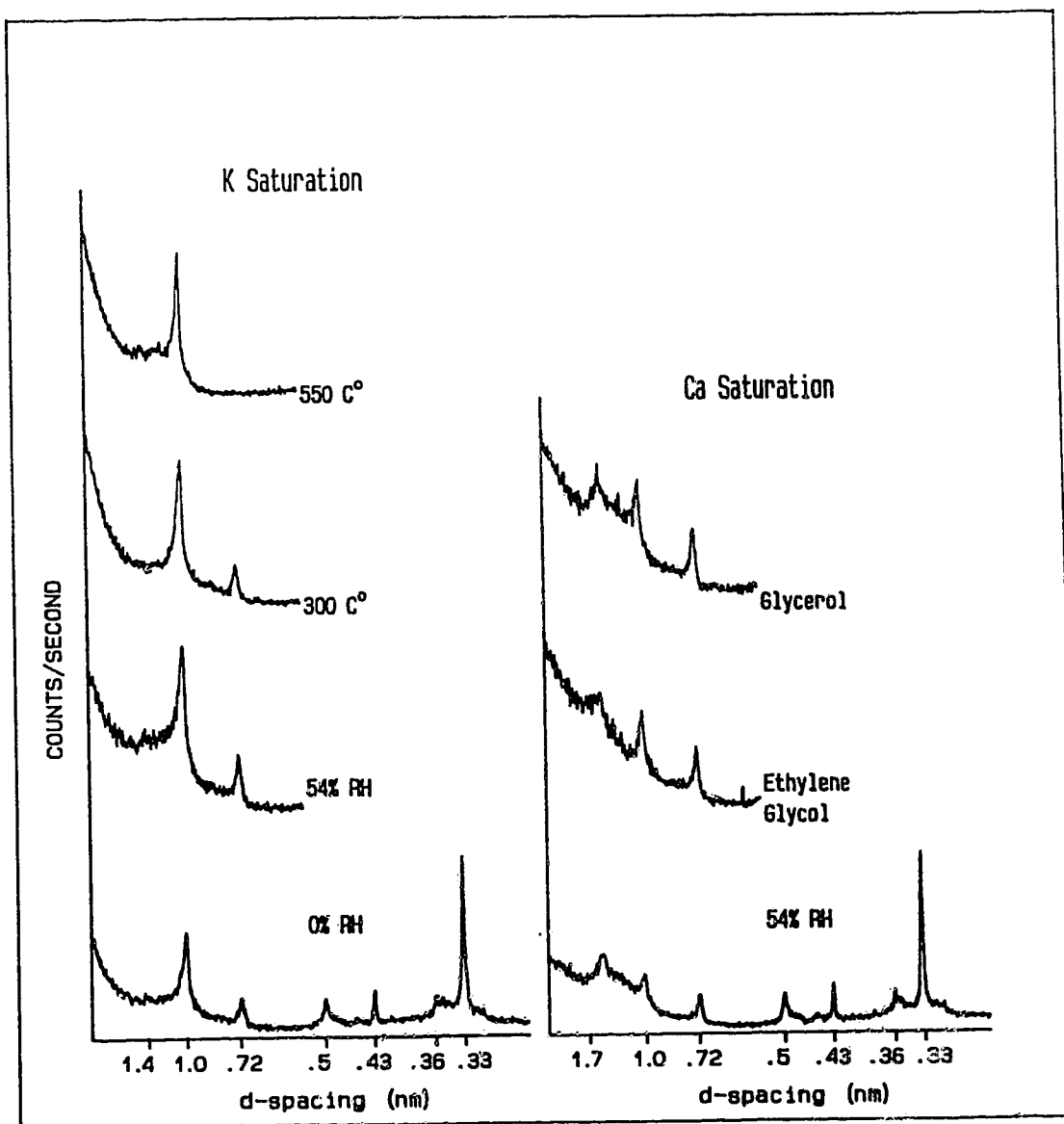


Figure 8. X-ray diffractogram of the clay separates from the Ah horizon of pedon 3.

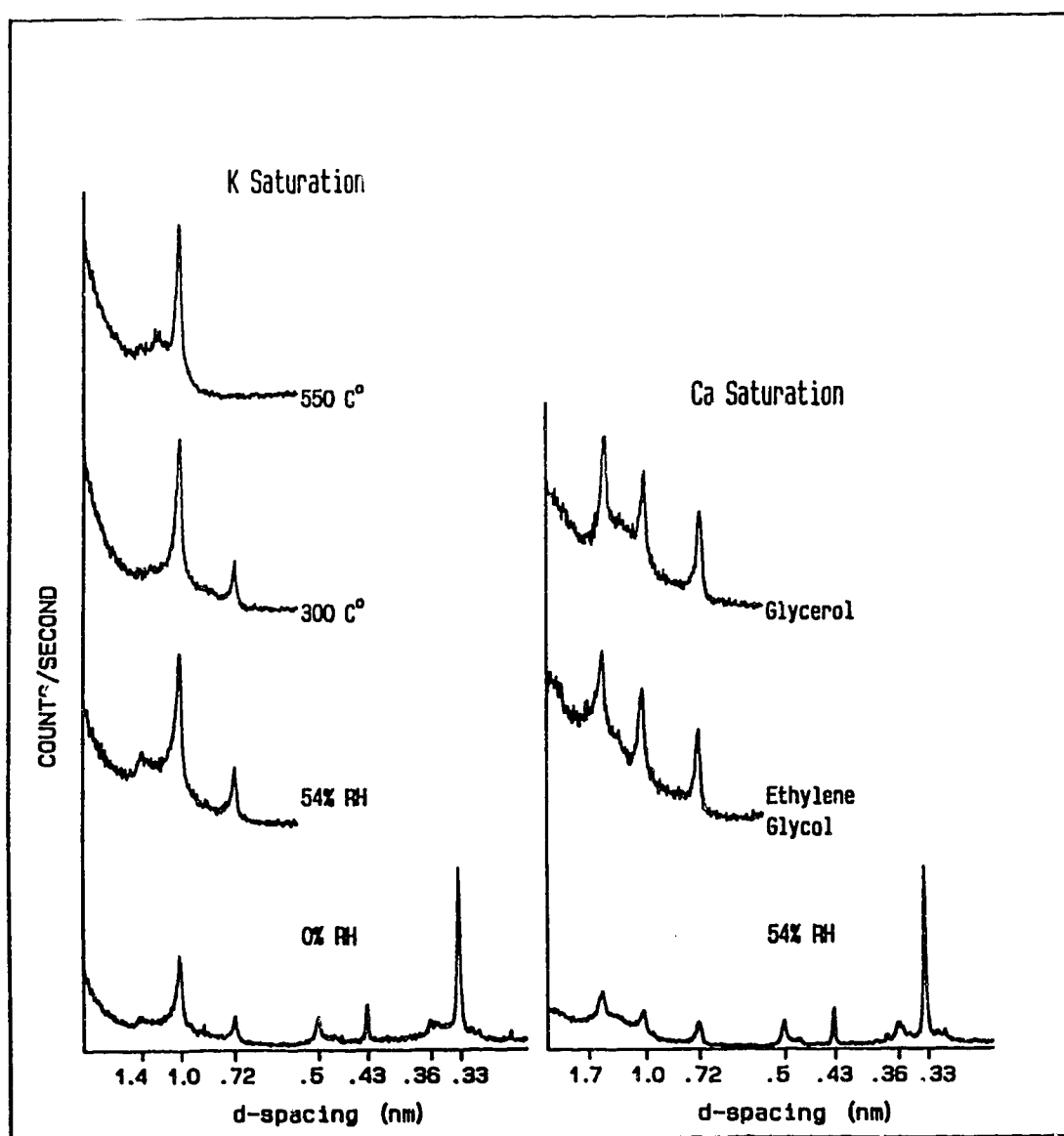


Figure 9. X-ray diffractogram of the clay separates from the E horizon of pedon 3.

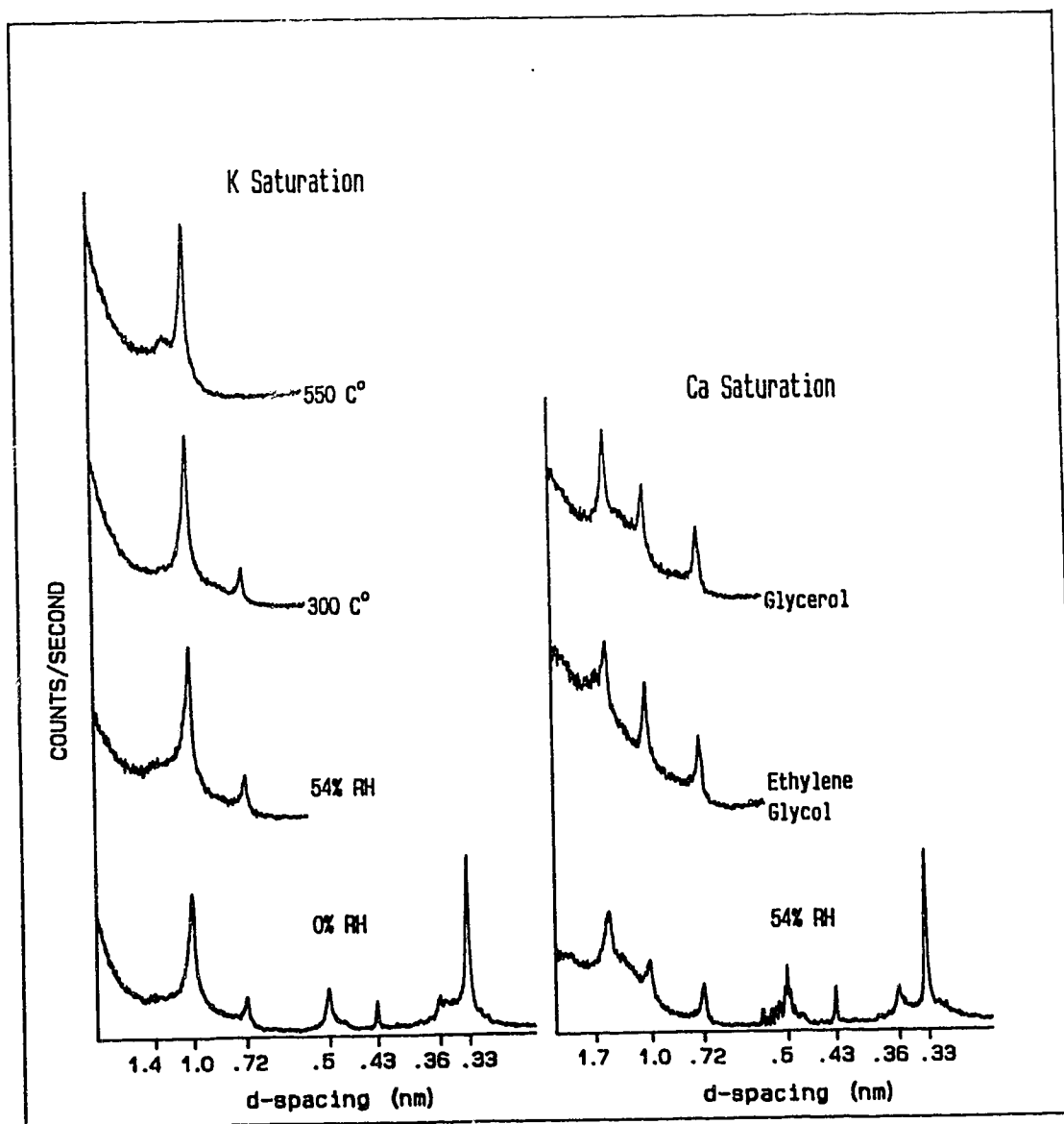


Figure 10. X-ray diffractogram of the clay separates from the Bt1 horizon of pedon 3.

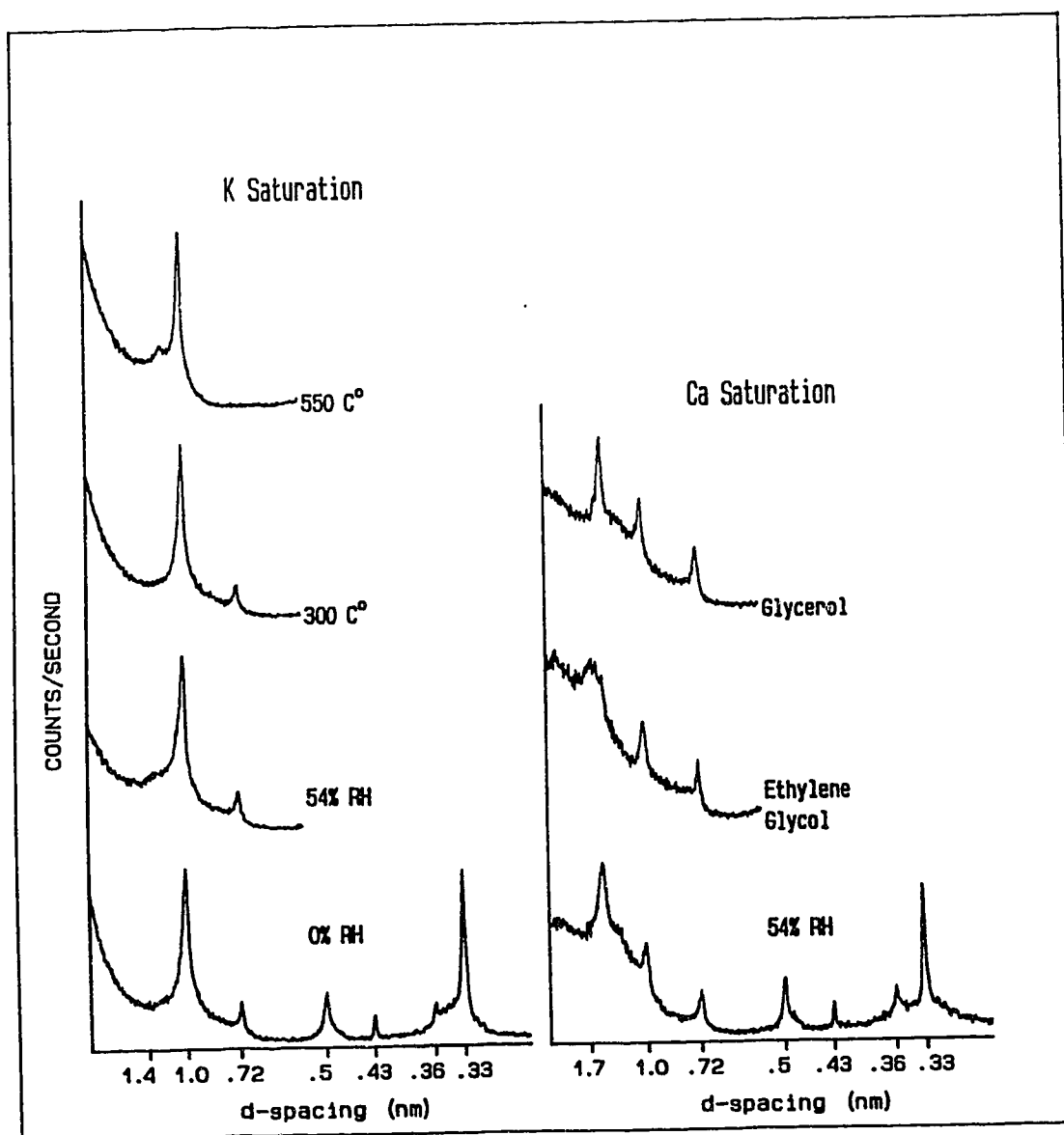


Figure 11. X-ray diffractogram of the clay separates from the Bt2 horizon of pedon 3.



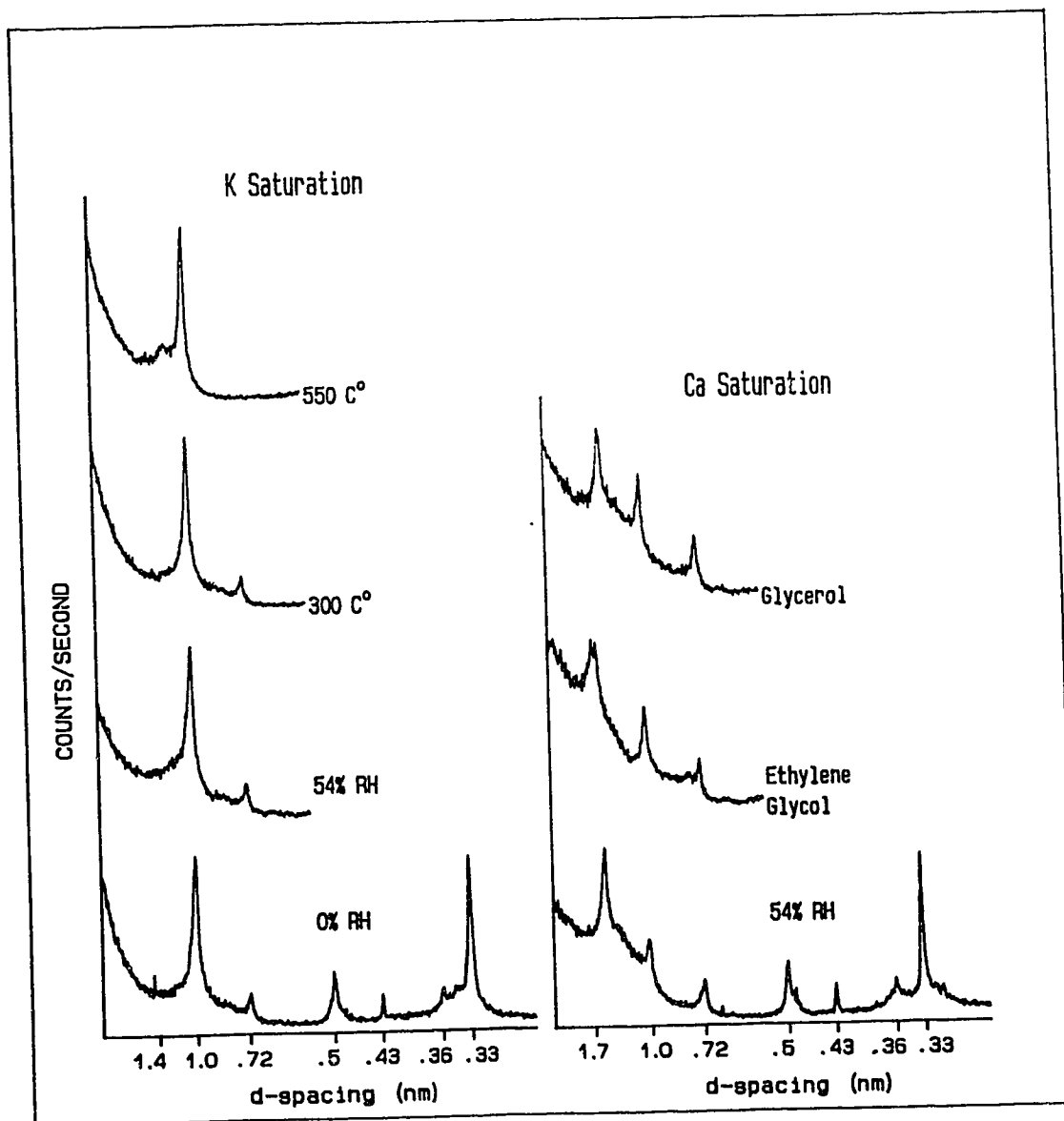


Figure 12. X-ray diffractogram of the clay separates from the Bt3 horizon of pedon 3.

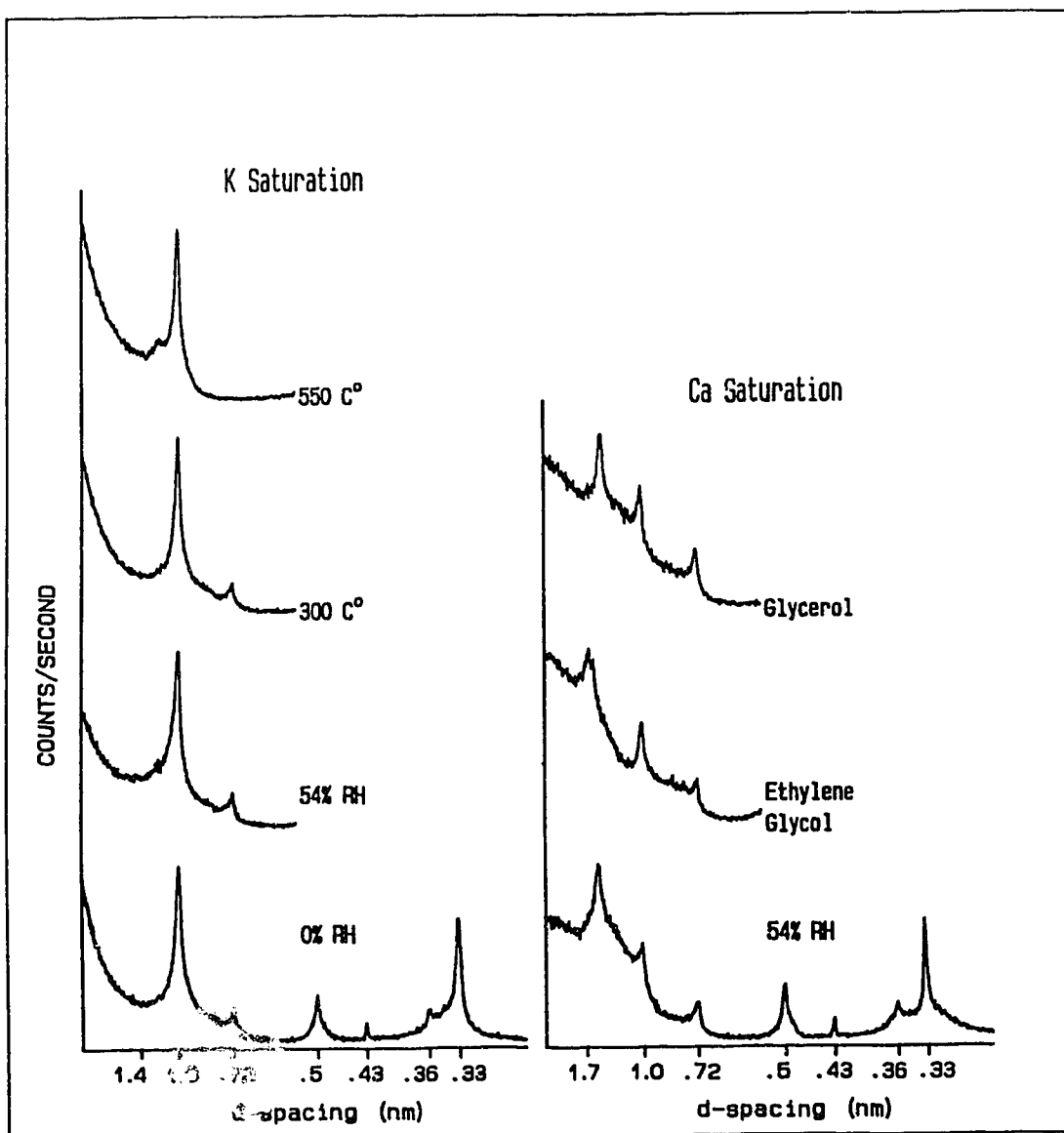


Figure 13. X-ray diffractogram of the clay separates from the C1 horizon of pedon 3.

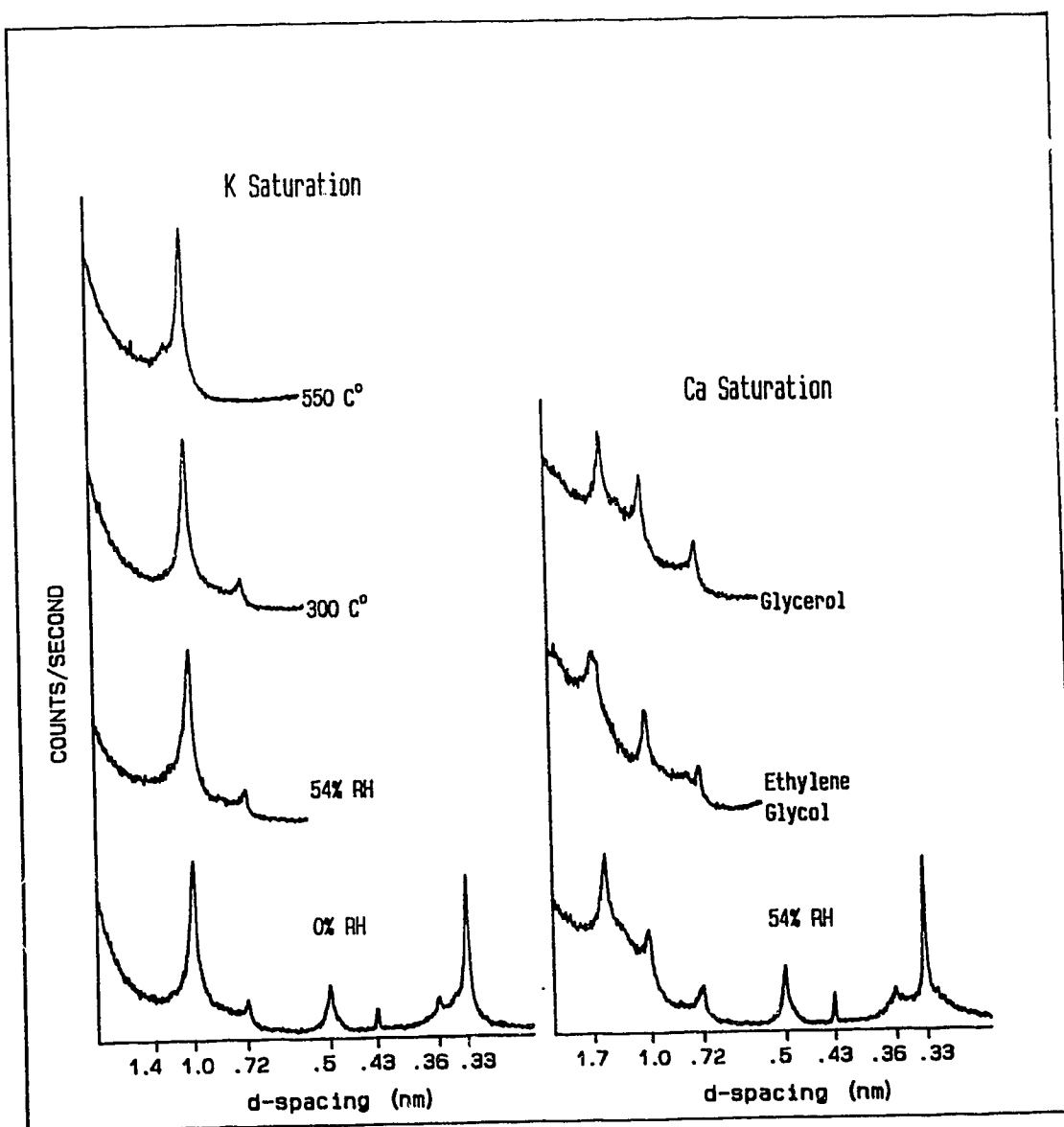


Figure 14. X-ray diffractogram of the clay separates from the C2 horizon of pedon 3.

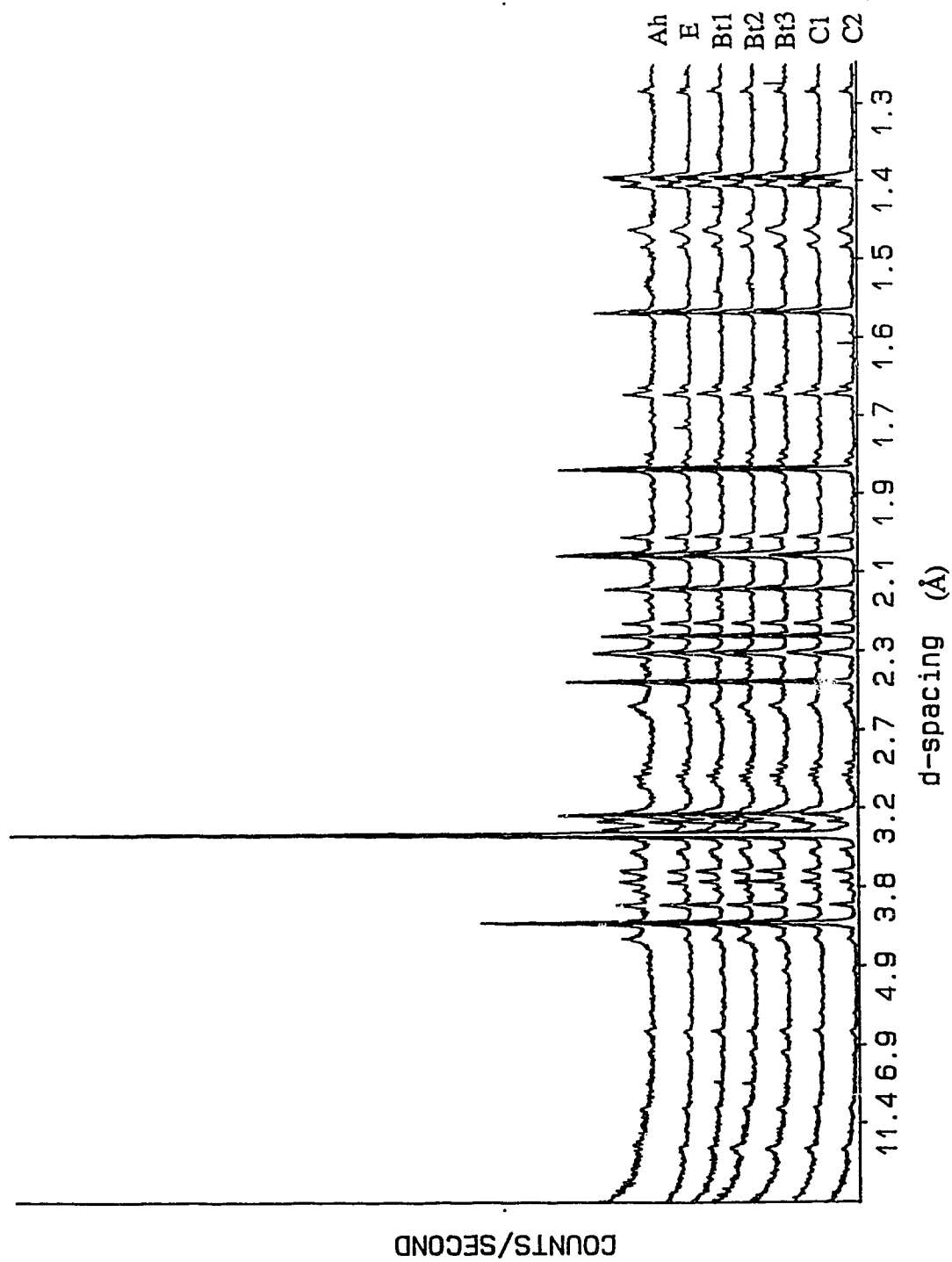


Figure 15. X-ray diffractogram of the total silt fraction of pedon 1.

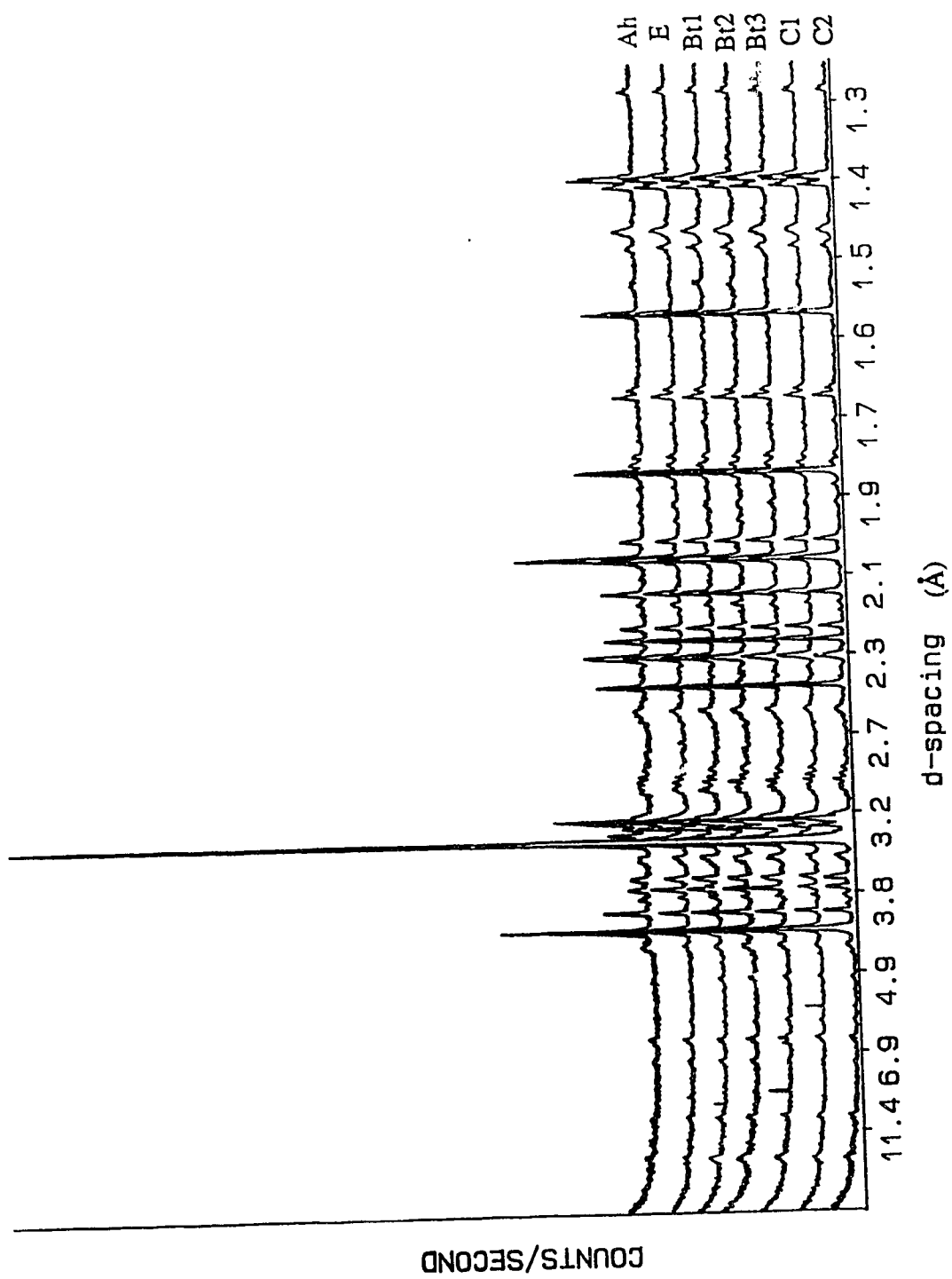


Figure 16. X-ray diffractogram of the total silt fraction of pedon 2.

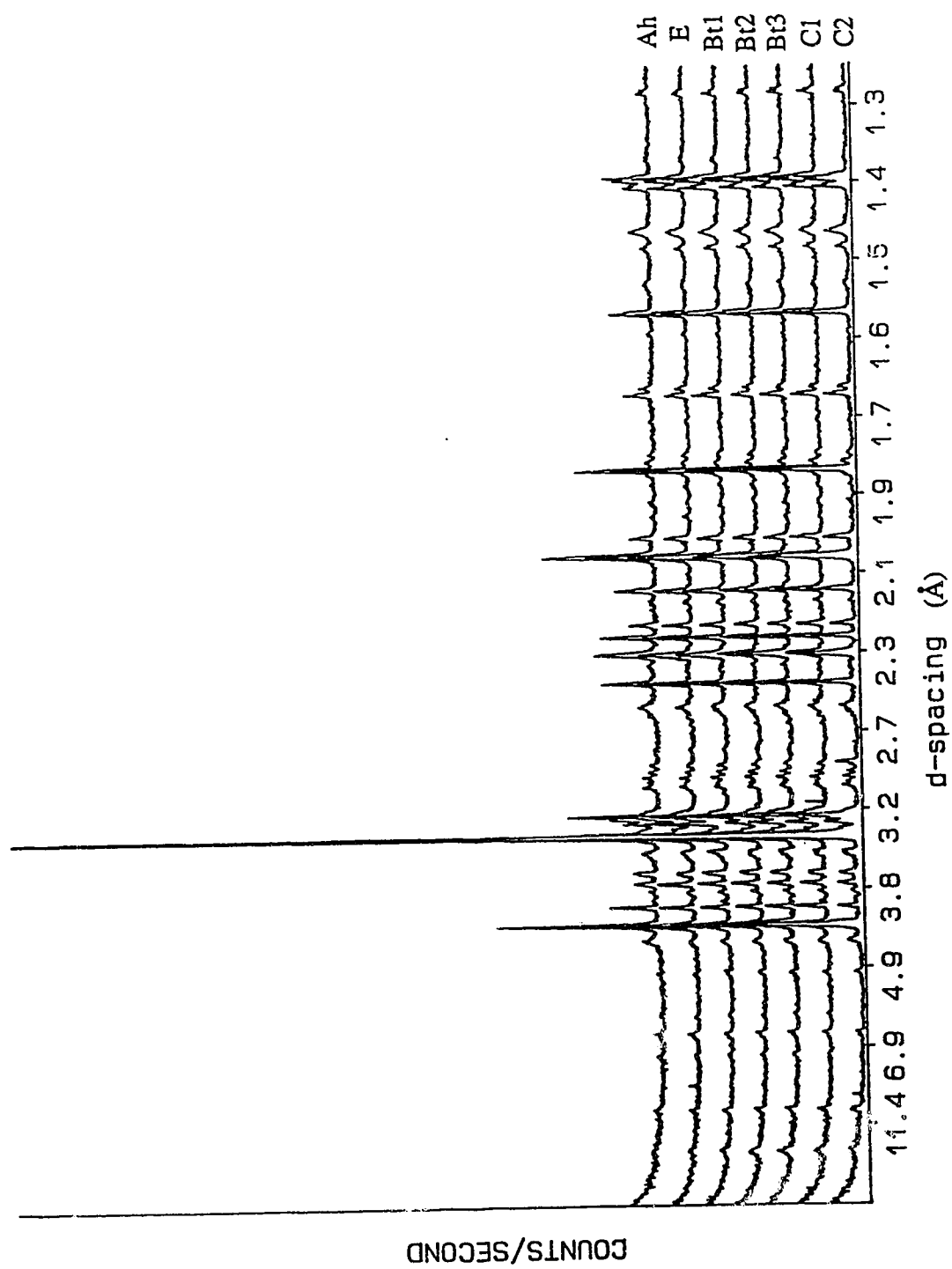


Figure 17. X-ray diffractogram of the total silt fraction of pedon 3.

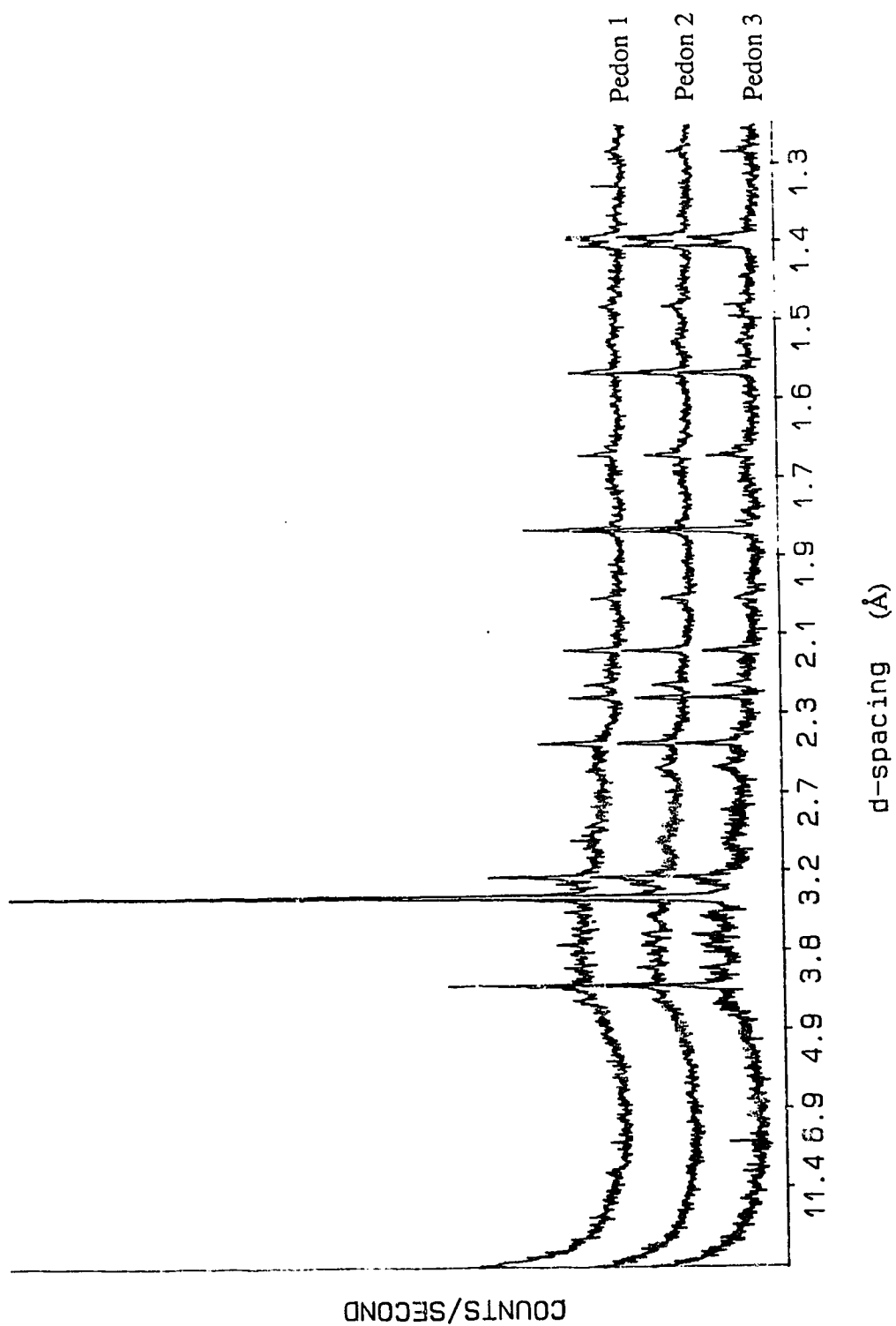


Figure 18. X-ray diffractogram of the Fe-Mn nodules from the E horizons of three pedons.





## APPENDIX II

Table 1. Profile distribution of total trace elements in bulk soil samples of pedon 1.

Element	(mg/kg)						
	A	Ae	Bt1	Bt2	Bt3	C1	C2
Ag	<†0.2	<0.2	<0.2	<0.2	<0.2	<0.2	<0.2
As	10	23	9.6	12	12	11	12
Au(µg/kg)	1.0	1.0	<1.0	1.0	1.0	1.0	1.0
B	37	47	42	41	42	42	42
Ba	620	630	580	560	650	500	550
Br	9.1	0.90	0.90	1.1	0.70	0.40	0.40
Cl	<10	<10	<10	<10	<10	<10	<10
Co	11	35	7.1	9.9	14	16	17
Cr	26	35	56	61	57	49	38
Cs	4.1	4.8	5.6	7.1	8.7	8.5	9.8
Ga	<5.0	<5.0	21	12	25	26	<5.0
Hf	5.3	7.5	5.9	5.4	5.4	5.8	5.7
Hg(µg/kg)	64	23	29	50	52	48	54
I	4.8	4.3	<0.5	1.8	4.5	3.1	<0.5
Mn	1500	1700	330	400	780	1000	1100
Mo	<0.4	0.6	<0.4	<0.4	<0.4	<0.9	<0.4
Ni	<50	<50	<50	<50	<50	<50	<50
Rb	120	120	130	130	130	160	140
Sb	1.1	1.7	1.4	1.1	1.3	1.1	1.3
Sc	9.9	9.9	14	15	15	13	13
Se	<0.5	<0.5	<0.5	1.8	<0.5	<0.5	<0.5
Sr	130	130	120	110	110	120	110
Ta	<0.1	1.2	0.9	<0.1	0.6	<0.1	0.6
Th	11	14	13	9.9	10	9.3	12
Ti	4900	5000	4800	4700	4700	4800	4600
U	3.3	4.0	3.6	3.7	3.5	3.3	3.5
V	82	66	110	120	110	88	99
W	<1.0	<1.0	<1.0	<1.0	<1.0	2.0	2.0
Zn	88	57	91	120	140	130	120
Zr	270	340	270	230	230	270	270

† denotes less than.

Table 2. Profile distribution of total trace elements in bulk soil samples of pedon 3.

Element	(mg/kg)						
	A	Ae	Bt1	Bt2	Bt3	C1	C2
Ag	<0.2	<0.2	<0.2	<0.2	<0.2	<0.2	<0.2
As	11	16	8.2	10	13	11	11
Au( $\mu\text{g/kg}$ )	<1.0	<1.0	<1.0	<1.0	<1.0	<1.0	1.0
B	41	43	42	42	41	41	39
Ba	650	540	520	600	650	540	590
Br	7.5	0.80	0.90	1.3	1.1	0.40	0.40
Cl	<10	<10	<10	<10	<10	<10	<10
Co	12	21	8.8	8.1	15	11	15
Cr	57	55	52	65	61	45	36
Cs	7.0	4.2	9.5	9.4	9.5	9.8	7.2
Ga	<5.0	<5.0	17	<5.0	<5.0	17	<5.0
Hf	6.2	6.4	5.9	5.7	6.1	5.8	6.0
Hg( $\mu\text{g/kg}$ )	49	25	38	45	41	45	45
I	4.4	<0.5	<0.5	7.6	<0.5	3.1	<0.5
Mn	1000	1300	330	790	800	570	640
Mo	<0.4	0.9	<0.4	<0.4	<0.4	<0.4	<0.4
Ni	<50	<50	<50	<50	<50	<50	<50
Rb	140	150	170	170	180	150	150
Sb	1.1	2.1	1.5	1.3	2.0	1.7	1.5
Sc	11	9.8	13	15	15	14	12
Se	<0.5	<0.5	<0.5	<0.5	<0.5	<0.5	<0.5
Sr	130	130	110	120	110	120	120
Ta	0.90	1.3	0.70	0.90	1.1	0.70	0.80
Th	13	17	14	14	14	14	11
Ti	4900	4800	4800	4400	4400	4100	4200
U	3.4	4.0	3.6	3.9	3.5	3.6	3.6
V	69	87	87	170	100	97	100
W	1.0	<1.0	<1.0	<1.0	2.0	<1.0	<1.0
Zn	84	71	97	120	120	120	120
Zr	290	300	270	240	260	250	240

Table 3. Profile distribution of total trace elements in clay separates of pedon 1.

Element	(mg/kg)						
	A	Ae	Bt1	Bt2	Bt3	C1	C2
Ag	<†0.2	<0.2	4.1	5.9	5.6	6.0	5.9
As	13	15	18	16	17	18	21
Au(µg/kg)	3.0	9.0	6.0	6.0	4.0	3.0	5.0
B	41	47	34	37	39	37	35
Ba	590	420	470	410	430	450	450
Br	22	4.8	3.4	3.0	2.1	0.80	0.70
Cl	150	80	20	20	40	30	40
Co	13	14	11	13	14	12	15
Cr	98	110	110	120	110	110	110
Cs	1.0x10	11	17	18	18	12	14
Hg(µg/kg)	‡	‡	‡	‡	‡	‡	‡
Hf	4.4	5.1	5.1	4.7	4.1	4.1	4.8
I	180	110	53	53	49	51	56
Mn	590	750	220	210	410	420	410
Mo	2.6	1.6	<0.4	<0.4	<0.4	<0.4	<0.4
Ni	95	<50	<50	110	110	65	5.0x10
Rb	210	210	230	230	210	210	200
Sb	1.7	1.7	1.8	1.7	1.9	1.7	2.0
Sc	22	25	26	26	27	26	27
Se	1.0	<0.5	4.0	6.8	7.2	2.5	4.6
Ta	0.7	1.2	1.1	1.0	1.2	1.1	1.1
Th	2.0x10	19	19	16	16	16	17
Ti	3000	3600	2000	2400	2400	3000	3100
U	3.7	5.7	4.4	3.8	3.7	3.7	4.0
V	120	110	100	110	110	130	120
W	2.0	4.0	3.0	2.0	2.0	3.0	2.0
Zn	99	100	110	110	110	95	100
Zr	‡	‡	‡	‡	‡	‡	‡

† denotes less than; ‡ denotes data unavailable.

Table 4. Profile distribution of total trace elements in clay separates of pedon 3.

Element	(mg/kg)						
	A	Ae	Bt1	Bt2	Bt3	C1	C2
Ag	1.4	<0.2	4.8	4.9	<0.2	6.1	5.7
As	15	19	19	20	210	19	17
Au( $\mu\text{g/kg}$ )	5.0	2.0	<1.0	4.0	7.0	5.0	4.0
Ba	570	600	520	480	540	570	450
Br	23	5.3	2.3	1.2	1.0	0.6	0.6
Cl	90	40	30	40	50	50	40
Co	13	14	9.9	10	14	15	13
Cr	90	100	100	100	100	100	100
Cs	12	13	14	16	13	16	16
Ga	24	49	54	42	25	27	47
Hg( $\mu\text{g/kg}$ )	‡	‡	‡	‡	‡	‡	‡
Hf	4.6	5.7	5.9	5.7	5.6	5.7	5.7
I	150	99	51	54	51	52	54
Mn	830	600	260	290	770	690	620
Mo	3.9	3.9	2.5	3.2	4.2	<0.4	<0.4
Ni	<50	<50	<50	110	110	75	<50
Rb	210	220	220	220	210	240	230
Sb	1.8	2.1	2.0	2.2	2.2	2.2	2.2
Sc	26	23	25	23	24	22	25
Se	1.3	7.4	7.7	<0.5	3.2	9.9	3.7
Ta	1.0	1.5	0.80	0.90	1.0	0.60	1.1
Th	20	21	20	18	19	19	17
Ti	3000	4600	2800	2600	2400	2400	2400
U	4.3	4.6	4.4	4.5	4.0	4.0	4.1
V	130	150	100	120	140	130	130
W	2.0	3.0	2.0	2.0	2.0	2.0	2.0
Zn	95	100	90	120	110	100	110
Zr	‡	‡	‡	‡	‡	‡	‡

Table 5. Profile distribution of rare earth elements (REE) in bulk soil samples of pedon 1.

(mg/kg)							
Element	A	Ae	Bt1	Bt2	Bt3	C1	C2
La	42	45	38	32	35	31	31
Ce	62	98	61	49	45	52	55
Nd	23	26	24	20	13	15	21
Sm	5.8	5.8	5.2	5.0	4.9	3.9	5.1
Eu	1.4	1.2	1.0	0.9	1.1	1.0	0.90
Gd	6.9	5.8	5.1	5.4	5.5	5.0	4.8
Tb	0.6	0.9	0.5	0.8	0.4	0.7	0.7
Dy	3.7	3.9	3.8	3.9	3.7	3.0	3.5
Yb	2.1	2.9	2.4	2.0	1.5	1.5	2.1
Lu	0.4	0.5	0.4	0.3	0.3	0.4	0.4
ΣREE	148	189	141	119	111	112	124
ΣLa/ΣLu	9.8	13	11	8.6	8.7	9.6	9.8

ΣLa = La to Eu.

ΣLu = Gd to Lu.

Table 6. Profile distribution of rare earth elements (REE) in bulk soil samples of pedon 3.

(mg/kg)							
Element	A	Ae	Bt1	Bt2	Bt3	C1	C2
La	37	44	39	41	49	36	33
Ce	79	88	75	61	56	64	59
Nd	23	31	24	27	24	15	11
Sm	5.4	6.5	5.5	5.7	5.4	4.1	4.3
Eu	1.3	1.1	0.9	1.1	1.2	0.90	0.90
Gd	6.6	5.0	5.3	6.2	5.9	5.3	4.7
Tb	0.9	0.5	0.7	0.8	0.7	0.7	0.7
Dy	4.0	3.4	3.6	3.8	3.7	3.7	3.2
Yb	2.7	2.9	2.8	2.9	2.4	2.3	2.0
Lu	0.5	0.4	0.4	0.5	0.6	0.4	0.4
ΣREE	161	183	158	149	149	132	119
ΣLa/ΣLu	9.8	14	11	10	11	9.7	9.8

Table 7. Profile distribution of rare earth elements (REE) in clay separates of pedon 1.

(mg/kg)							
Element	A	Ae	Bt1	Bt2	Bt3	C1	C2
La	62	75	64	49	53	38	36
Ce	87	120	99	89	83	91	94
Nd	41	58	35	39	26	22	22
Sm	8.1	9.2	8.2	7.8	8.2	5.1	5.0
Eu	1.8	2.5	2.0	1.4	1.4	1.1	1.1
Gd	6.4	8.9	8.5	5.4	5.1	4.2	3.3
Tb	0.90	0.90	1.2	0.60	1.1	0.60	0.40
Dy	6.2	7.5	4.5	4.2	5.1	4.1	4.3
Yb	3.9	4.5	4.0	4.0	3.9	3.5	3.8
Lu	0.6	0.6	0.6	0.6	0.6	0.5	0.6
$\Sigma$ REE	217	287	231	202	187	170	171
$\Sigma$ La/ $\Sigma$ Lu	11	12	11	13	11	12	13

Table 8. Profile distribution of rare earth elements (REE) in clay separates of pedon 3.

(mg/kg)							
Element	A	Ae	Bt1	Bt2	Bt3	C1	C2
La	71	77	63	57	58	49	49
Ce	121	127	113	104	105	104	100
Nd	39	42	40	39	41	30	29
Sm	9.0	9.1	6.5	6.7	9.3	6.4	6.2
Eu	1.8	1.6	1.3	1.4	1.4	1.1	1.1
Gd	6.1	7.0	5.8	4.0	5.0	3.9	6.1
Tb	1.5	1.1	1.1	0.80	1.1	0.80	0.90
Dy	6.2	6.4	6.1	5.6	6.7	4.4	5.1
Yb	4.1	4.6	4.2	4.3	4.7	4.3	4.2
Lu	0.6	0.6	0.6	0.6	0.7	0.5	0.6
$\Sigma$ REE	261	276	241	223	233	204	202
$\Sigma$ La/ $\Sigma$ Lu	13	13	13	14	12	14	11